Universität Zürich[UZH]

# Amplitude analyses of multibody hadronic decays at LHCb


Rafael Silva Coutinho

Universität Zürich - SNF Ambizione
On behalf of the LHCb Collaboration


**CERN LHC Seminar**
**December 11th, 2018**

Julie Oppermann
[Untitled (2013) - Acrylic on yupo paper]

# Portrait of the underlying physics

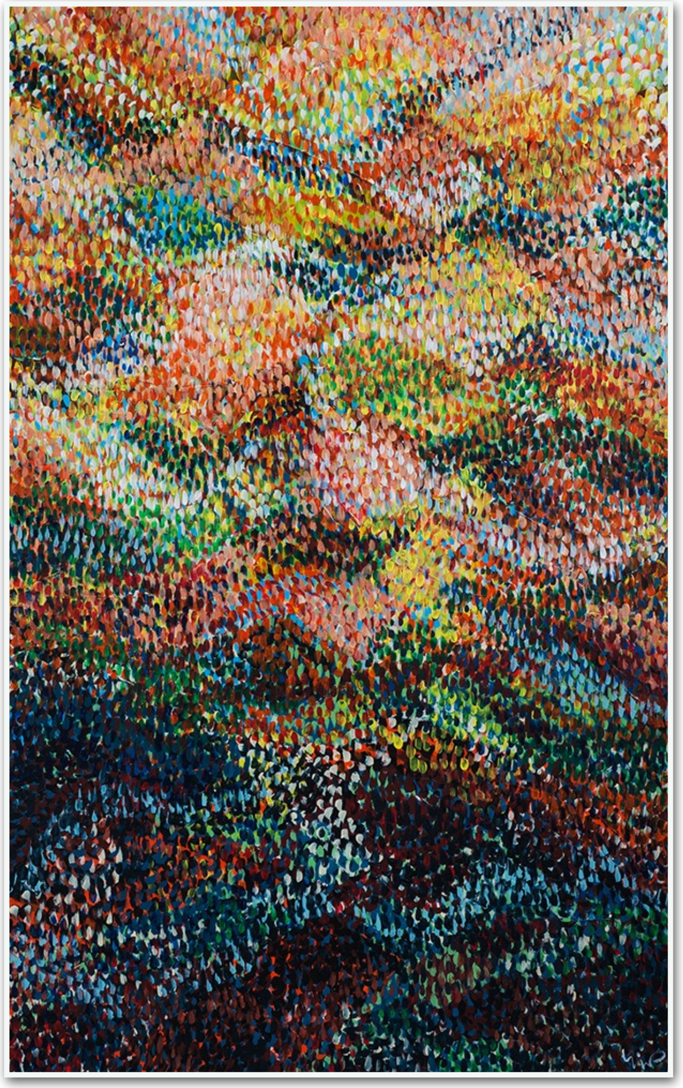

Norm YIP
[Ecstasy, No. 1 (2015) - Acrylic on canvas]

*"… the specks and flickers of paint dance like energy particles throughout the painting."*

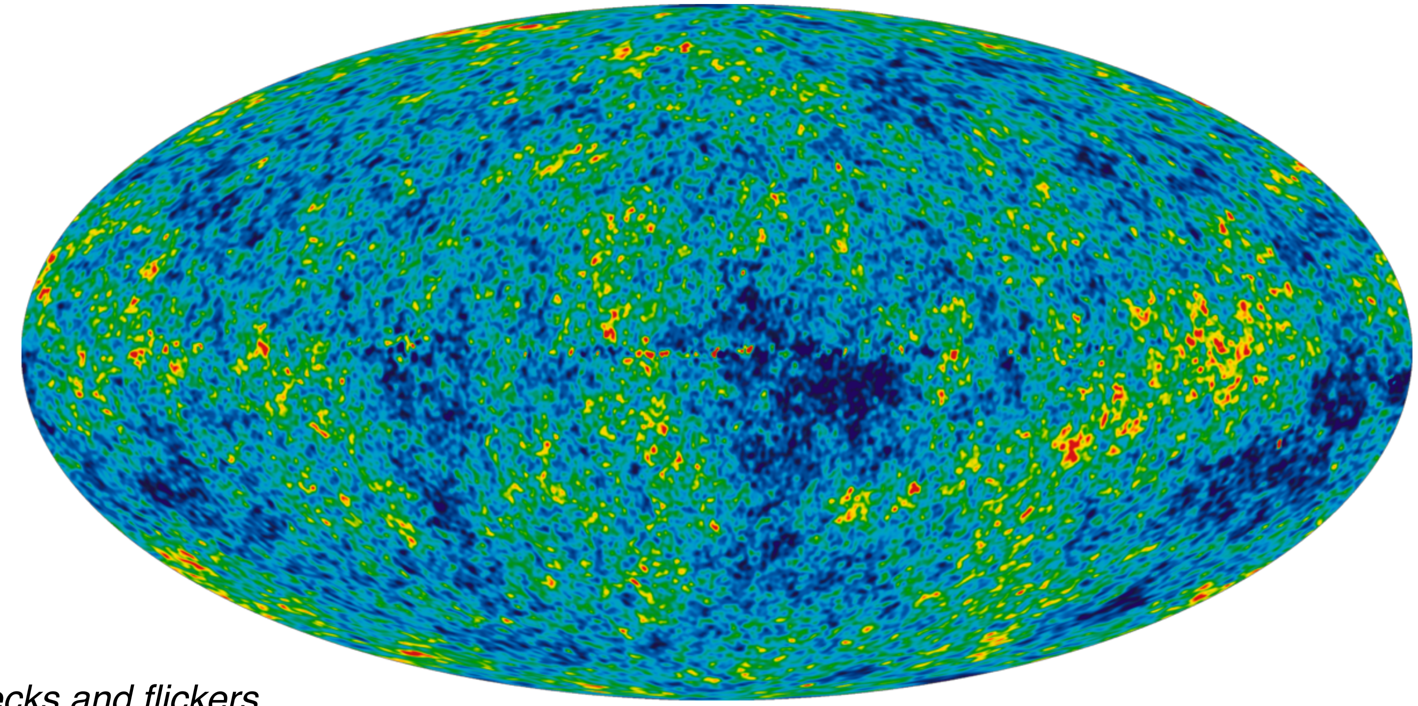

[Cosmic Microwave background, WMAP, NASA]

*"Observations of the CMB [its anisotropies] have played a key role in […] our understanding of the very early universe."*

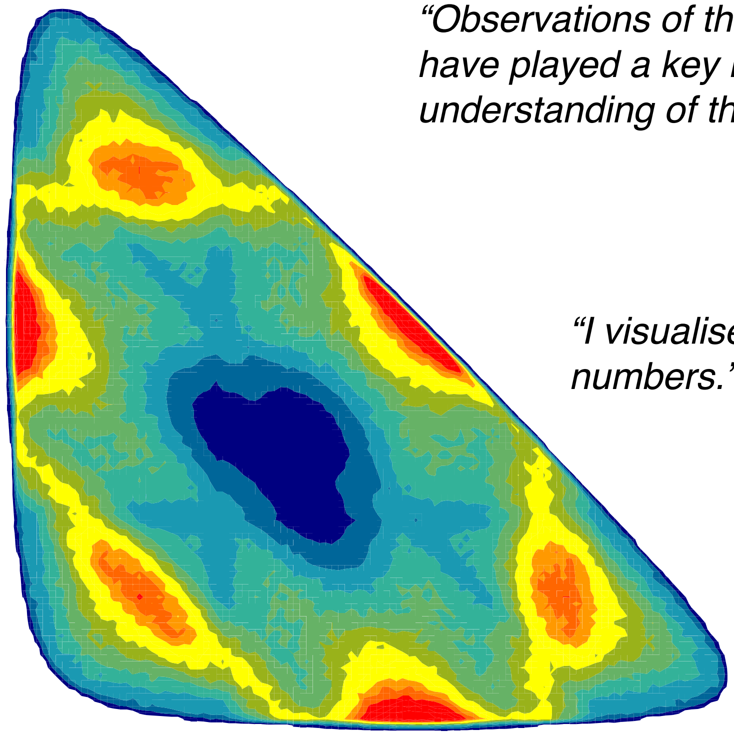

*"I visualise geometry better than numbers."* [Richard Dalitz]

[Crystal Barrel LEAR]

# Flavour physics: the CKM matrix

In the SM quarks can change their flavour by emission of a W boson, with transition probability governed by the CKM matrix

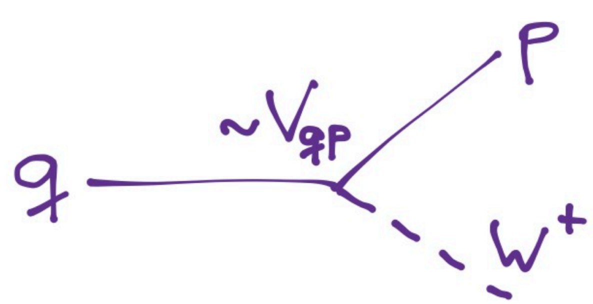


$$V_{\mathrm{CKM}} = \begin{pmatrix} V_{ud} & V_{us} & V_{ub} \\ V_{cd} & V_{cs} & V_{cb} \\ V_{td} & V_{ts} & V_{tb} \end{pmatrix}$$

Described by 4 independent parameters, in particular a single complex phase

$$V = \begin{pmatrix} 1-\lambda^2/2 & \lambda & A\lambda^3(\rho - i\eta) \\ -\lambda & 1-\lambda^2/2 & A\lambda^2 \\ A\lambda^3(1-\rho-i\eta) & -A\lambda^2 & 1 \end{pmatrix} + \mathcal{O}(\lambda^4)$$

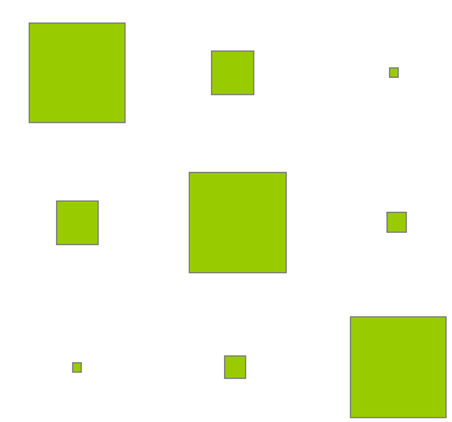

# The portrait of flavour physics: Unitary Triangle

[CKM fitter group (J. Charles et al, Eur. Phys. J. C41, 1-131 (2005)]

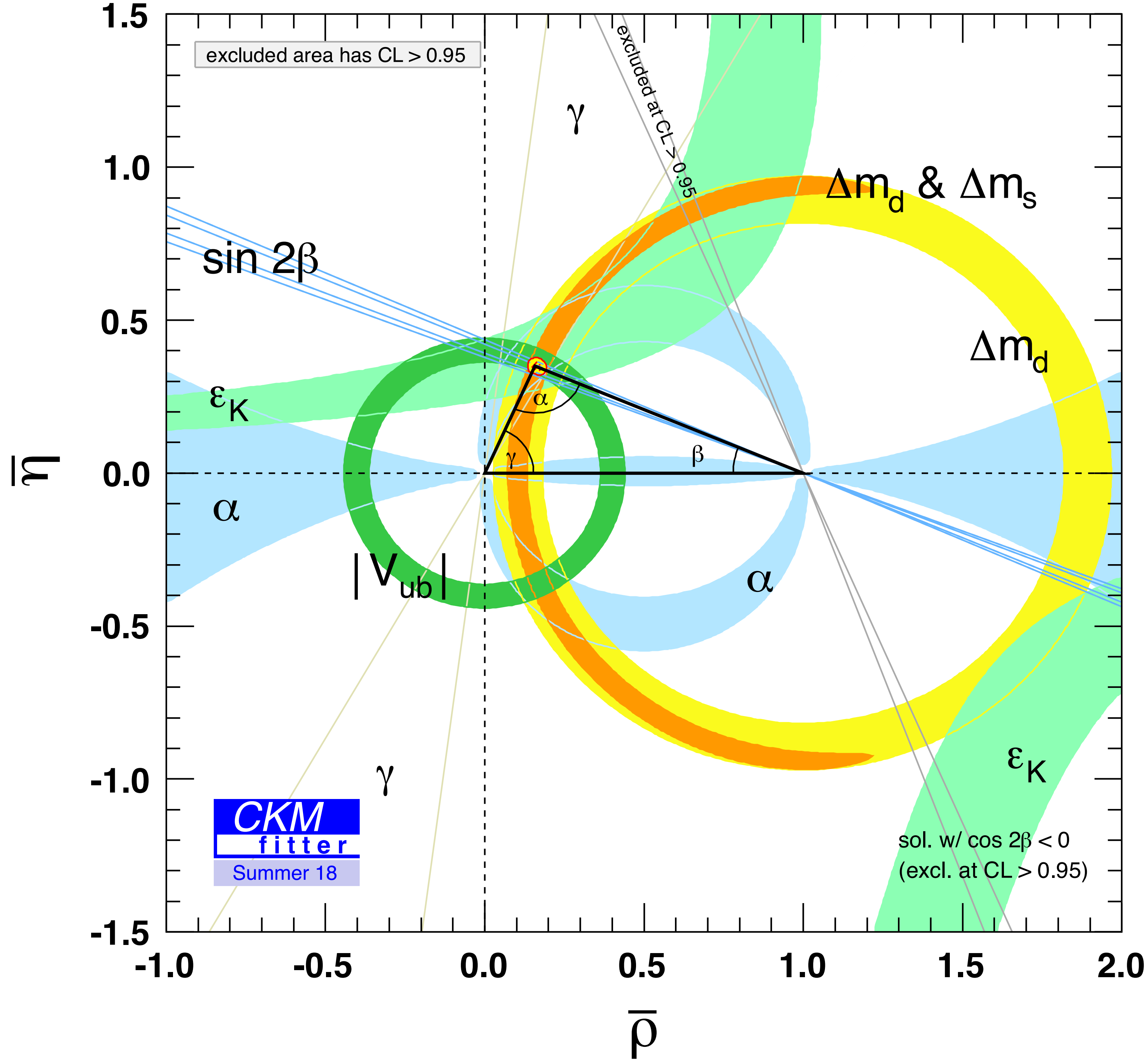


So far a huge success for the Standard Model!

~20% contribution from New Physics still possible within current precision

# CP violation in B decays

[LHCb, PRL 110 (2013) 221601]

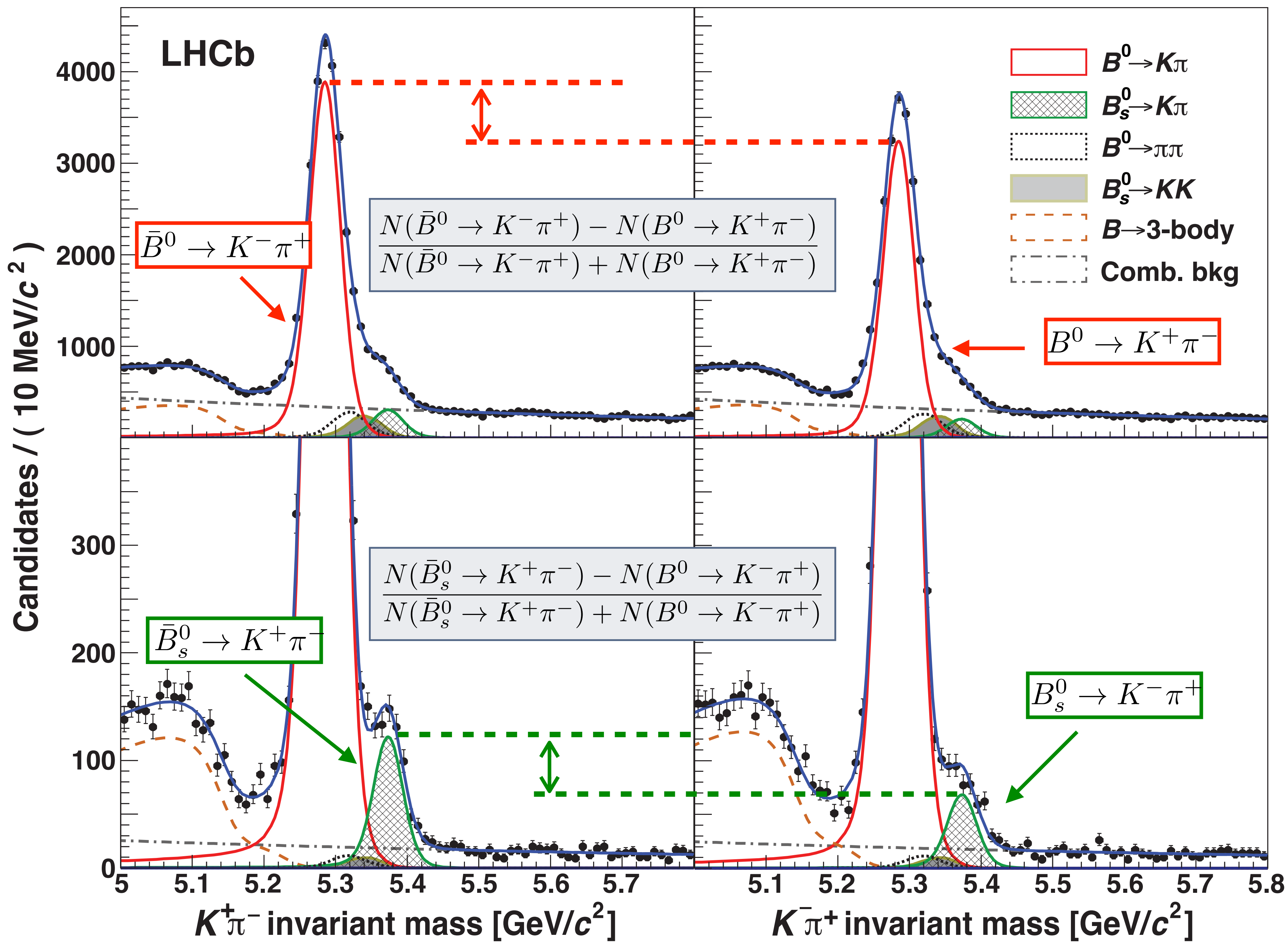

# Two-body decays physics case

## Hadronic 2-body $B \to K\pi$ decays show an interesting $A^{CP}$ pattern:

### $A^{CP}$ measurements

| | BaBar | Belle |
|---|---|---|
| $B^0 \to K^0\pi^0$ | $+0.13 \pm 0.13 \pm 0.03$ | $+0.14 \pm 0.13 \pm 0.06$ |
| $B^+ \to K^0\pi^+$ | $-0.029 \pm 0.039 \pm 0.010$ | $-0.011 \pm 0.021 \pm 0.006$ |
| $B^0 \to K^+\pi^-$ | $-0.107 \pm 0.016^{+0.006}_{-0.004}$ | $-0.069 \pm 0.014 \pm 0.007$ |
| $B^+ \to K^+\pi^0$ | $+0.030 \pm 0.039 \pm 0.010$ | $+0.043 \pm 0.024 \pm 0.002$ |

Spectator exchange of d ↔ u: naïvely $B^+ \to K^+\pi^0$ should follow $B^+ \to K^+\pi^-$

| | $B^0 \to K^+\pi^-$ | $B^+ \to K^+\pi^0$ |
|---|---|---|
| LHCb | $-0.088 \pm 0.011 \pm 0.008$ | $n/a$ |
| World average | $-0.082 \pm 0.006$ | $0.040 \pm 0.021$ |

### $K\pi$ "puzzle"

$$\Delta\mathcal{A}^{CP}(K\pi) = 0.122 \pm 0.022 \quad 5\sigma$$

QCD effects, or ... ?

[LHCb, JHEP 1210 (2012) 037]

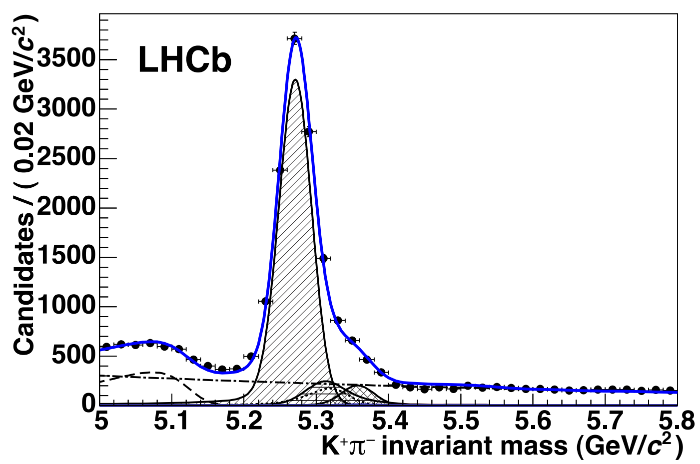


[LHCb, PLB 726 (2013)]

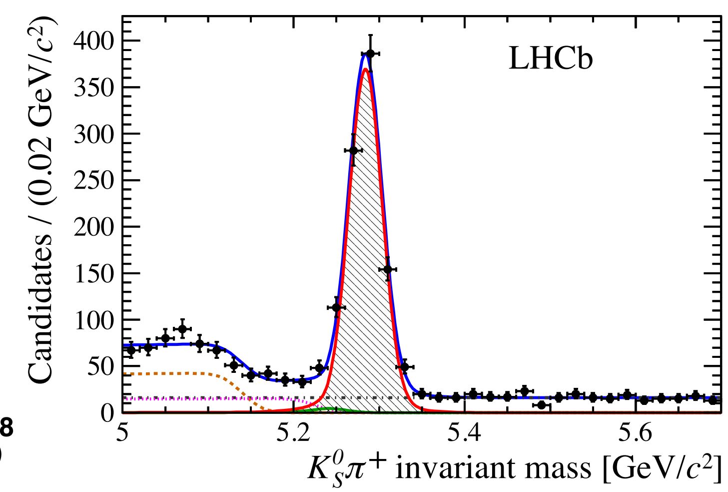


[Belle, Nature 452 (2008) 332]

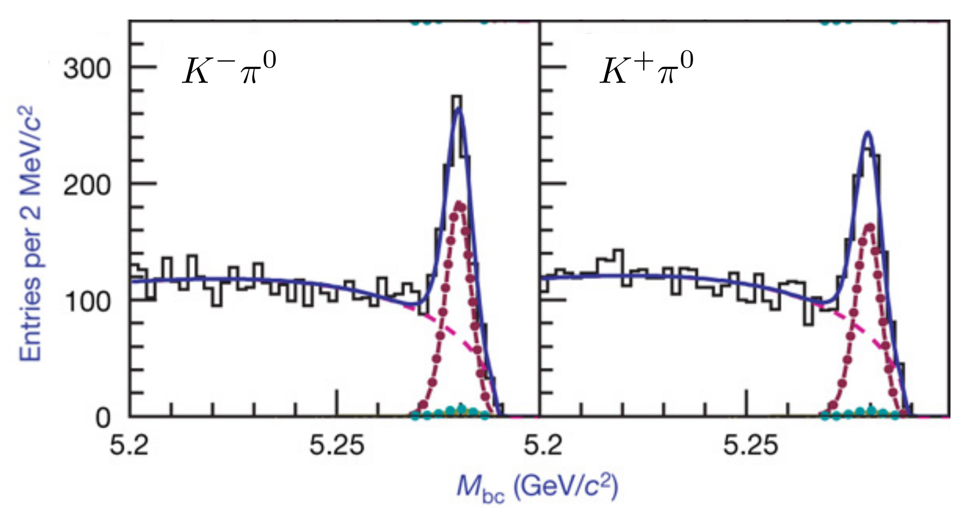


[Belle,PRL 99 (2007) 121601]

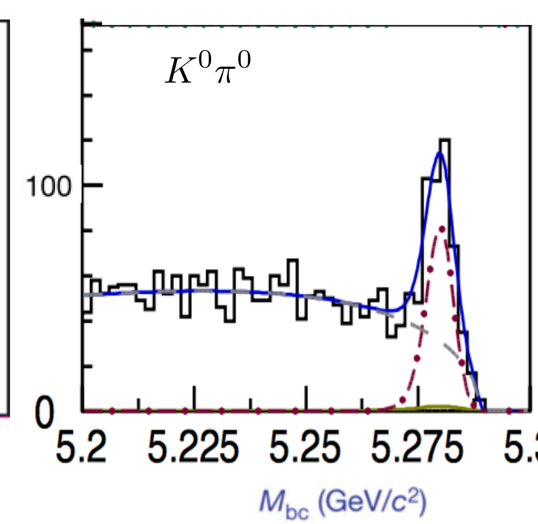

# *CP* violation sensitivity in two-body decays

**An asymmetry can be visualised as**

$$\mathcal{A}^{CP} = \frac{|\bar{A}_{\bar{f}}|^2 - |A_f|^2}{|\bar{A}_{\bar{f}}|^2 + |A_f|^2} = \frac{2|A_T||A_P|\sin\delta\sin\phi}{|A_T|^2 + |A_P|^2 + 2|A_T||A_P|\cos\delta\cos\phi}$$

where $\delta$ and $\varphi$ are the *CP* conserving and *CP* violating relative phases between amplitudes.

**Limited information available in two-body decays:**

- Observables are the Branching ratio and $A^{CP}$; unknowns, e.g. $A_T$, $A_P$, $\delta$ and $\varphi$

**Premise: additional information can be obtained via multi-body decays (n >2)**

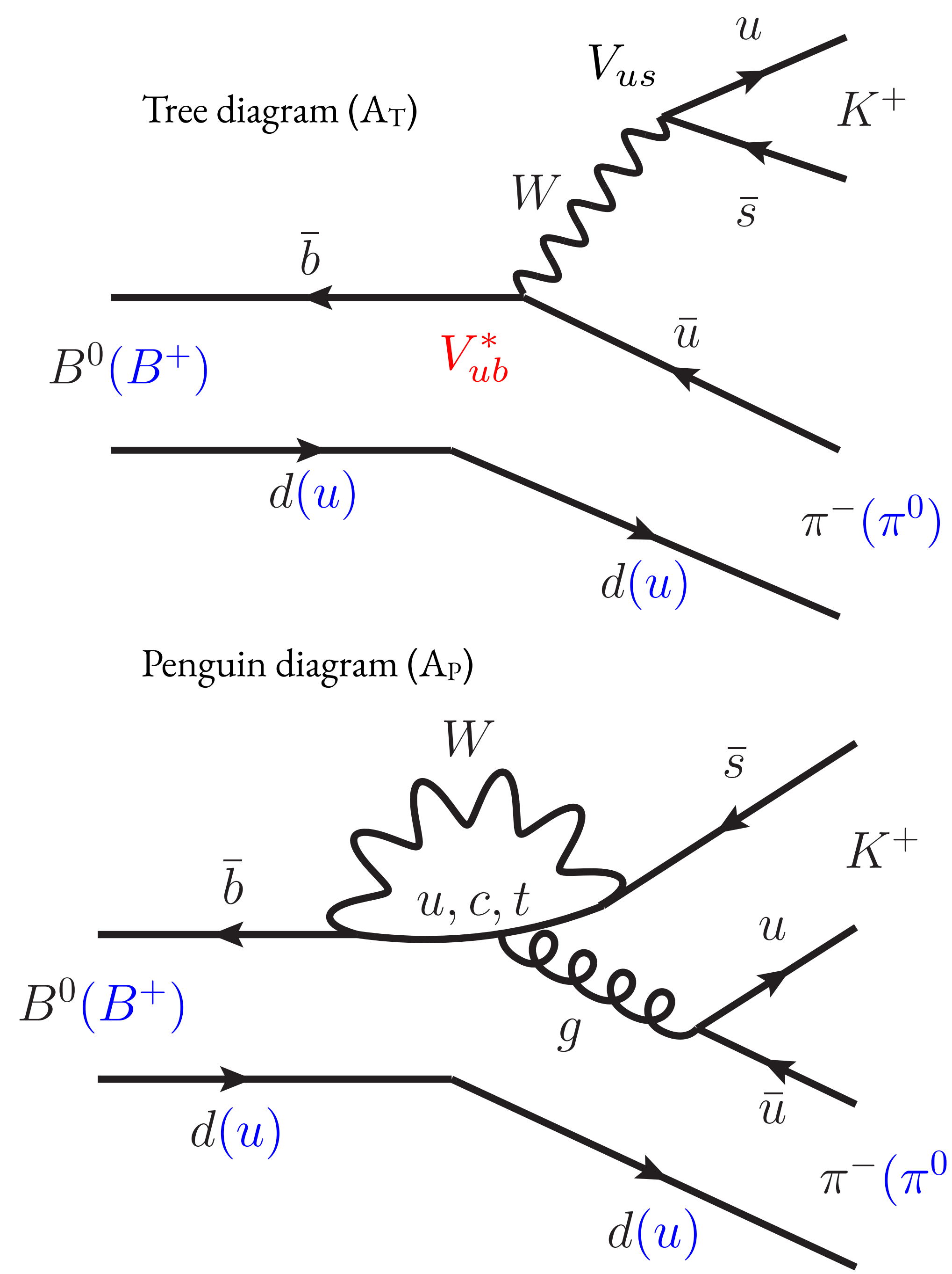

# Interference pattern for multi-channels

Multibody decays proceed through several intermediate states which interfere

→ The phase-space has interference pattern analogous to the double-slit experiment

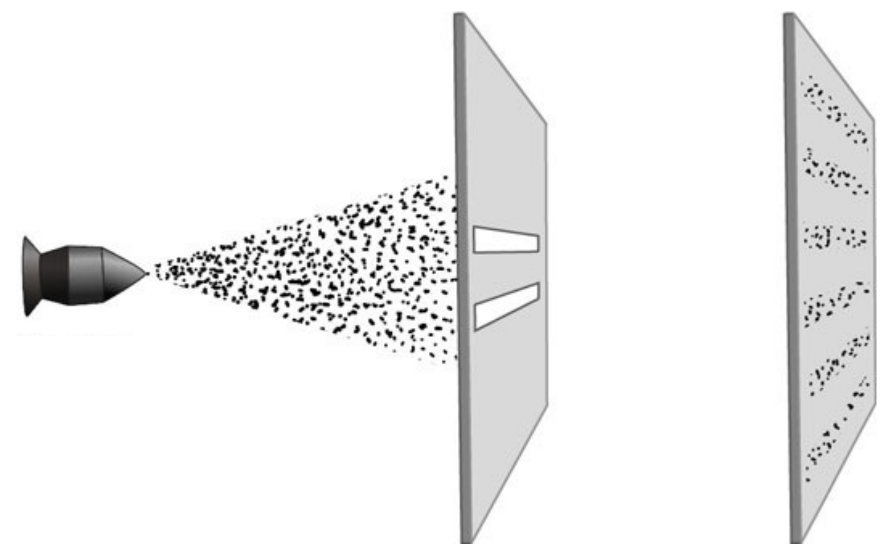

The coupling of initial and final states is given by the invariant amplitudes of the process

Wave-particle duality of light for the classroom
A. Weis and T. L. Dimitrova

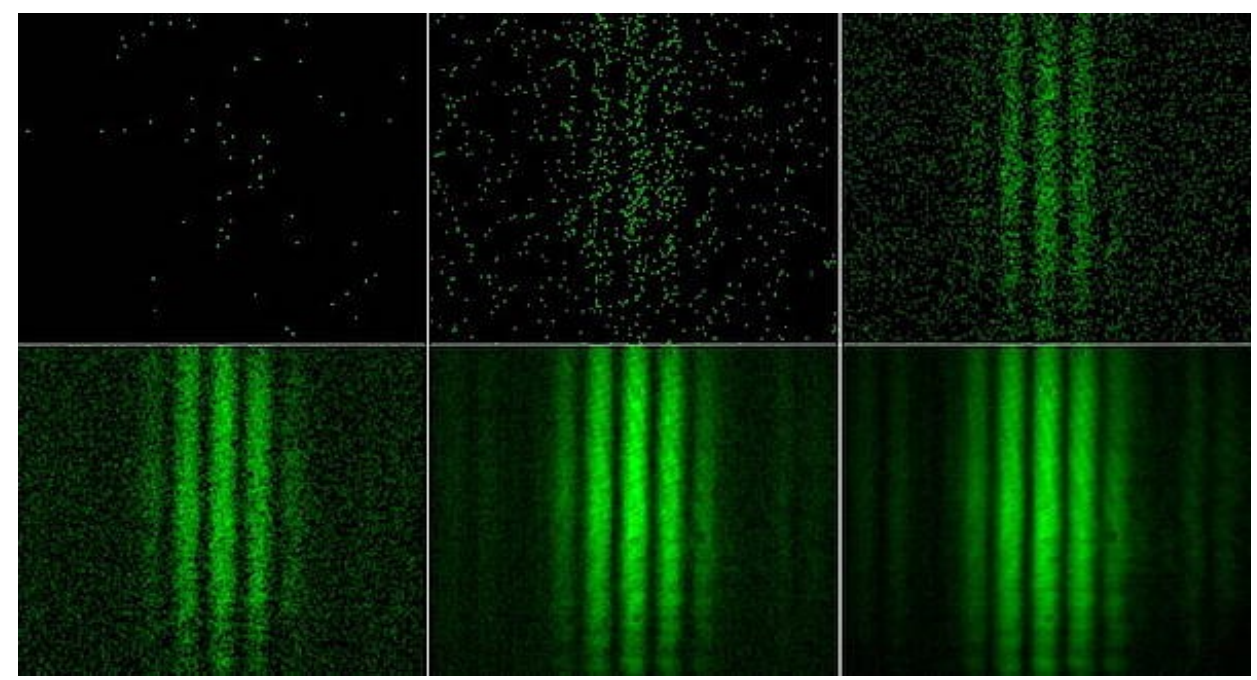

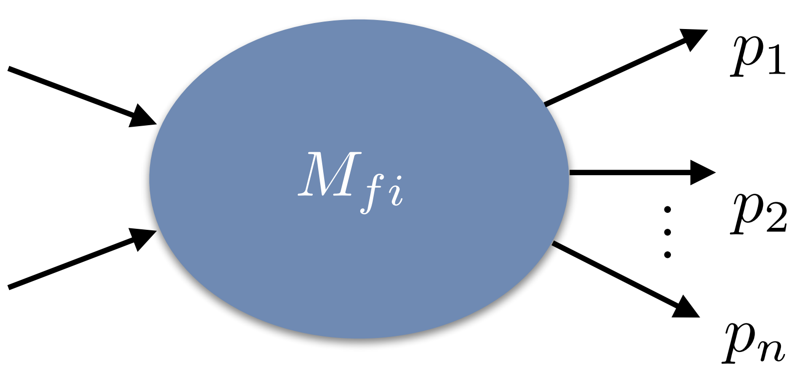


**Fermi's Golden rule**

$$d\sigma \propto |M_{fi}|^2 d\phi_N$$

Matrix element

N-body phase-space element

# Three-body decays (spinless) case

**For n = 3 final state spin-0 particles this is given by**

$$d\sigma \sim |M_{fi}|^2 d\phi_3 \sim |M_{fi}|^2 dm^2_{ij} dm^2_{jk}$$

| | | |
|---|---|---|
| Lorentz four-vector | → | 12 |
| Meson masses | → | -3 |
| p, E conservation | → | -4 |
| Arbitrary orientation | → | -3 |
| Independent variables | | 2 |

Graphical representation of the 3-body phase-space: *i.e.* **Dalitz plot!**

$$m^2_{12} + m^2_{13} + m^2_{23} = M^2 + m^2_1 + m^2_2 + m^2_3$$

[PDG (M. Tanabashi et al), PRD 98 (2018) 010001]

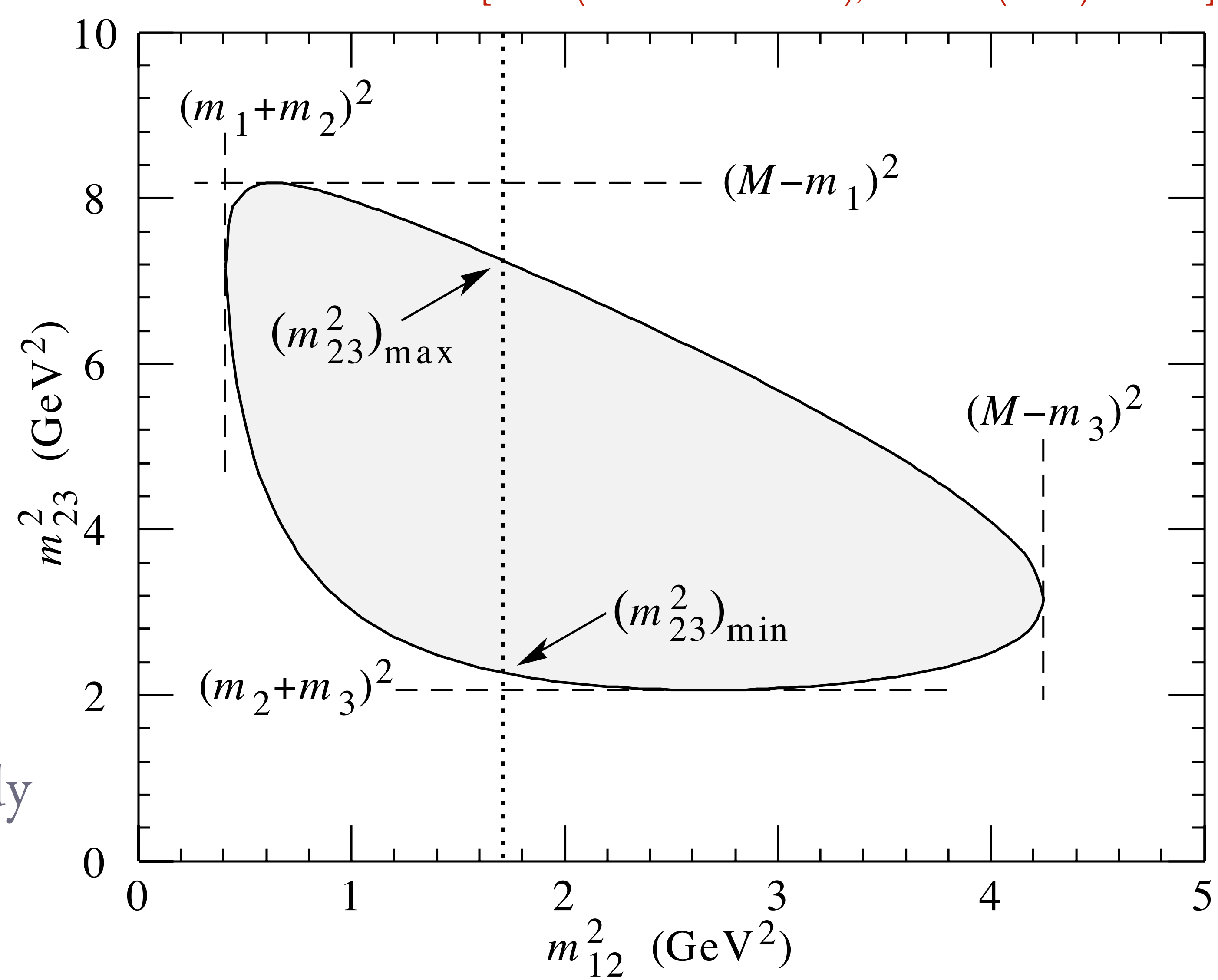

# Dalitz plot analysis features

Universität Zürich[UZH]

**Technique named after Richard Dalitz (1925-2006) applied to study $K_L$ decays**

Spin/parity determination of the known $\tau/\theta$ particle in its decay to three pion final state

"On the analysis of tau-meson data and the nature of the tau-meson."

[R. H. Dalitz, Phil. Mag. 44 (1953) 1068]

**"I visualise geometry better than numbers"**
**Richard Dalitz**

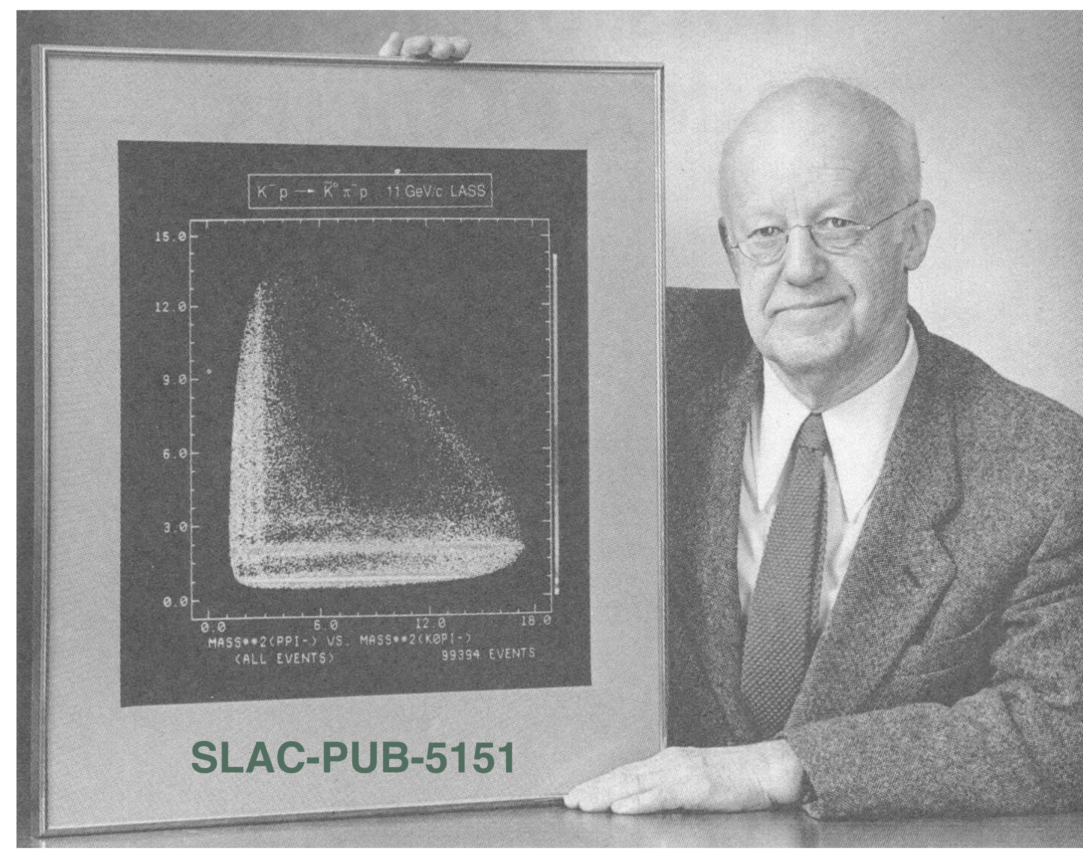


"A work of art" - gift from B. Ritcher, W. Panofsky, S. Drell, D. Leith, D. Aston, W. Dunwoodie and B. Ratcliff

**Scatter-plot visualisation as**

- Matrix element constant: Dalitz-plot uniformly populated
- Non-uniform distributions, *i.e.* dynamics
- Interference patterns between intermediate states can be studied/model

# Dalitz plot analysis features

[Laura++, Comput. Phys. Commun. 231 (2018) 198-242]

## Intensity along bands indicates magnitude and the spin resonances

### Resonant DP illustration:

- **Nonresonant (phase space)**
- $K^*(892)$ [vector]: green and blue
- $K^*_0(1430)$, $f_0(980)$ [scalar]: grey and red
- $K^*_2(1430)$ [tensor]: magenta and cyan
- $\rho(770)$ [vector]: yellow

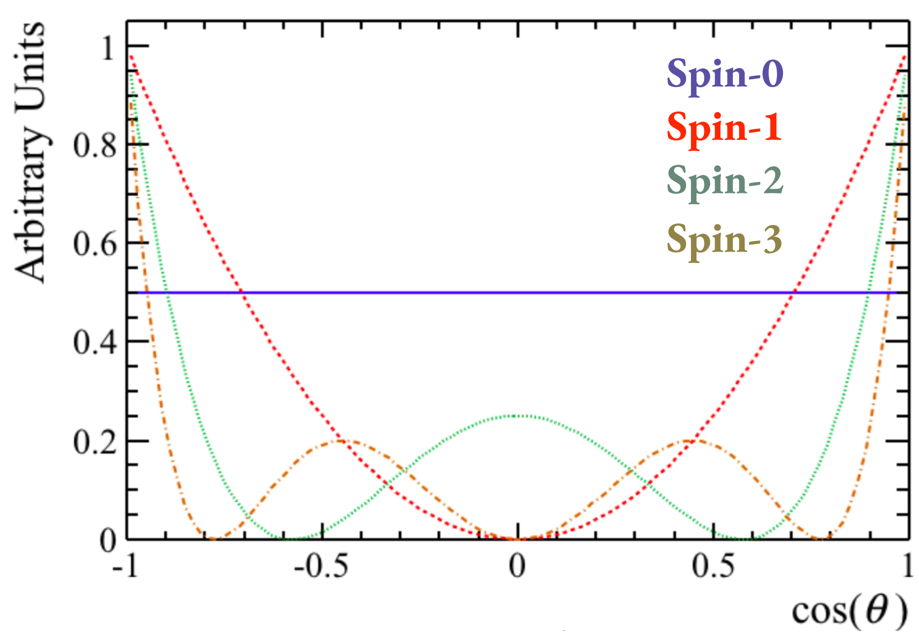


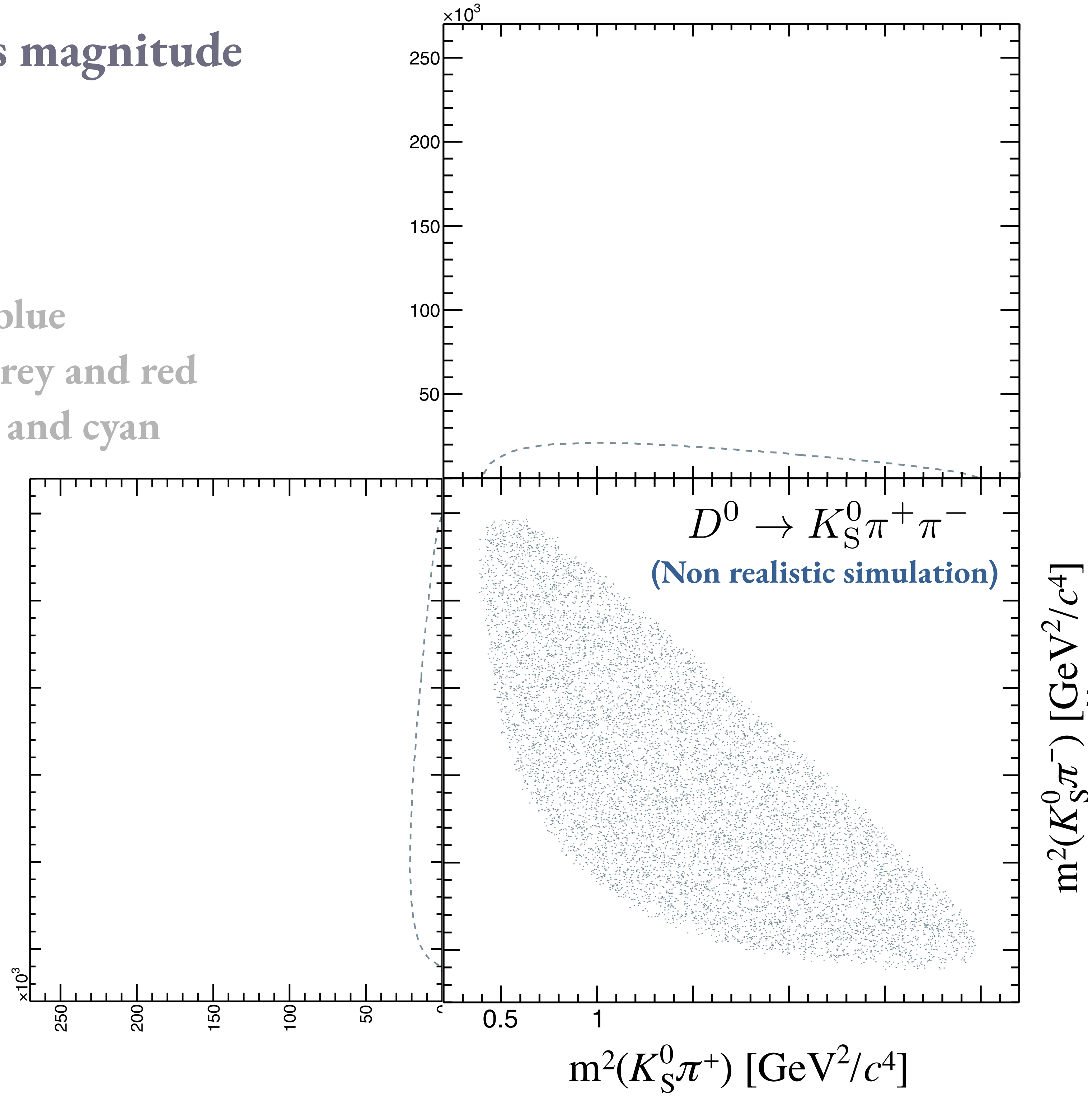

# Dalitz plot analysis features

[Laura++, Comput. Phys. Commun. 231 (2018) 198-242]

## Intensity along bands indicates magnitude and the spin resonances

### Resonant DP illustration:

- Nonresonant (phase space)
- $K^*(892)$ [vector]: green and blue
- **$K^*_0(1430)$, $f_0(980)$ [scalar]: grey and red**
- $K^*_2(1430)$ [tensor]: magenta and cyan
- $\rho(770)$ [vector]: yellow

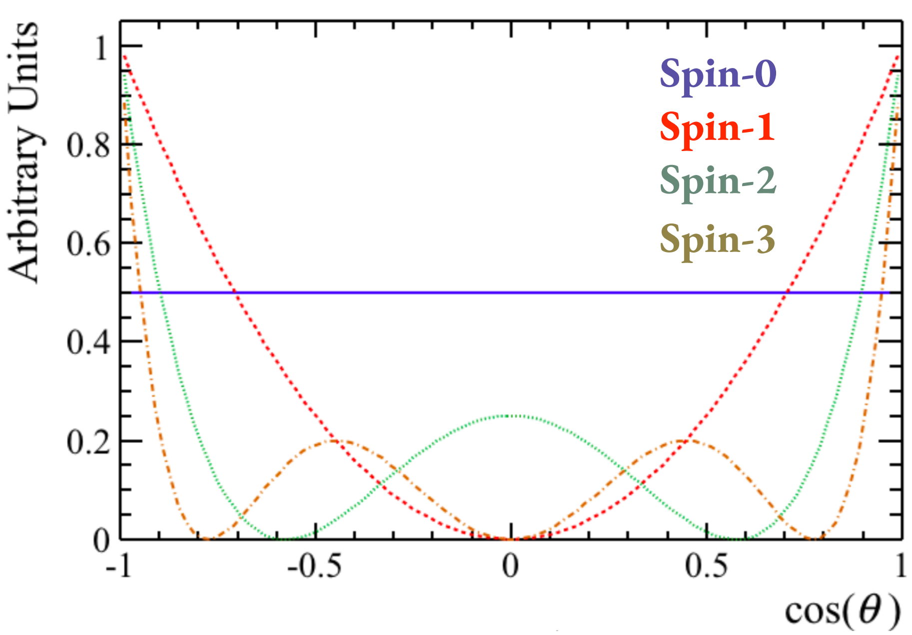


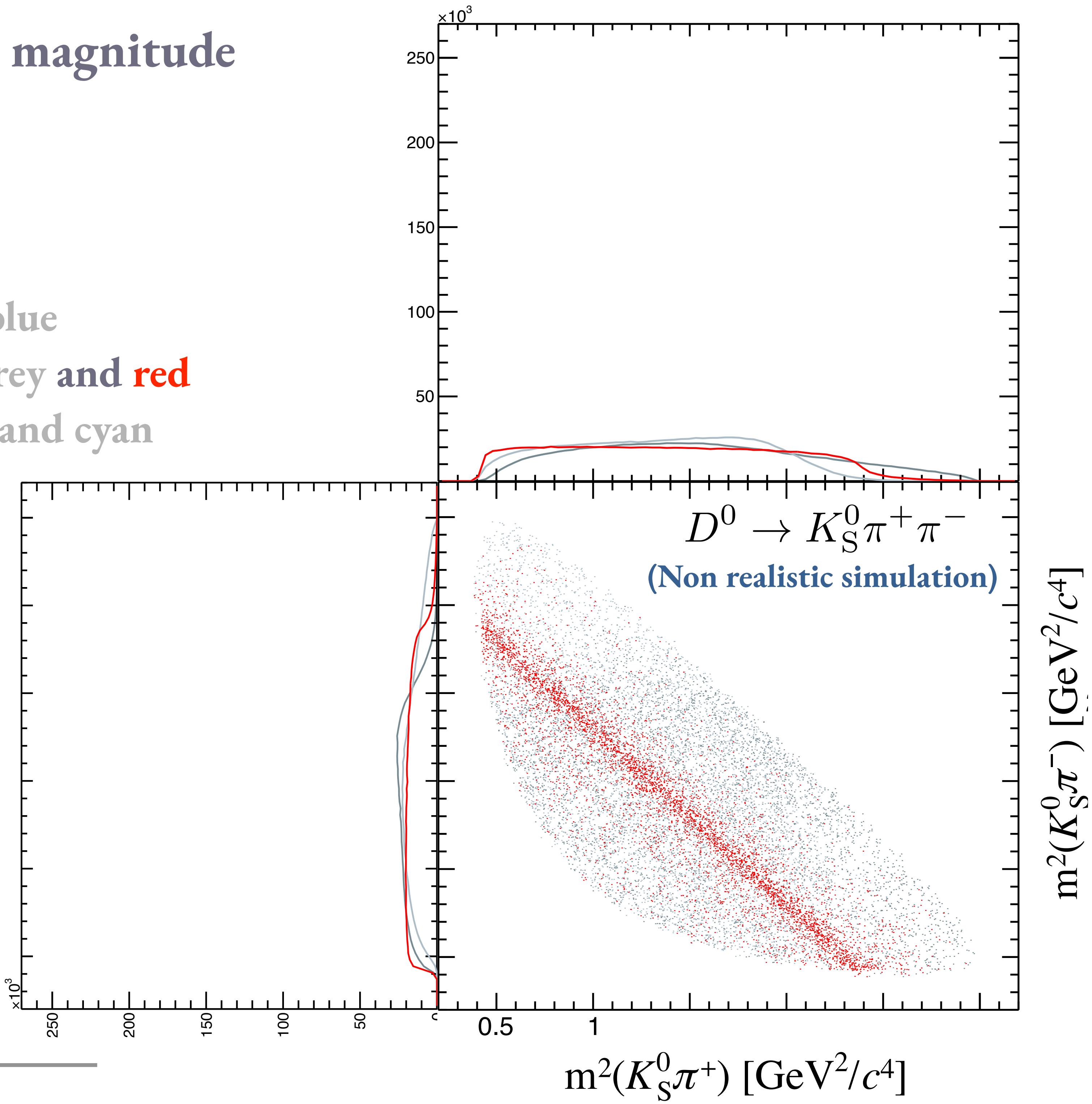

# Dalitz plot analysis features

[Laura++, Comput. Phys. Commun. 231 (2018) 198-242]

**Intensity along bands indicates magnitude and the spin resonances**

**Resonant DP illustration:**

- Nonresonant (phase space)
- $K^*(892)$ [vector]: green and blue
- $K^*_0(1430)$, $f_0(980)$ [scalar]: grey and red
- $K^*_2(1430)$ [tensor]: magenta and cyan
- $\rho(770)$ [vector]: yellow

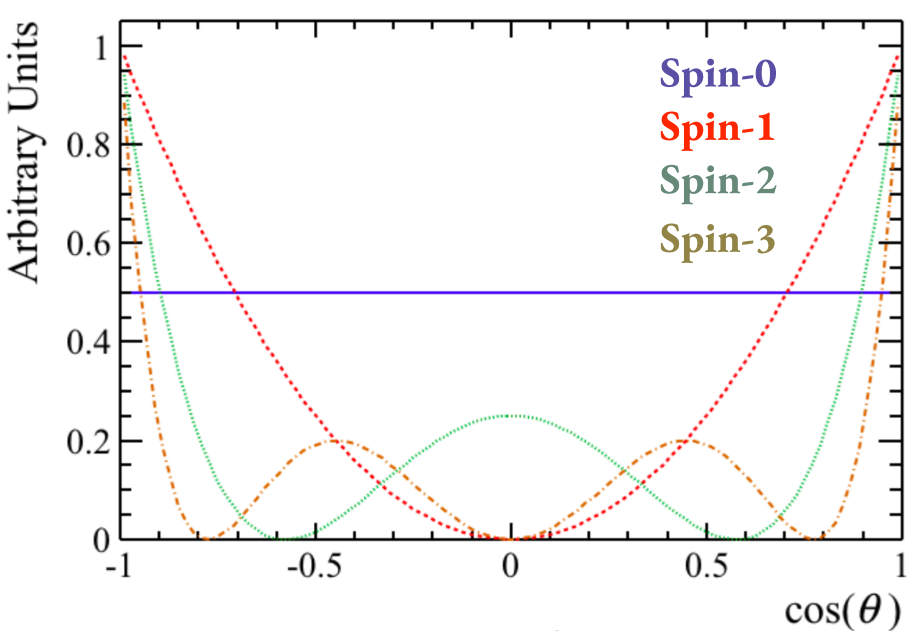


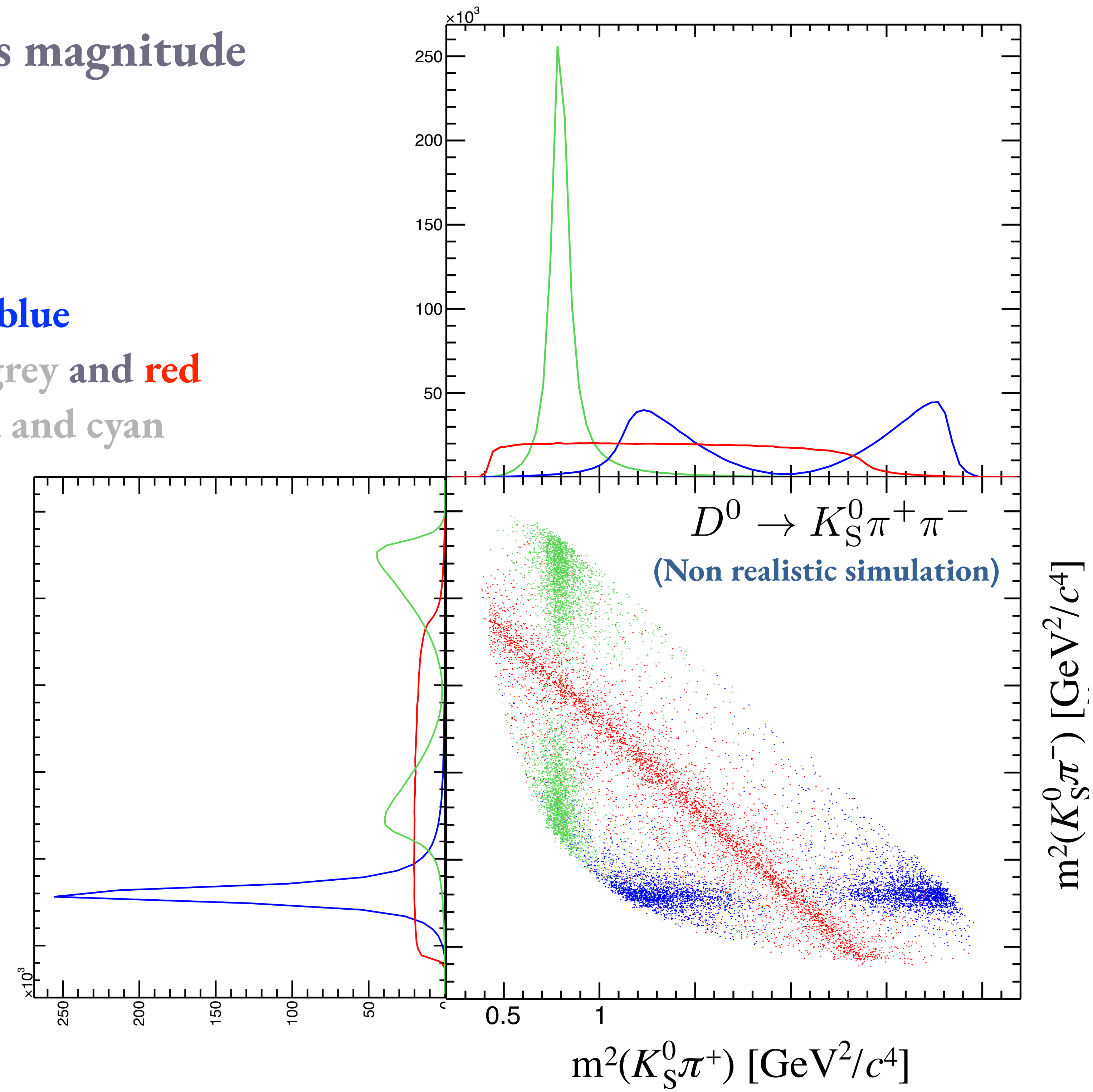

# Dalitz plot analysis features

[Laura++, Comput. Phys. Commun. 231 (2018) 198-242]

## Intensity along bands indicates magnitude and the spin resonances

### Resonant DP illustration:

- Nonresonant (phase space)
- $K^*(892)$ [vector]: green and blue
- $K^*_0(1430)$, $f_0(980)$ [scalar]: grey and red
- $K^*_2(1430)$ [tensor]: magenta and cyan
- $\rho(770)$ [vector]: yellow

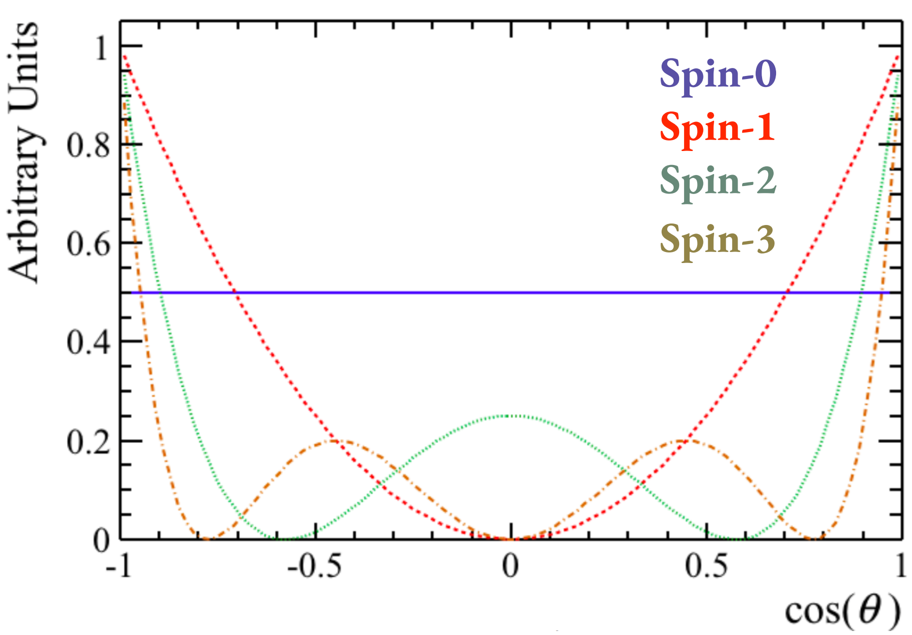


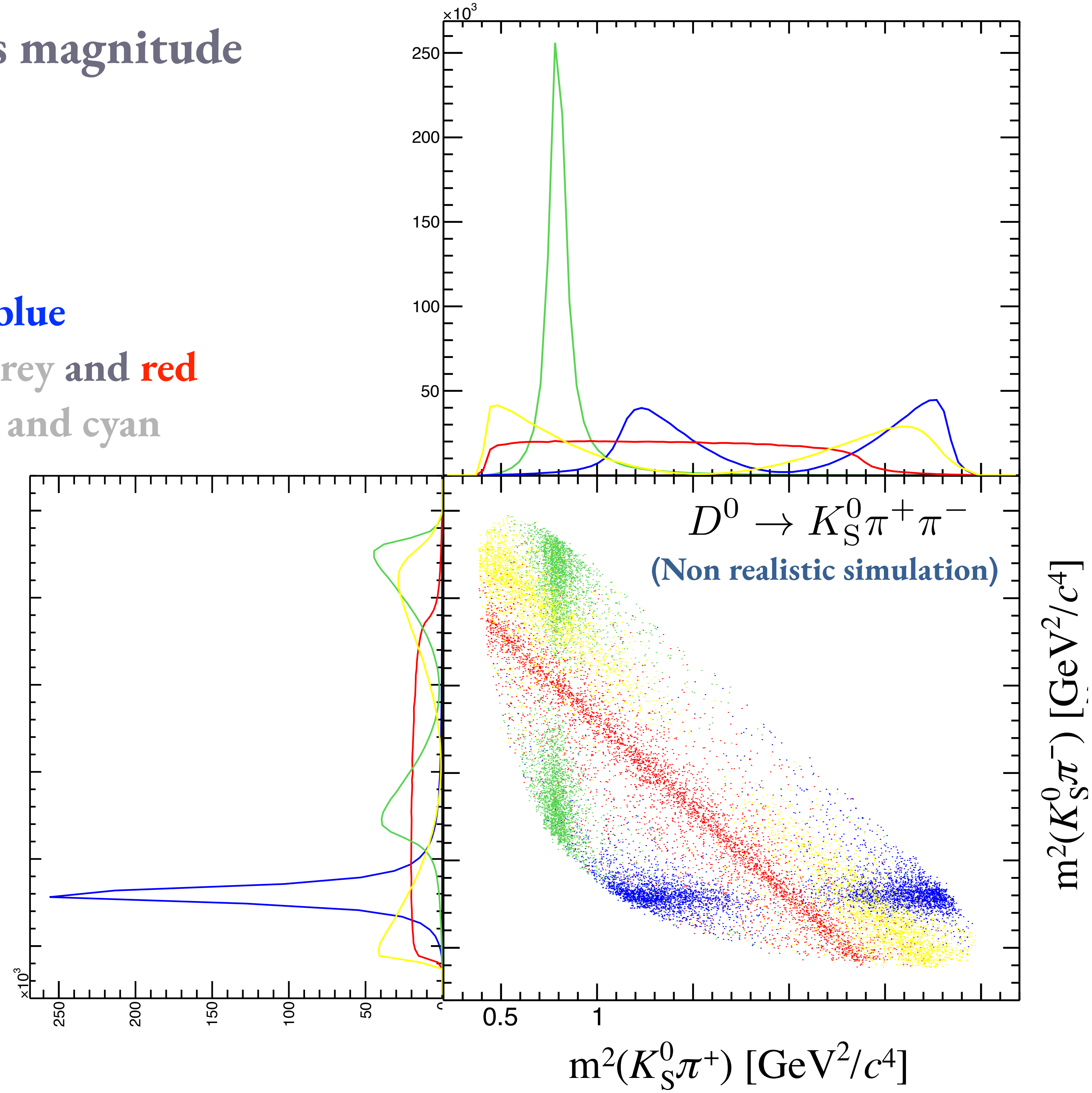

# Dalitz plot analysis features

[Laura++, Comput. Phys. Commun. 231 (2018) 198-242]

## Intensity along bands indicates magnitude and the spin resonances

### Resonant DP illustration:

- Nonresonant (phase space)
- $K^*(892)$ [vector]: green and blue
- $K^*_0(1430)$, $f_0(980)$ [scalar]: grey and red
- $K^*_2(1430)$ [tensor]: magenta and cyan
- $\rho(770)$ [vector]: yellow

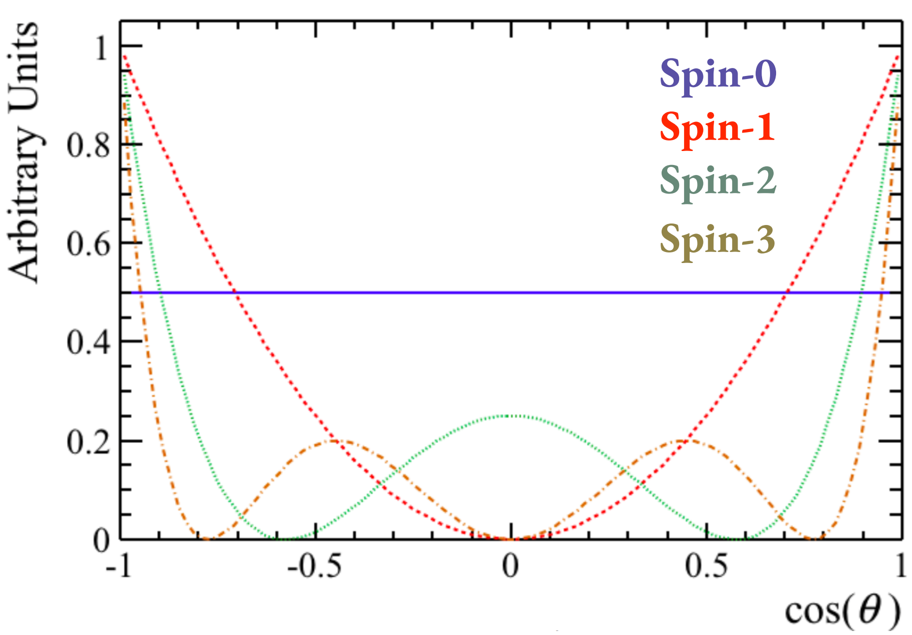


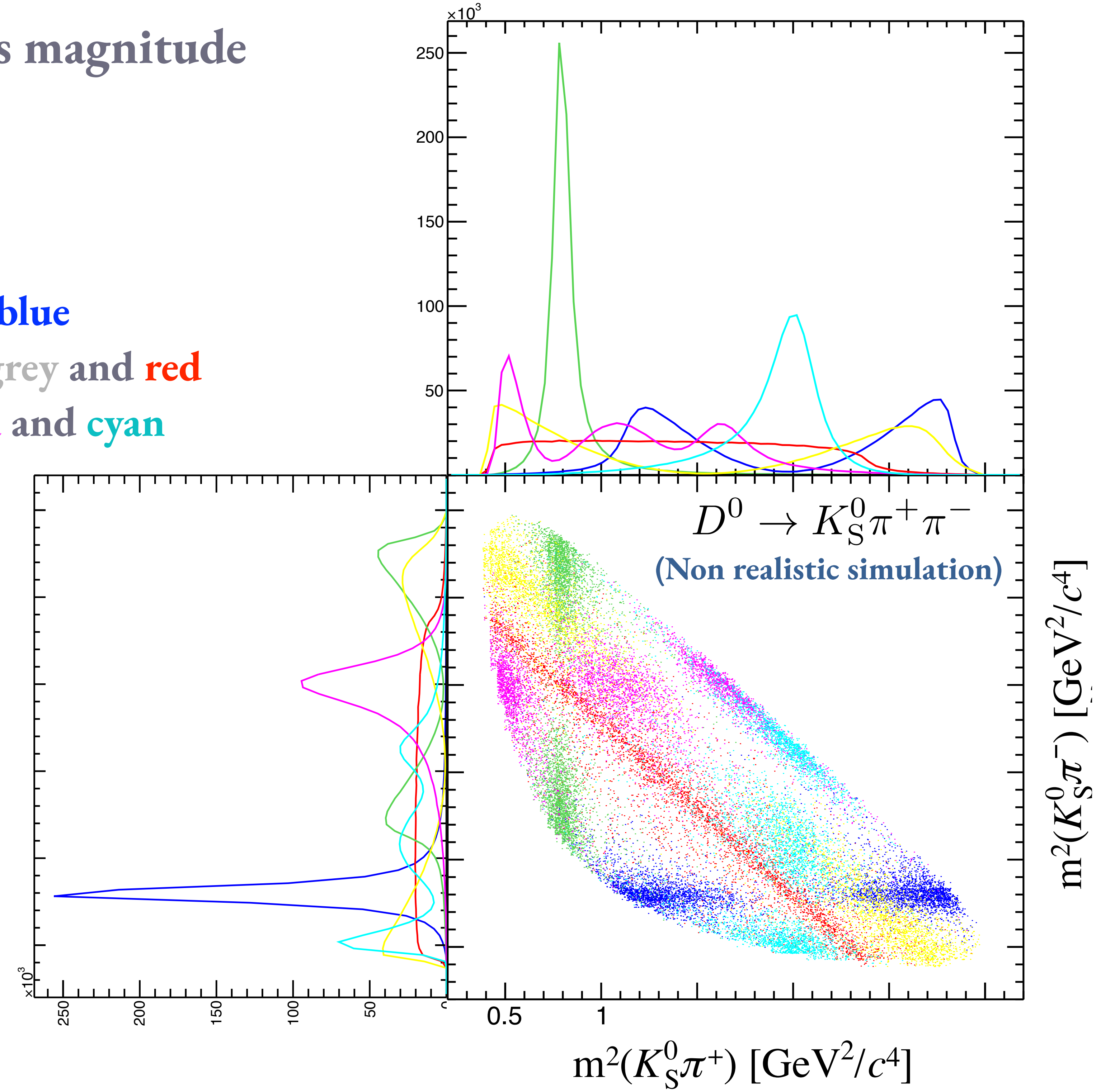

# Dalitz plot analysis features

**In reality, interference plays a significant role in these distributions and in the physics sensitivity**

[BaBar, PRL 103 (2009) 211801]

Amplitude analysis can explore several information features of multi body decays

- Relative phases between states
- Sensitivity to CP violating effects
- Resolve ambiguities in weak phases
- Hadron spectroscopy

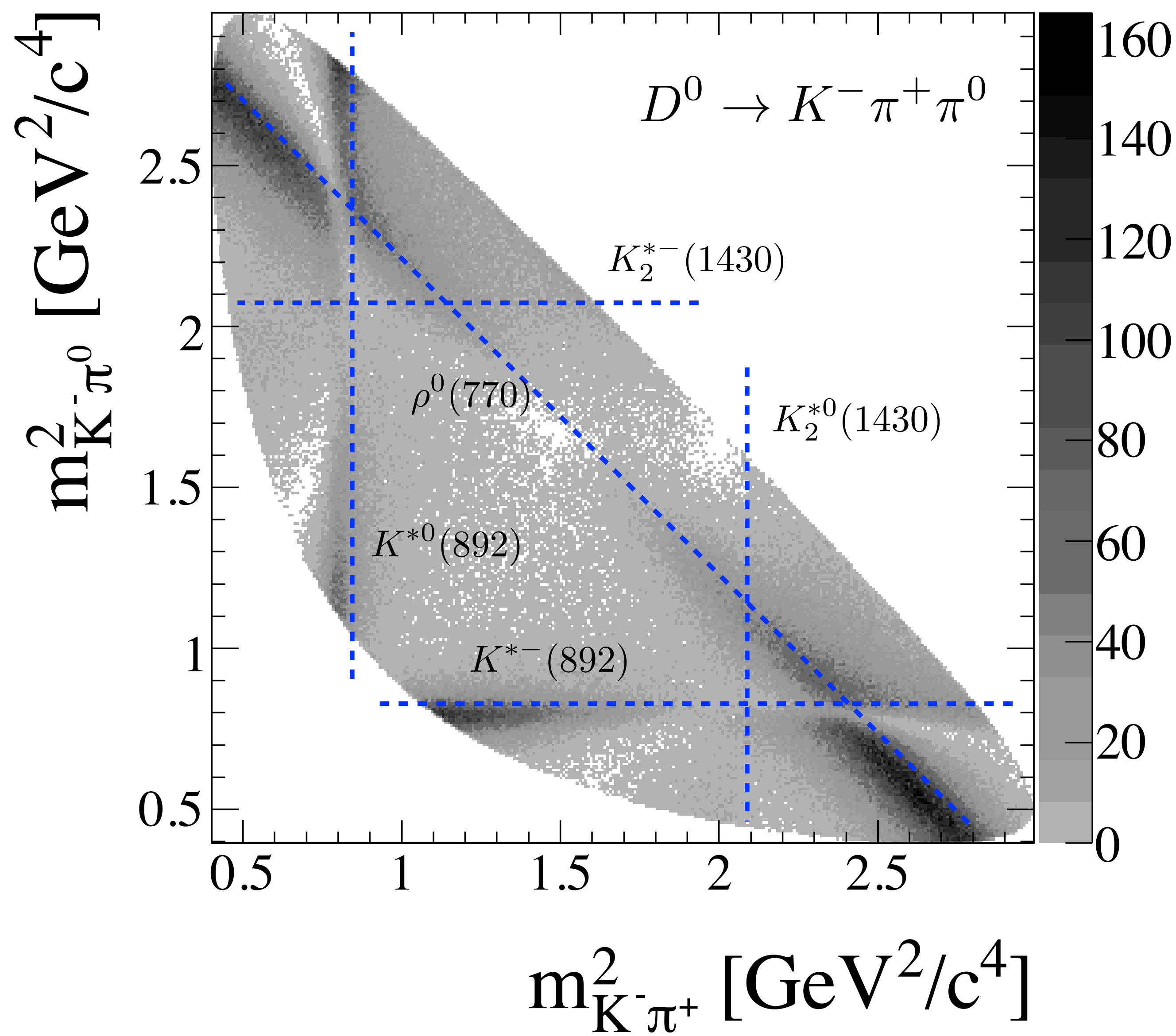

# Dalitz plot analysis features

[Laura++, Comput. Phys. Commun. 231 (2018) 198-242]

**Low-energy resonant states while dominate in D decays, in B decays are clustered around the edges**

Amplitude analysis can explore several information features of multi body decays

- Relative phases between states
- Sensitivity to CP violating effects
- Resolve ambiguities in weak phases
- Hadron spectroscopy

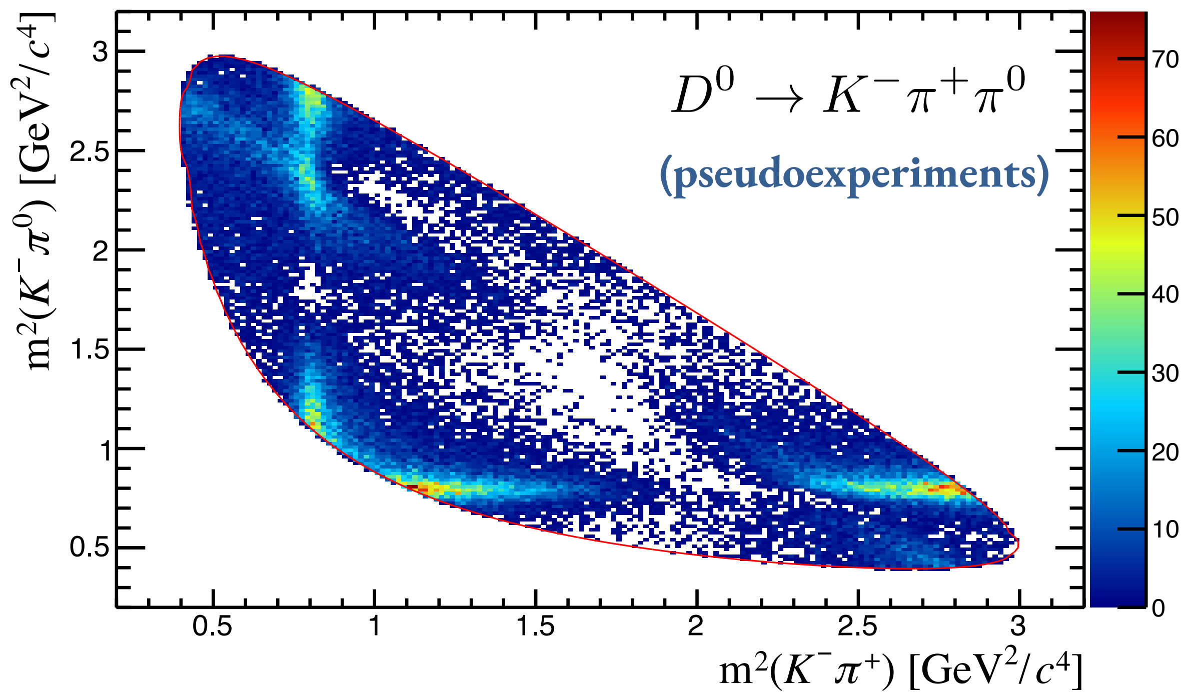


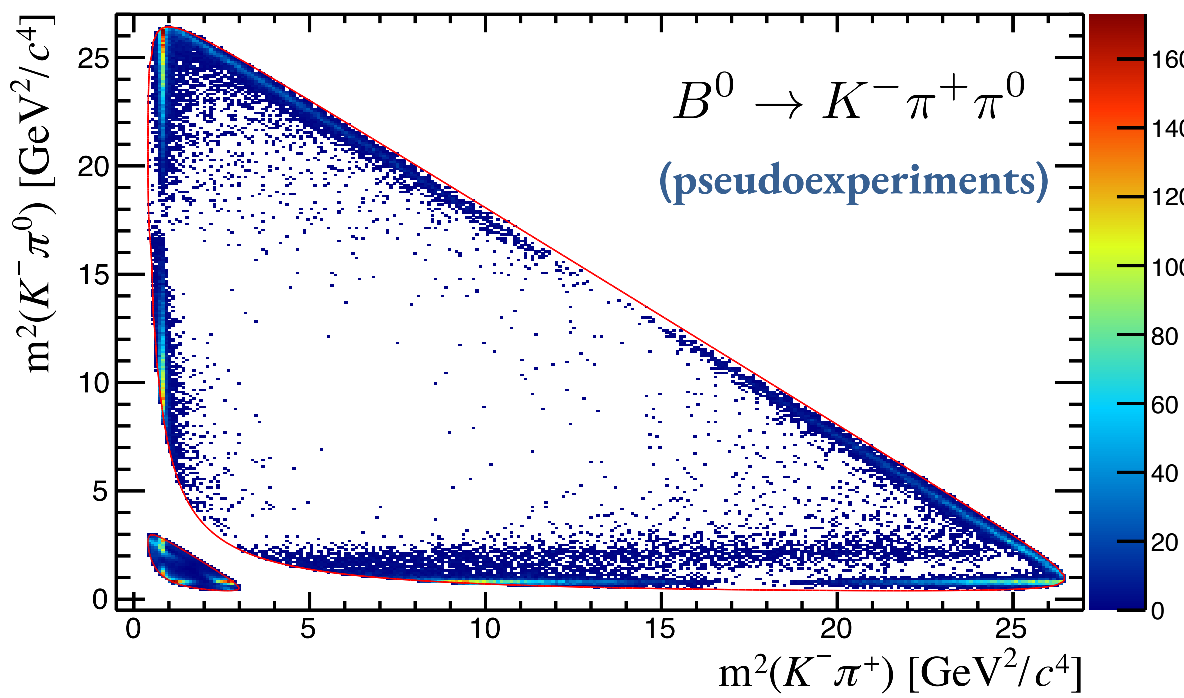

# Dalitz plot - Isobar Model approach

**Amplitude analysis most commonly performed in the "Isobar Model"**

**Total amplitude is approximated as coherent sum of quasi-two-body contributions:**

*CP* violating — Strong dynamics *CP* conserving

$$\mathcal{A}(m_{12}^2, m_{23}^2) = \sum_{j=1}^{N} \boxed{c_j} \boxed{F_j(m_{12}^2, m_{23}^2)}$$

$c_i$ : complex coefficients describing the relative magnitude and phase of the different isobars

$F_i$ : dynamical amplitudes that contain the lineshape and spin-dependence of the hadronic part

$$F_j(L, m_{12}^2, m_{23}^2) = \boxed{R_j(m_{12}^2)} \times \boxed{X_L(|\vec{p}\,|\, r)} \times \boxed{X_L(|\vec{q}\,|\, r)} \times \boxed{T_j(L, \vec{p}, \vec{q}\,)}$$

Resonance mass term (e.g. Breit–Wigner) — Barrier factors - *p*, *q*: momenta of bachelor and resonance — Angular probability distribution

More sophisticated approaches can be pursued, *e.g.* **partial wave analysis**

# The LHCb experiment

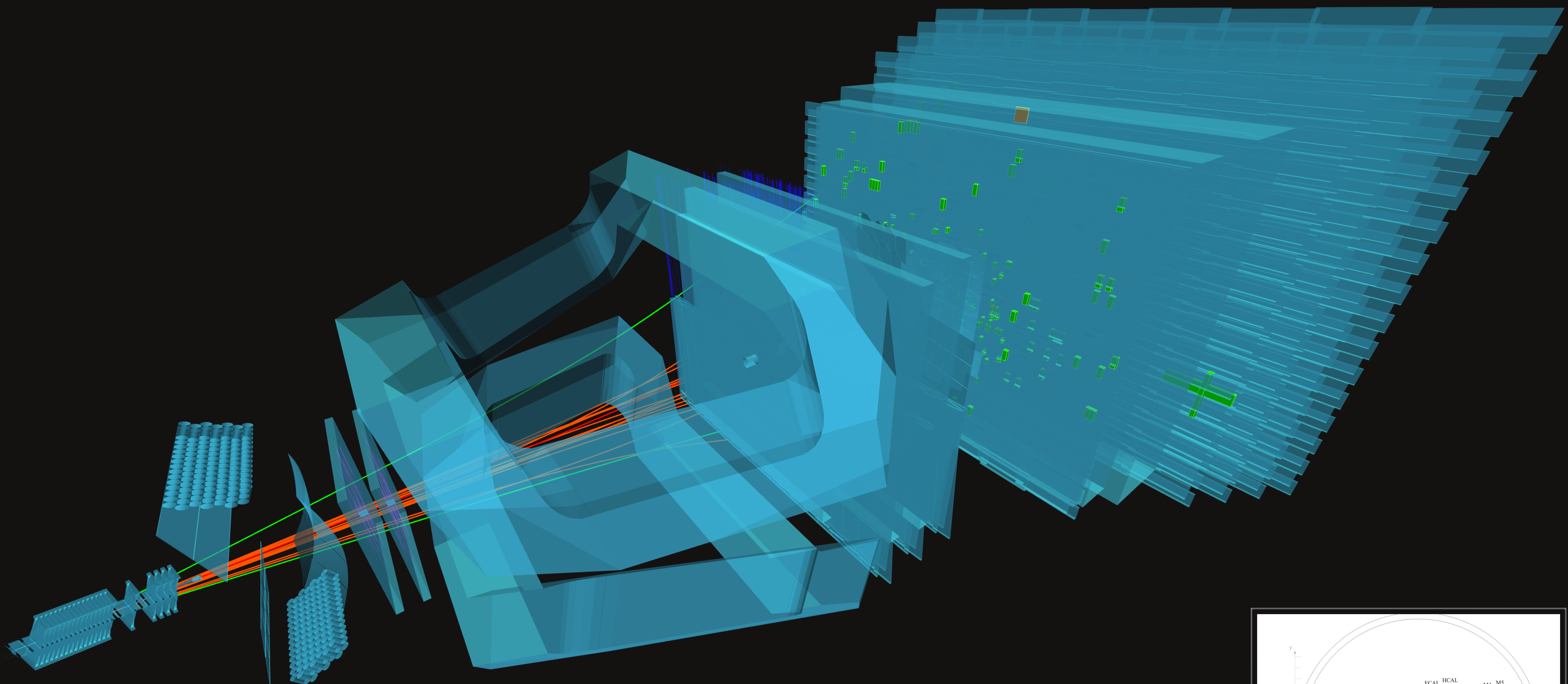

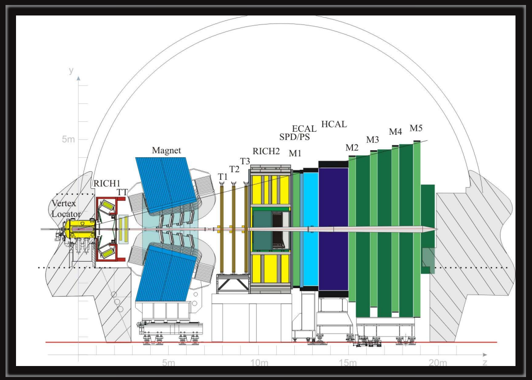


[Int. J. Mod. Phys. A30, (2015) 1530022]

# The LHCb experiment

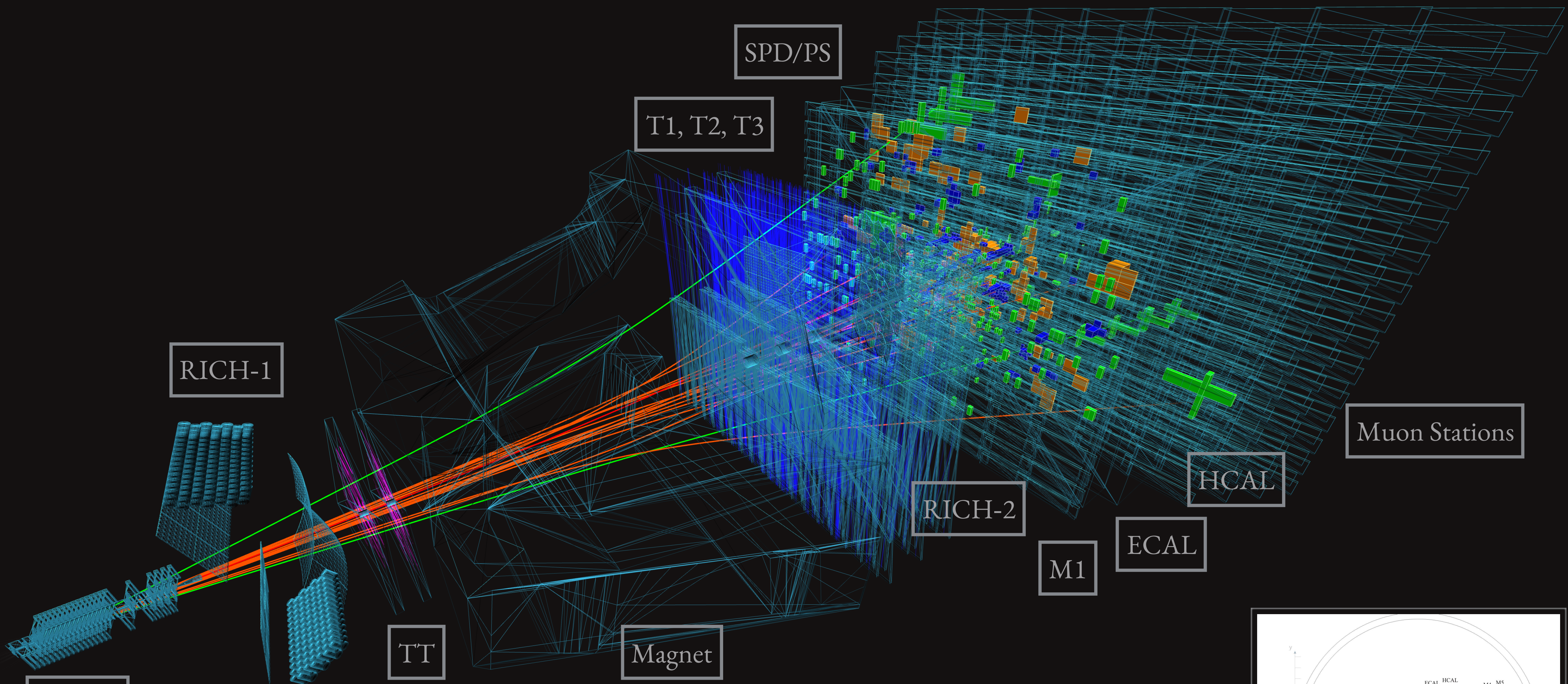


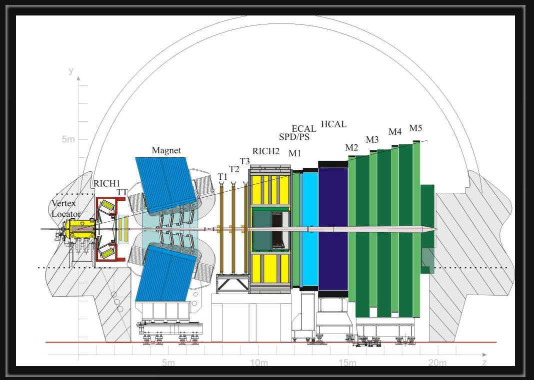

- Primary vertex, IP [≈ 200$\mu$m] and $\tau$ resolution [≈ 45 fs]
- Momentum resolution [≈ 0.5 %]
- Particle ID/misID, [e.g. $\epsilon$(K) ≈ 95%]

[Int. J. Mod. Phys. A30, (2015) 1530022]

# The LHCb experiment

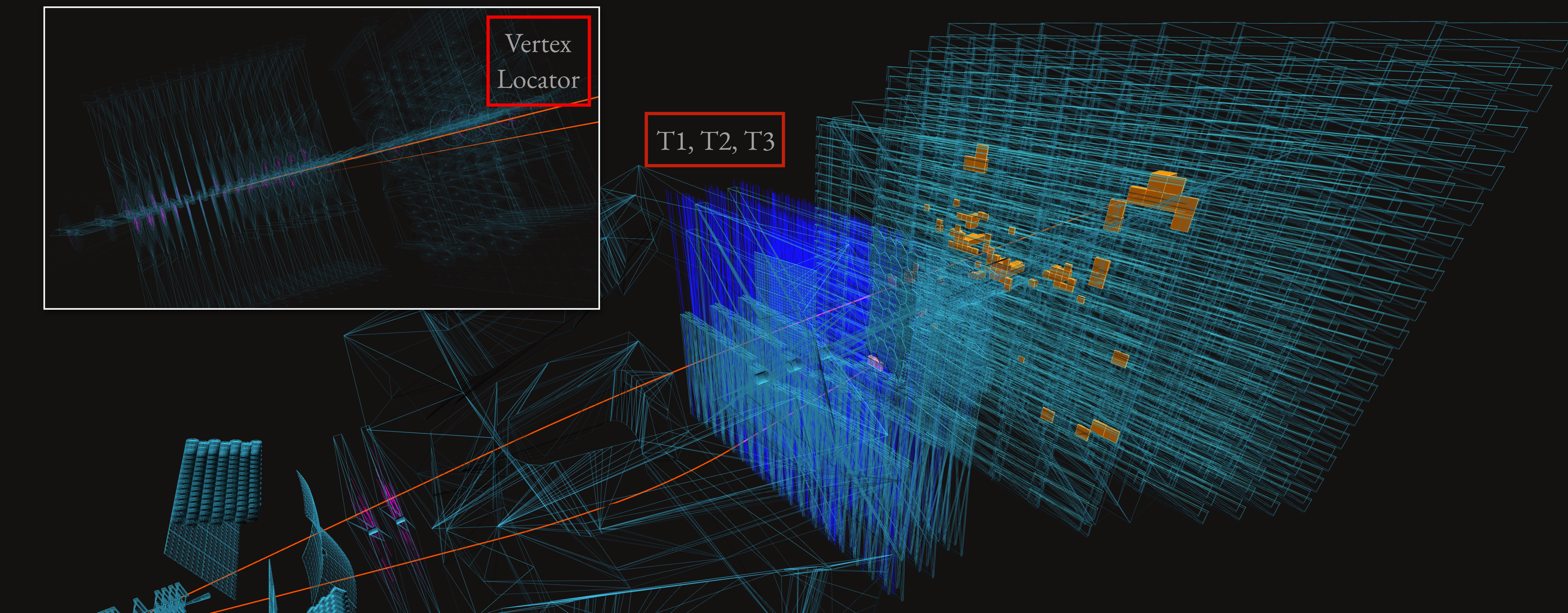


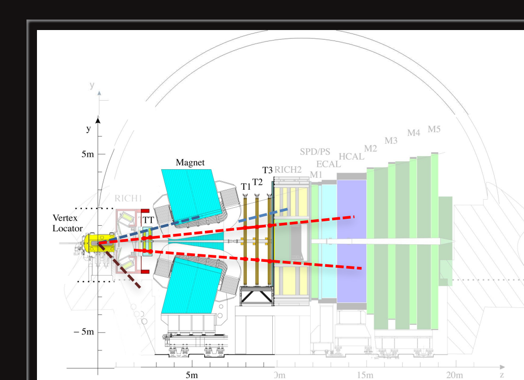


- Charged particles trajectories are classified according to the hits in the several modules of the detector

[Int. J. Mod. Phys. A30, (2015) 1530022]

# The LHCb experiment

| Year | 2011 | 2012 | 2015 | 2016 | 2017 | 2018 |
|---|---|---|---|---|---|---|
| $\int \mathcal{L}\,(\mathrm{fb}^{-1})$ | 1.0 | 2.0 | 0.3 | 1.7 | 1.7 | 2.2 |

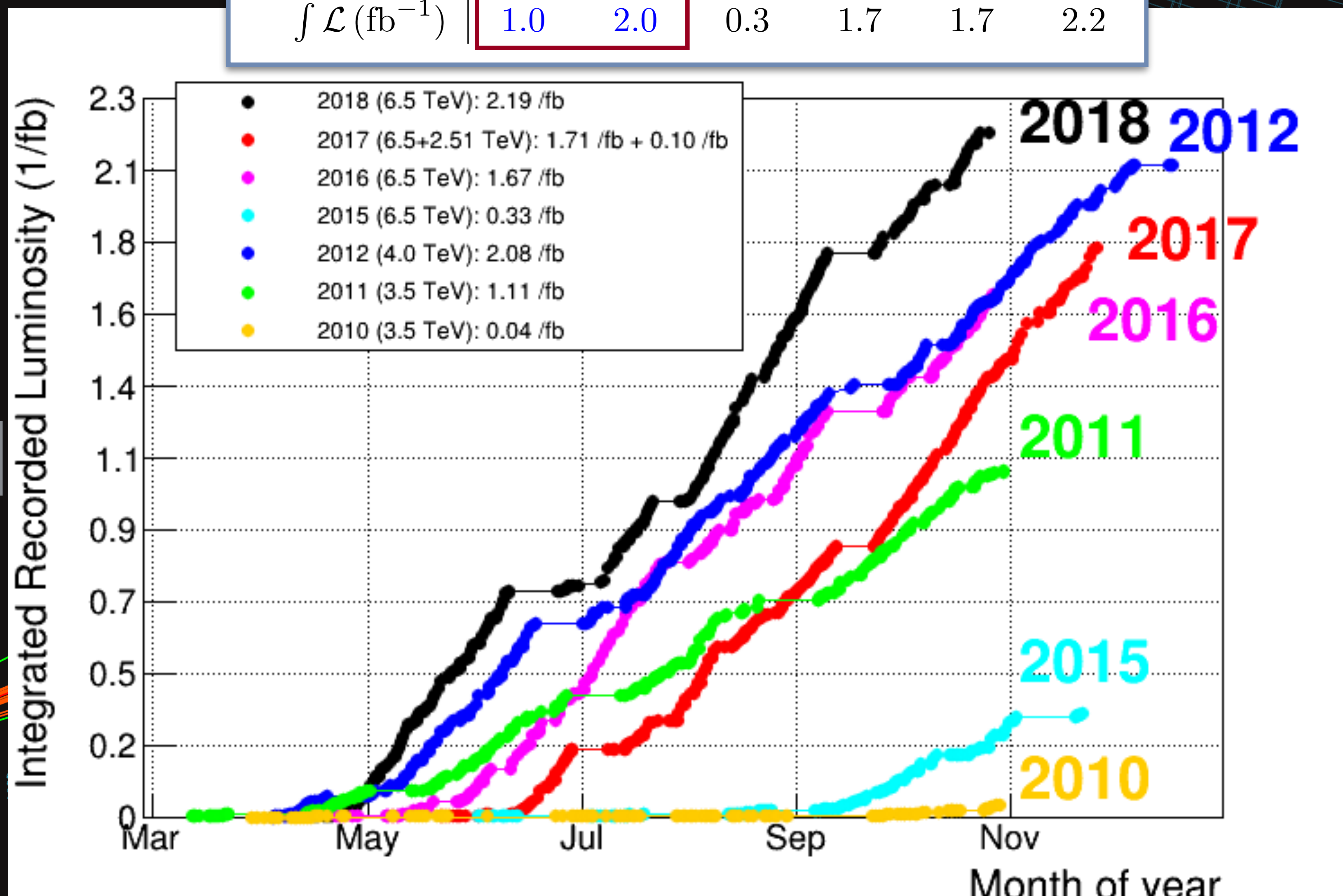


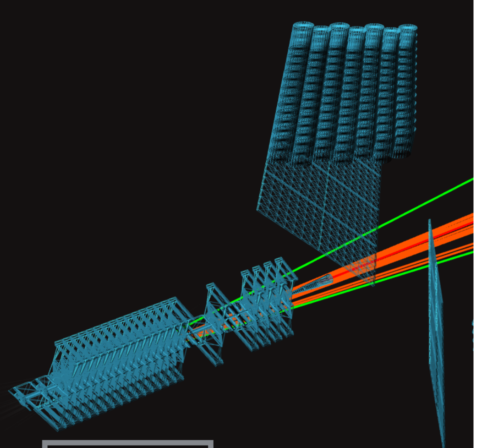


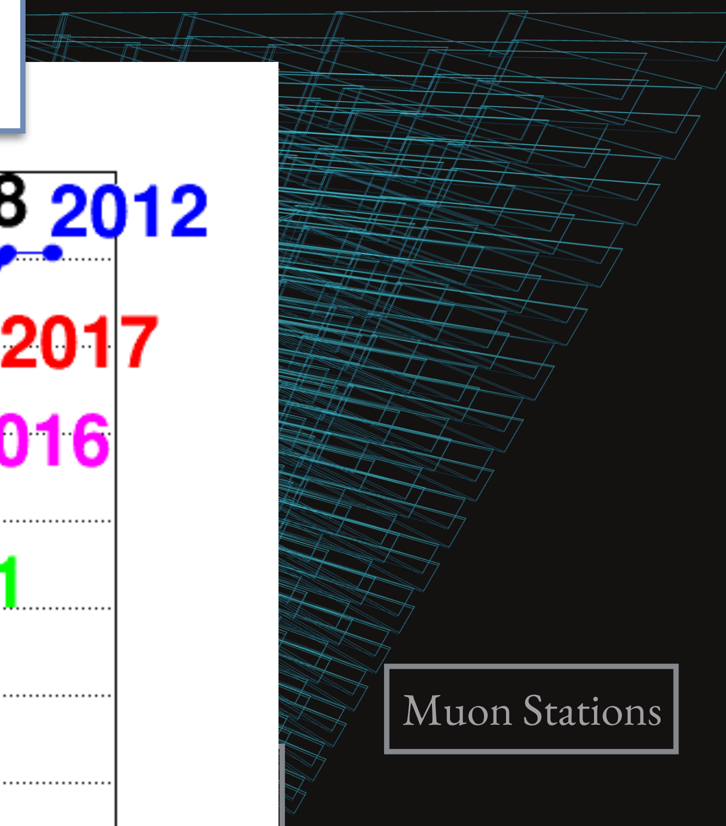


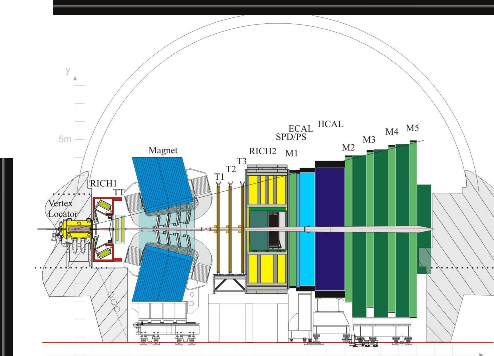

Thanks a lot to the LHC team!

[Int. J. Mod. Phys. A30, (2015) 1530022]

Universität Zürich[UZH]

# First Dalitz plot analysis of $B^0_s \to \overset{(\overline{\phantom{K}})}{K}{}^0 K^\pm \pi^\mp$ decays

LHCb results : $\mathcal{L} = 3\,\mathrm{fb}^{-1}$ – 2011 + 2012 dataset

**Isobar approach - the "artisan" approach**

[LHCb-PAPER-2018-045]

Leif Nilsson
[Gate to the Studio - noon]

# The $B^0_s \to \overset{(-)}{K^0} K^\pm \pi^\mp$ decay

**Search for ~~CP~~ in charmless 3-body decays of neutral B mesons to final states containing a K⁰ meson**

- CKM angle γ using $B^0_s \to K^*K$ and flavour symmetries
- U-spin multiplet $B^0_s \to K^{*0}\bar{K}^0(\bar{K}^{*0}K^0)$ to $B^0 \to K^*K$

Study of $B^0_{(s)} \to K^0_S h^+ h'^-$ decays with first observation of $B^0_s \to K^0_S K^\pm \pi^\mp$ and $B^0_s \to K^0_S \pi^+\pi^-$
[LHCb, JHEP 10 (2013) 143]

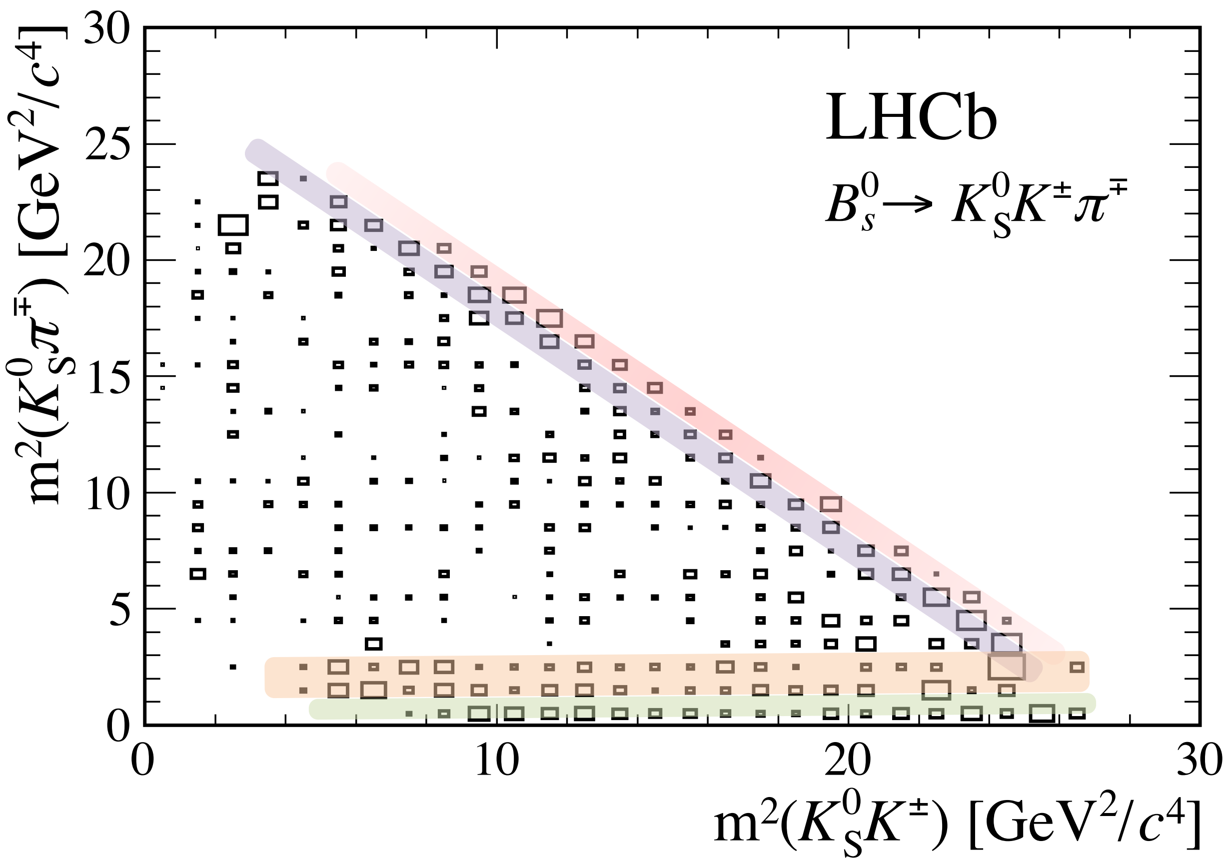


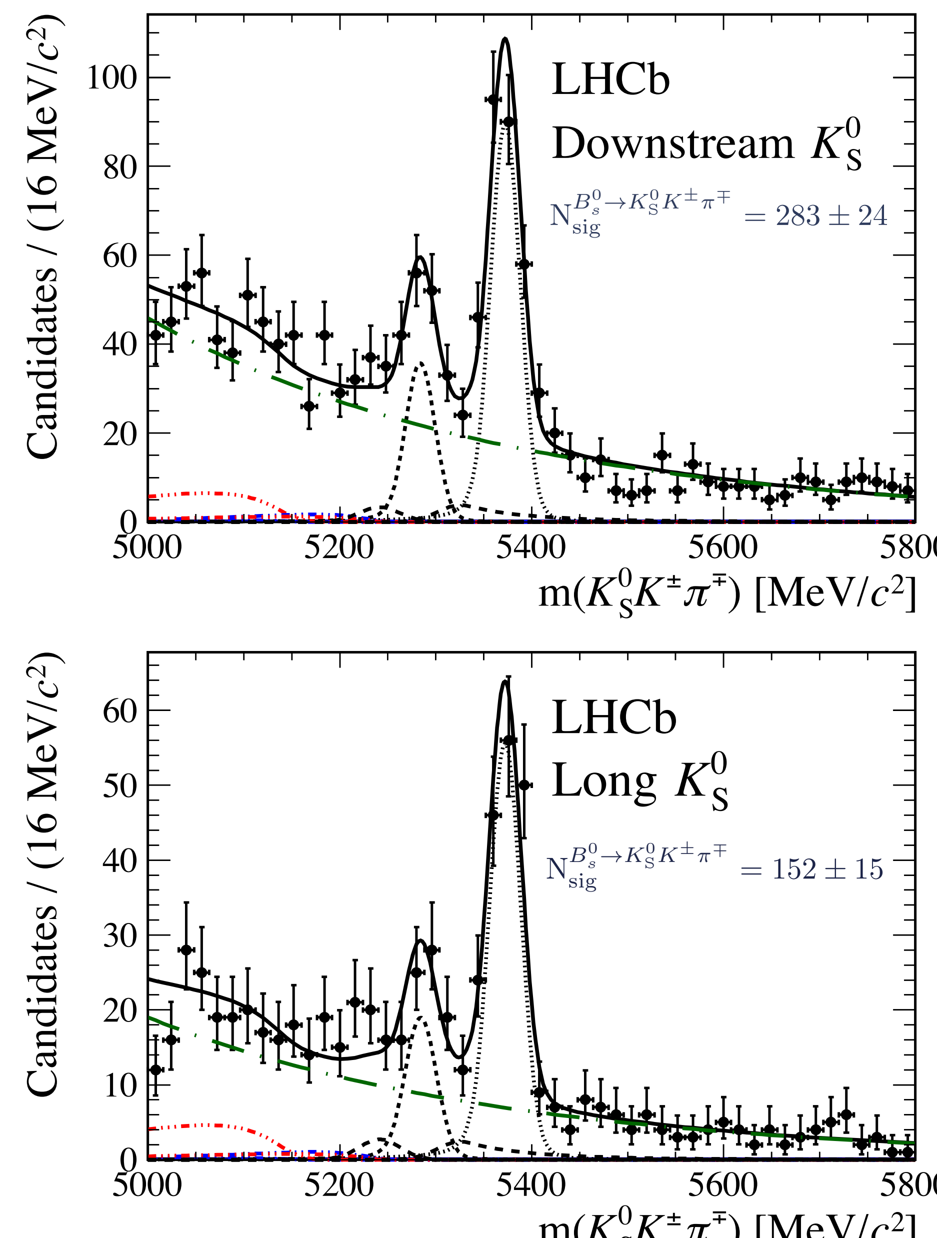

# The $B^0_s \to \overset{(-)}{K^0} K^{\pm}\pi^{\mp}$ decay

**Search for ~~CP~~ in charmless 3-body decays of neutral B mesons to final states containing a $K^0$ meson**

- CKM angle γ using $B^0_s \to K^*K$ and flavour symmetries
- U-spin multiplet $B^0_s \to K^{*0}\bar{K}^0(\bar{K}^{*0}K^0)$ to $B^0 \to K^*K$

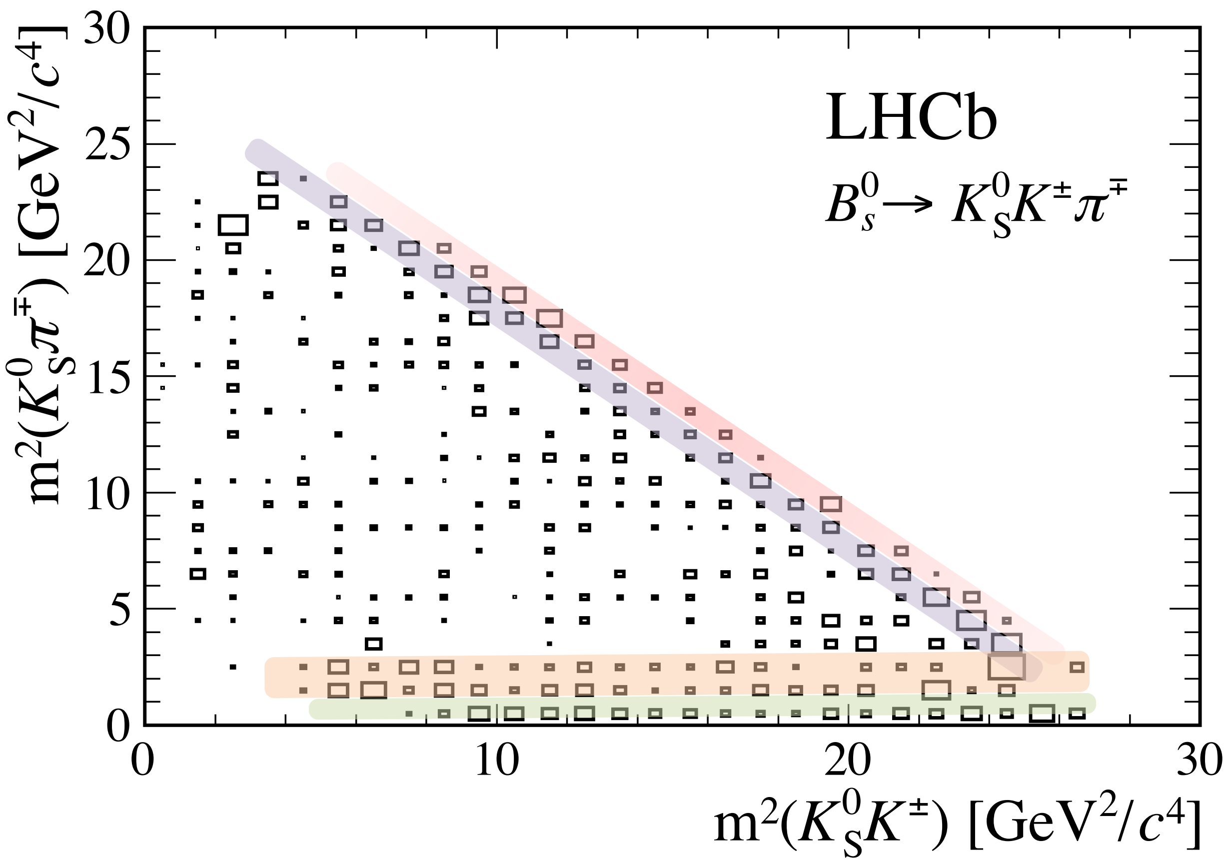


[LHCb, New J. Phys. 16 (2014) 12, 123001]

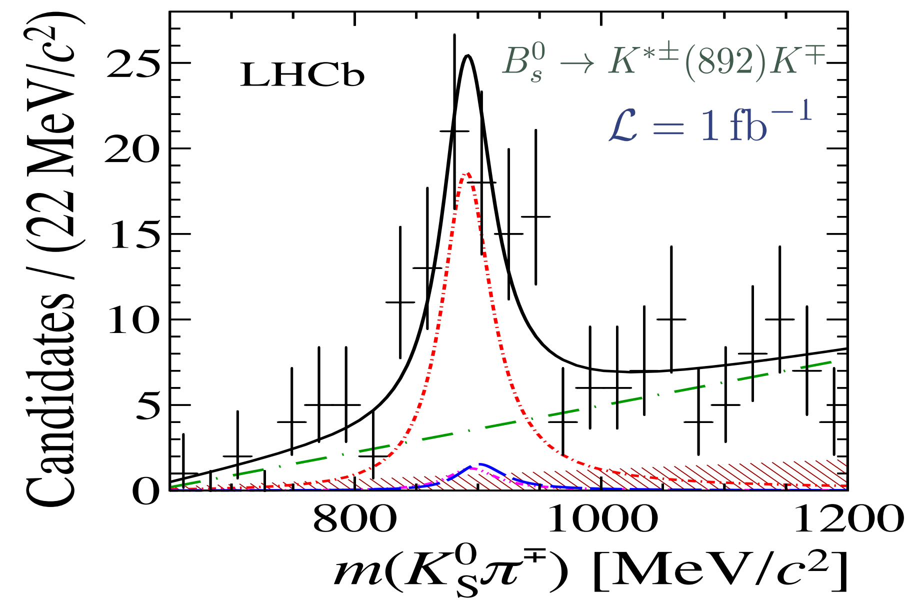


[LHCb, JHEP 1601 (2016) 012]

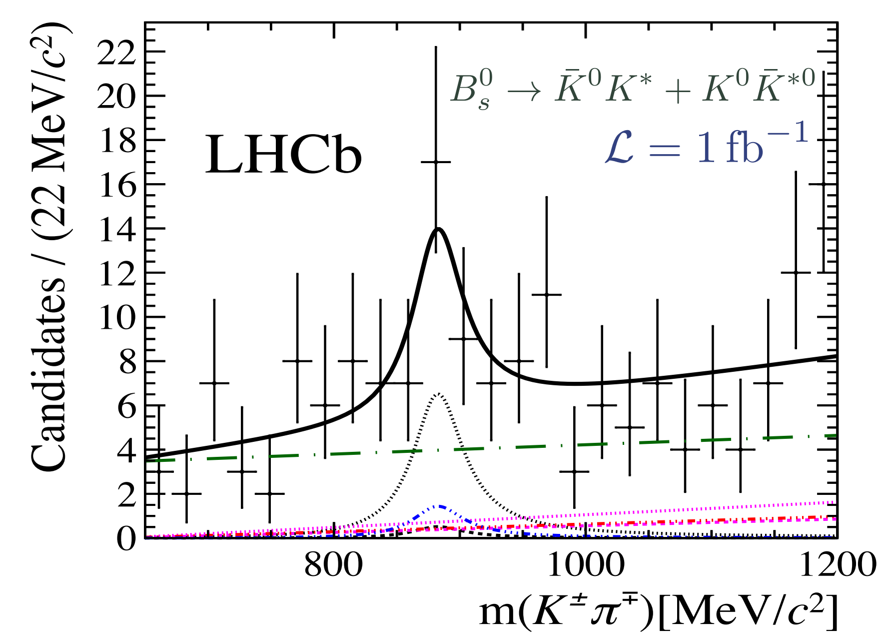

# The $B^0_s \to \overset{(-)}{K}{}^0 K^{\pm}\pi^{\mp}$ decay

Universität Zürich[UZH]

## Channel can be seen as a four different Dalitz plots

$[\mathcal{A}_f]$ $B^0_s \to K^0_S K^+\pi^-$ $\qquad$ $[\bar{\mathcal{A}}_f]$ $\bar{B}^0_s \to K^0_S K^+\pi^-$

CP $\qquad$ Mixing $\qquad$ CP

$\bar{B}^0_s \to K^0_S K^-\pi^+$ $[\bar{\mathcal{A}}_{\bar{f}}]$ $\qquad$ $B^0_s \to K^0_S K^-\pi^+$ $[\mathcal{A}_{\bar{f}}]$

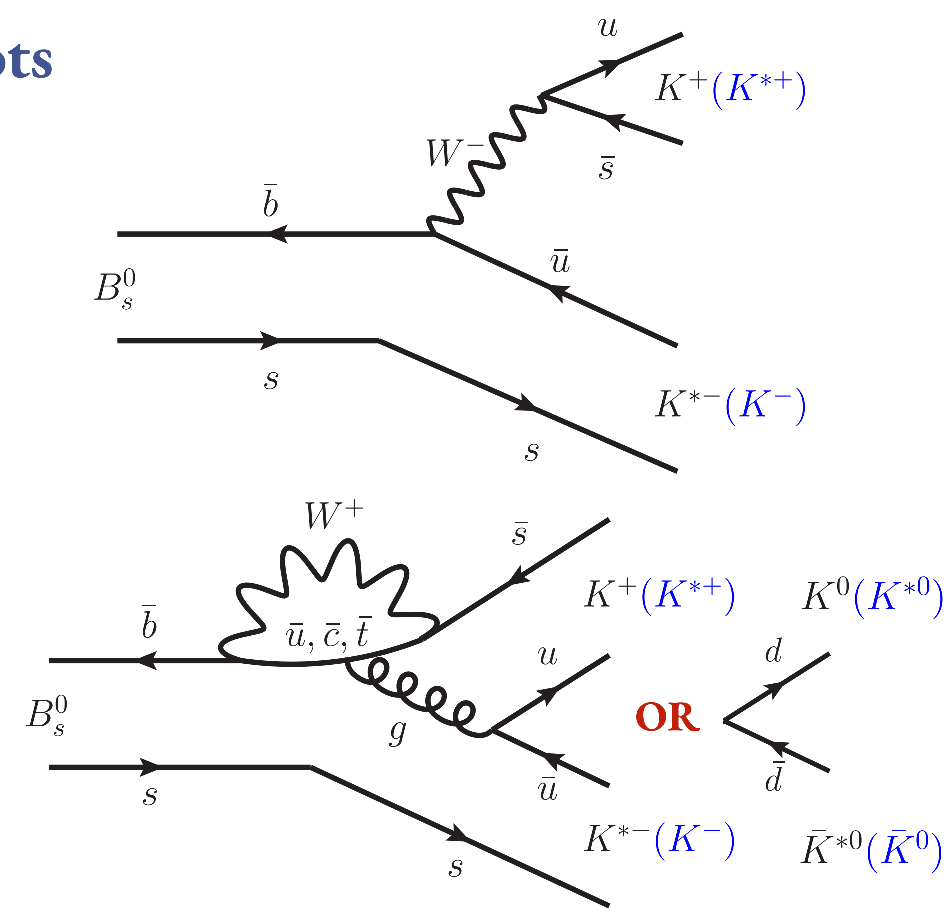


[Theory predictions]

| $\bar{B}^0_s \to \bar{K}^0 K^+\pi^-$ | Reference PRD 89 (074025) | Reference arXiv:1401.5948 | $\bar{B}^0_s \to \bar{K}^0 K^-\pi^+$ | Reference PRD 89 (074025) | Reference arXiv:1401.5948 |
|---|---|---|---|---|---|
| $K^{*0}\bar{K}^0$ | $1.5^{+2.4}_{-0.9}$ | $0.7^{+1.7}_{-0.5}$ | $\bar{K}^{*0}K^0$ | $3.8^{+0.8}_{-0.7}$ | $2.3^{+0.6}_{-0.5}$ |
| $K^{*-}K^+$ | $3.5^{+0.7}_{-0.7}$ | $2.3^{+0.6}_{-0.5}$ | $K^{*+}K^-$ | $2.6^{+2.7}_{-1.1}$ | $1.3^{+2.0}_{-0.9}$ |
| $K_0^{*0}(1430)\bar{K}^0$ | $0.6^{+0.9}_{-0.4}$ | $0.5^{+1.2}_{-0.4}$ | $\bar{K}_0^0(1430)K^0$ | $14.5^{+3.3}_{-2.9}$ | $16.6^{+5.1}_{-4.3}$ |
| $K_0^{*-}(1430)K^+$ | $14.5^{+3.2}_{-2.9}$ | $15.5^{+4.5}_{-3.9}$ | $K_0^{*+}(1430)K^-$ | $1.0^{+1.0}_{-0.4}$ | $0.9^{+1.4}_{-0.5}$ |
| Non resonant | $23.8^{+9.9}_{-6.7}$ | $12.3^{+12.6}_{-6.3}$ | Non Resonant | $24.2^{+0.9}_{-5.1}$ | $12.9^{+13.2}_{-6.6}$ |
| Total | $35.3^{+15.7}_{-9.8}$ | $33.7^{+20.9}_{-12.0}$ | Total | $36.7^{+14.9}_{-9.0}$ | $34.2^{+21.1}_{-12.0}$ |

# The $B^0_s \to \overset{(-)}{K}{}^0 K^\pm \pi^\mp$ analysis

**Flavour-tagging is unattractive with current statistics → even in the absence of ~~CP~~, two amplitudes remain (i.e. $A_f$ and $\bar{A}_f$) in an untagged decay-time integrated method**

$$\Gamma_{\bar{B}^0_s \to f}(t) + \Gamma_{B^0_s \to f}(t) \propto \frac{e^{-t/\tau(B^0_s)}}{\tau(B^0_s)} \left[ \left(|\mathcal{A}_f|^2 + |\bar{\mathcal{A}}_f|^2\right) \cosh \frac{\Delta\Gamma_s t}{2} - 2\,\Re\left(\frac{q}{p}\mathcal{A}^*_f \bar{\mathcal{A}}_f\right) \sinh \frac{\Delta\Gamma_s t}{2} \right]$$

In an untagged analysis it is, in general, impossible to disentangle the two components, except:

- **[$B^0 \to K^+\pi^-\pi^0$]** - Final state assumed to be flavour-specific, so that one of the two possible contributions vanishes

  [BaBar, PRD 83 (2011) 112010]

- **[$B^0_{(s)} \to K^0_S\pi^+\pi^-$]** - In time-integrated DP, resonances are either flavour specific (*e.g.* $K^{*+}\pi^-$) or CP-conjugate (*e.g.* $K^0_S\rho^0$)

  [LHCb, PRL 120, 261801 (2018)]

**ToyMC Laura++**

[Com. Phys. Com. 231 (2018) 198-242]

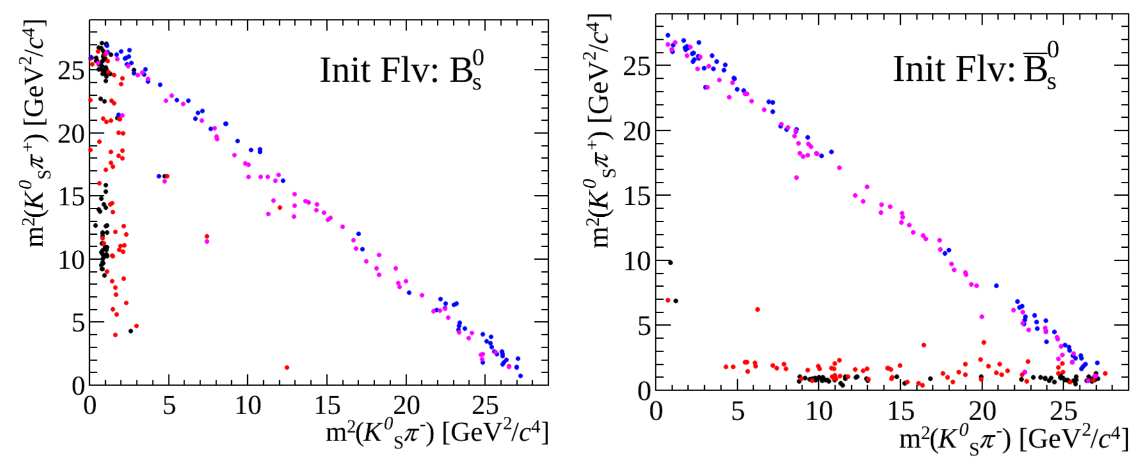


Conclusion: cannot perform an untagged Dalitz-plot analysis of a non-self-conjugate, non-flavour-specific final state without some assumption on $A_f$ and $\bar{A}_f$.

# $B^0_s \to \overset{(-)}{K^0} K^\pm \pi^\mp$ Dalitz-plot strategy

[LHCb-PAPER-2018-045]

## An effective DP model assumed [validated in simulation]

$$\mathcal{P}_f^{\rm sig}(s,t) = \frac{|\mathcal{A}_f(s,t)|^2}{\int\int_{DP}\ |\mathcal{A}_f(s,t)|^2\ ds\,dt}$$

$$\widehat{FF}_j = \frac{\int\int_{DP} |c_j F_j(s,t)|^2\, dsdt + \int\int_{DP'} \left|\bar{c}_j \bar{F}_j(s',t')\right|^2\, ds'dt'}{\int\int_{DP} \left|\sum_k c_k F_k(s,t)\right|^2\, dsdt + \int\int_{DP'} \left|\sum_k \bar{c}_k \bar{F}_k(s',t')\right|^2\, ds'dt'}$$

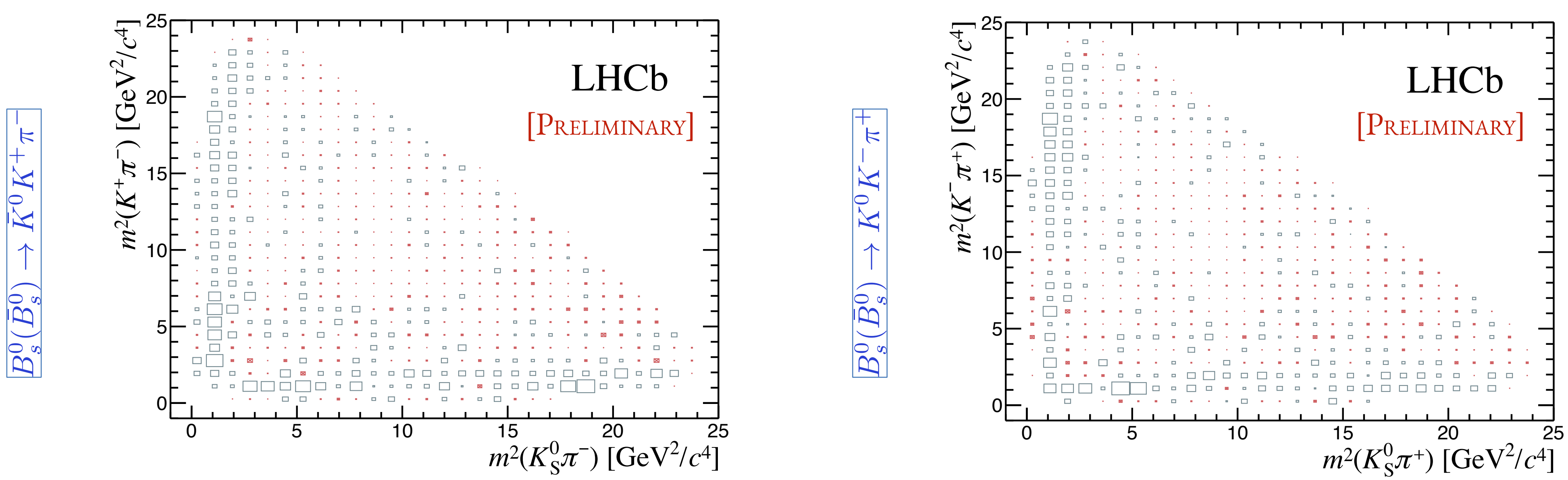


**Although the presence of ~~CP~~ can be investigated, the complex coefficients obtained are not of trivial interpretation: only fit fractions are unbiased**

# Selecting the signal

[LHCb-PAPER-2018-045]

Strategy designed to enhance the DP signal yield and the amplitude fit (Dalitz plot) sensitivity, *i.e.* isobar parameters

- Boosted Decision Tree and particle identification to reject comb/misID backgrounds
- Mass vetoes for unwanted contributions
- Analysis performed with ~900 signal events and purity of 84%

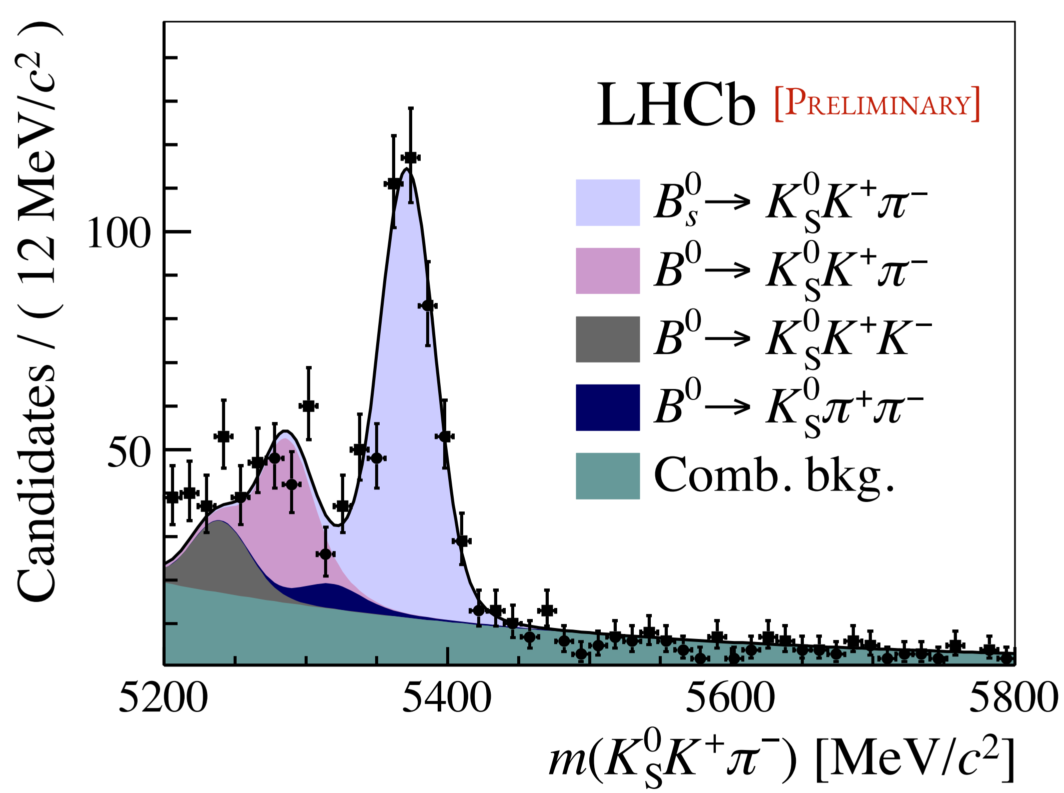


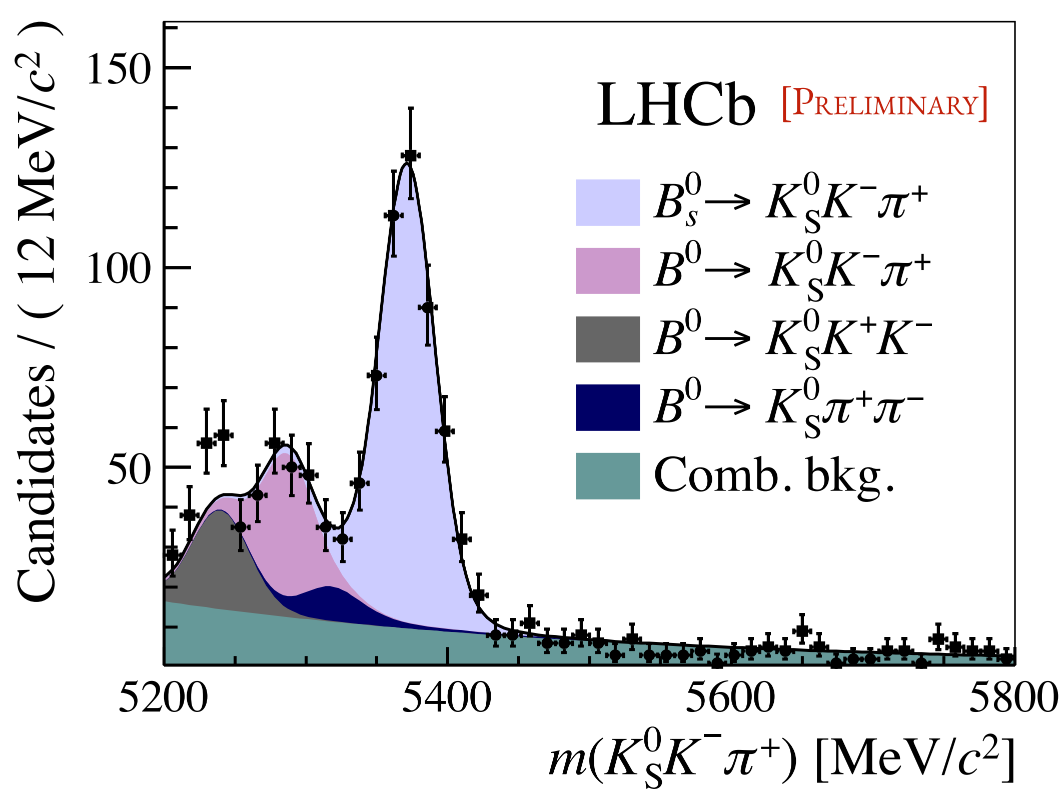

# Dalitz-plot fitting

[LHCb-PAPER-2018-045]

Simultaneous unbinned DP fit based on the JFit method within the Laura$^{++}$ framework is performed for each event $i$ and signal/background $k$ component as

[arXiv:1409.5080, Comput. Phys. Commun. 231 (2018) 198-242]

$$\mathcal{L} = \prod_i^{N_c} \left[ \sum_k N_k \mathcal{P}_k \left( m_i^2(K^\pm\pi^\mp), m_i^2(K_S^0\pi^\mp) \right) \right]$$

| Resonance | Spin | Model | Mass (MeV) | Width (MeV) |
|---|---|---|---|---|
| $\overset{(-)}{K}{}^*(892)^0$ | 1 | Rel BW | $895.81 \pm 0.19$ | $47.4 \pm 0.6$ |
| $K^*(892)^\pm$ | 1 | Rel BW | $891.66 \pm 0.26$ | $50.8 \pm 0.9$ |
| $\overset{(-)}{K}{}_0^*(1430)^0$ | 0 | LASS | $1425 \pm 50$ | $270 \pm 80$ |
| $K_0^*(1430)^\pm$ | 0 | LASS | $1425 \pm 50$ | $270 \pm 80$ |
| $\overset{(-)}{K}{}_2^*(1430)^0$ | 2 | Rel BW | $1432.4 \pm 1.3$ | $109 \pm 5$ |
| $K_2^*(1430)^\pm$ | 2 | Rel BW | $1425.6 \pm 1.5$ | $98.5 \pm 2.7$ |

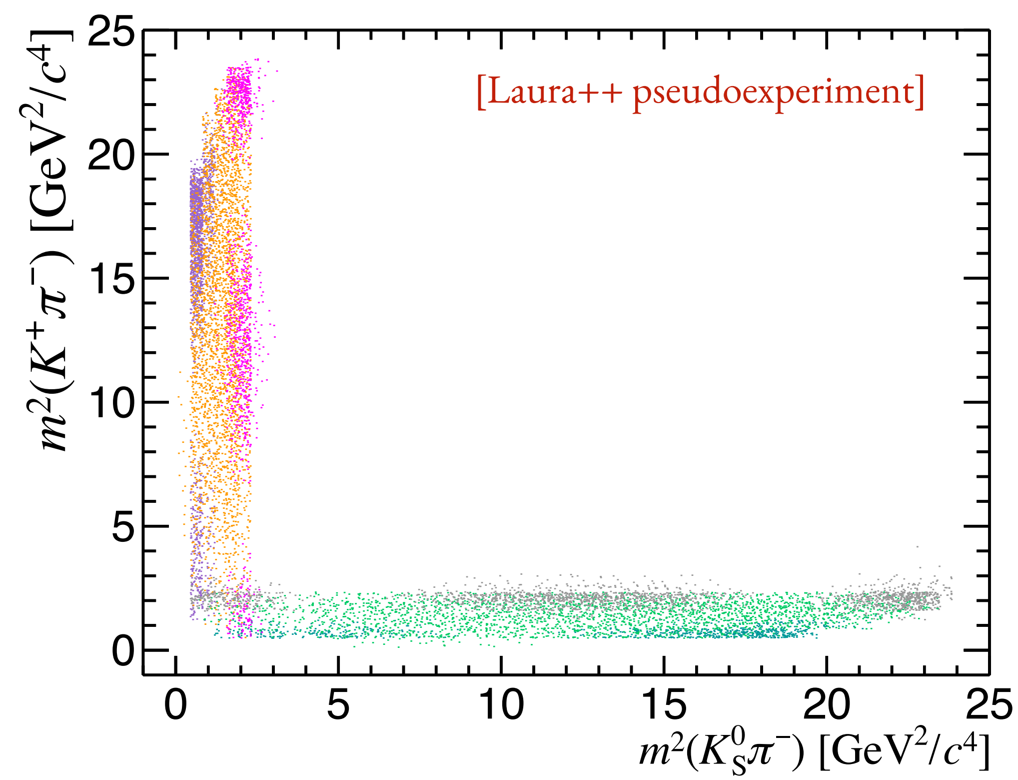


Signal model is built by:

- Significant changes in the negative log-likelihood, *i.e.* Wilks' theorem
  [Annals Math. Statist. 9 (1938) no.1, 60-62]
- Unbinned goodness-of-fit tests
  [JINST 4 (2010) P09004]

# Systematic uncertainties

Universität Zürich[UZH]

[LHCb-PAPER-2018-045]

The results for the various sources of systematic uncertainties are given below

| [PRELIMINARY] Fit fraction (%) uncertainties | | | | | | | | | |
|---|---|---|---|---|---|---|---|---|---|
| Resonance | Yields | Bkg. | Eff. | Fit bias | Add. res. | Fixed par. | Alt. model | Method | Total |
| $K^*(892)^-$ | 0.2 | 0.2 | 0.5 | 0.2 | – | 0.7 | 5.4 | 3.1 | 6.3 |
| $K_0^*(1430)^-$ | 0.1 | 0.2 | 0.6 | 0.3 | 0.1 | 2.1 | 22.0 | 2.9 | 22.3 |
| $K_2^*(1430)^-$ | 0.1 | 0.1 | 0.3 | 0.6 | 0.1 | 1.8 | 2.2 | 0.2 | 2.9 |
| $K^*(892)^0$ | 0.2 | 0.2 | 0.4 | 0.9 | – | 0.3 | 7.0 | 2.0 | 7.4 |
| $K_0^*(1430)^0$ | 0.2 | 0.3 | 0.9 | 0.4 | 0.1 | 4.4 | 3.3 | 1.3 | 5.7 |
| $K_2^*(1430)^0$ | 0.1 | 0.3 | 0.7 | 1.3 | 0.2 | 4.4 | 3.6 | 1.0 | 6.0 |
| $K^*(892)^+$ | 0.4 | 0.1 | 0.6 | 0.5 | 0.1 | 0.7 | 1.1 | 0.7 | 1.8 |
| $K_0^*(1430)^+$ | 0.5 | 0.4 | 0.7 | 0.8 | 0.2 | 6.4 | 13.0 | 4.5 | 15.2 |
| $K_2^*(1430)^+$ | 0.1 | 0.2 | 0.4 | 0.2 | 0.1 | 4.1 | 4.5 | 3.2 | 6.9 |
| $\overline{K}^*(892)^0$ | 0.4 | 0.3 | 0.4 | 0.2 | 0.2 | 0.5 | 3.0 | 7.9 | 8.5 |
| $\overline{K}_0^*(1430)^0$ | 0.4 | 0.4 | 0.6 | 0.8 | 0.7 | 0.9 | 3.9 | 5.4 | 6.8 |
| $\overline{K}_2^*(1430)^0$ | 0.1 | 0.2 | 0.4 | 0.8 | 0.1 | 1.0 | 5.5 | 2.7 | 6.3 |

Dominant uncertainties come from the Kπ S-wave model, e.g. the choice of the alternative line shapes to the LASS model for the $K^{*\pm,0}(1430)$ states

# Fit results - isobar parameters

[LHCb-PAPER-2018-045]

[PRELIMINARY]

| $B_s^0 \to K_S^0 K^+ \pi^-$ | | $B_s^0 \to K_S^0 K^- \pi^+$ | |
|---|---|---|---|
| Resonance | Fit fraction (%) | Resonance | Fit fraction (%) |
| $K^*(892)^-$ | $15.6 \pm 1.5$ | $K^*(892)^+$ | $13.4 \pm 2.0$ |
| $K_0^*(1430)^-$ | $30.2 \pm 2.6$ | $K_0^*(1430)^+$ | $28.5 \pm 3.6$ |
| $K_2^*(1430)^-$ | $2.9 \pm 1.3$ | $K_2^*(1430)^+$ | $5.8 \pm 1.9$ |
| $K^*(892)^0$ | $13.2 \pm 2.4$ | $\overline{K}^*(892)^0$ | $19.2 \pm 2.3$ |
| $K_0^*(1430)^0$ | $33.9 \pm 2.9$ | $\overline{K}_0^*(1430)^0$ | $27.0 \pm 4.1$ |
| $K_2^*(1430)^0$ | $5.9 \pm 4.0$ | $\overline{K}_2^*(1430)^0$ | $7.7 \pm 2.8$ |

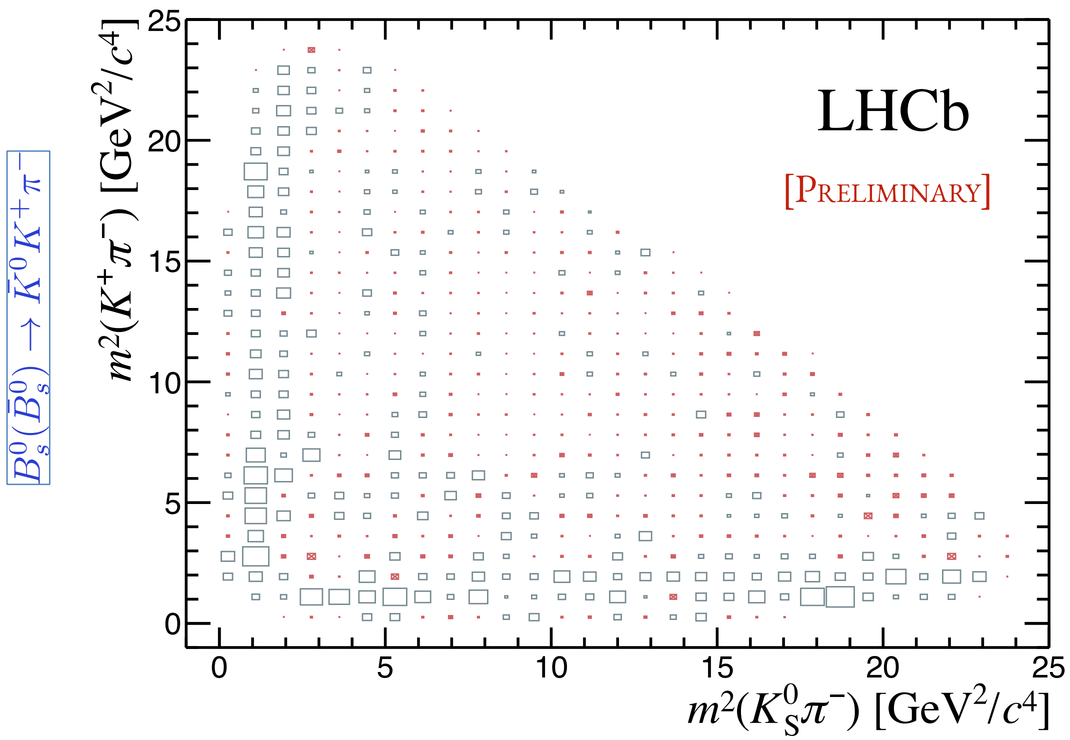


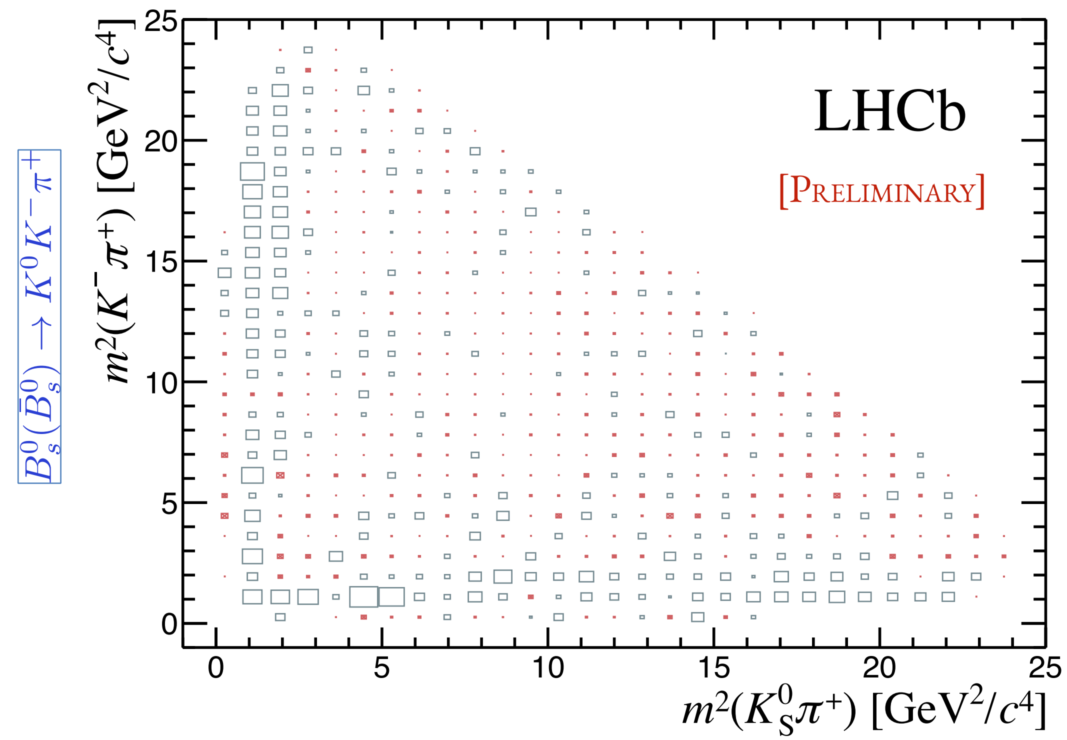

# Fit results - projections

[LHCb-PAPER-2018-045]

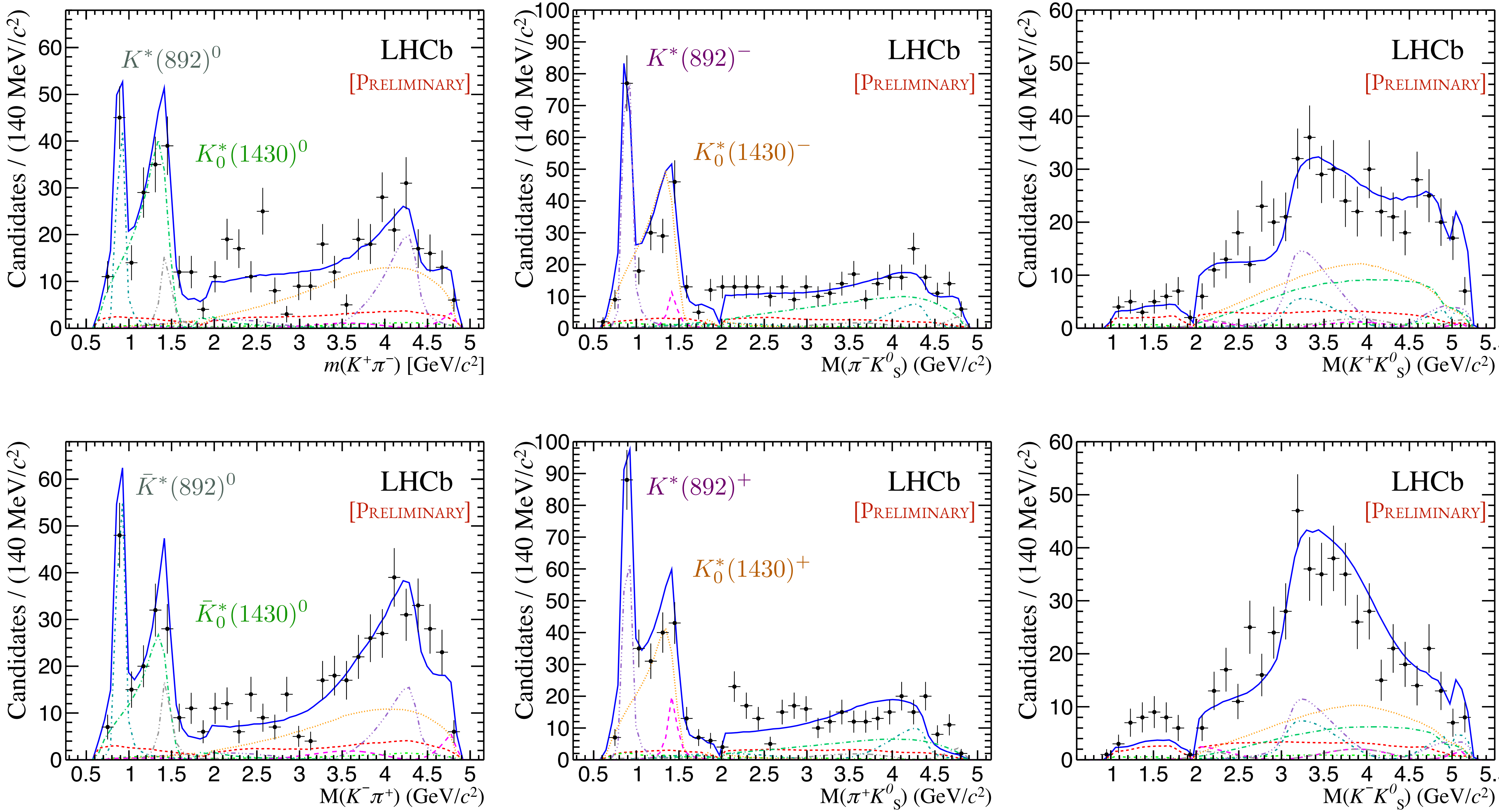

# Branching ratio results

[LHCb-PAPER-2018-045]

The fit fractions of the resonant components can be converted into quasi-two-body BF:

$$\mathcal{B}\left(B_s^0 \to K^*K; K^* \to K\pi\right) = \widehat{FF}_j \times \mathcal{B}\left(B_s^0 \to \overset{(-)}{K}{}^0 K^\pm\pi^\mp\right)$$

[PRELIMINARY]

$^*\mathcal{B}(B_s^0 \to \overset{(-)}{K}{}^0 K^\pm\pi^\mp) = (84.3 \pm 3.5 \pm 7.4 \pm 3.4) \times 10^{-6}$

$$\begin{aligned}
\mathcal{B}\left(B_s^0 \to K^*(892)^\pm K^\mp\right) &= (18.6 \pm 1.2 \pm 0.8 \pm 4.0 \pm 2.0) \times 10^{-6} \\
\mathcal{B}\left(B_s^0 \to K_0^*(1430)^\pm K^\mp\right) &= (31.3 \pm 2.3 \pm 0.7 \pm 25.1 \pm 3.3) \times 10^{-6} \\
\mathcal{B}\left(B_s^0 \to K_2^*(1430)^\pm K^\mp\right) &= (10.3 \pm 2.5 \pm 1.1 \pm 16.3 \pm 1.1) \times 10^{-6} \\
\mathcal{B}\left(B_s^0 \to \overset{(-)}{K}{}^*(892)^0 \overset{(-)}{K}{}^0\right) &= (19.8 \pm 2.8 \pm 1.2 \pm 4.4 \pm 2.1) \times 10^{-6} \\
\mathcal{B}\left(B_s^0 \to \overset{(-)}{K}{}_0^*(1430)^0 \overset{(-)}{K}{}^0\right) &= (33.0 \pm 2.5 \pm 0.9 \pm 9.1 \pm 3.5) \times 10^{-6} \\
\mathcal{B}\left(B_s^0 \to \overset{(-)}{K}{}_2^*(1430)^0 \overset{(-)}{K}{}^0\right) &= (16.8 \pm 4.5 \pm 1.7 \pm 21.2 \pm 1.8) \times 10^{-6}
\end{aligned}$$

[Summary]

- **Results are in good agreement with, and more precise than, the previous measurements**
- **Contribution from $K^*_0(1430)^{(\pm,0)}$ states are observed for the first time with significance above 10 standard deviations**
- **Further theoretical understanding of the S-wave modelling is paramount**

Universität Zürich[UZH]

LHCb

# Amplitude analysis of $B^0 \to (\pi^+\pi^-)(K^+\pi^-)$ decays

LHCb results : $\mathcal{L} = 3\,\text{fb}^{-1} - 2011 + 2012$ dataset

**Study of the B0 $\to \rho(770)^0 K^*(892)^0$ mode**

[LHCb-PAPER-2018-042]

Pablo Picasso
[Portrait of Daniel-Henry Kahnweiler]

# Amplitude analysis of quasi-two-body decays

**A natural extension of the DP approach is to consider 4-body final states, which further increases the degrees of freedom of the system**

$B^0 \rightarrow (p_1p_2)(p_3p_4)$ decays are described using (e.g. $B^0 \rightarrow \rho^0 K^*$)

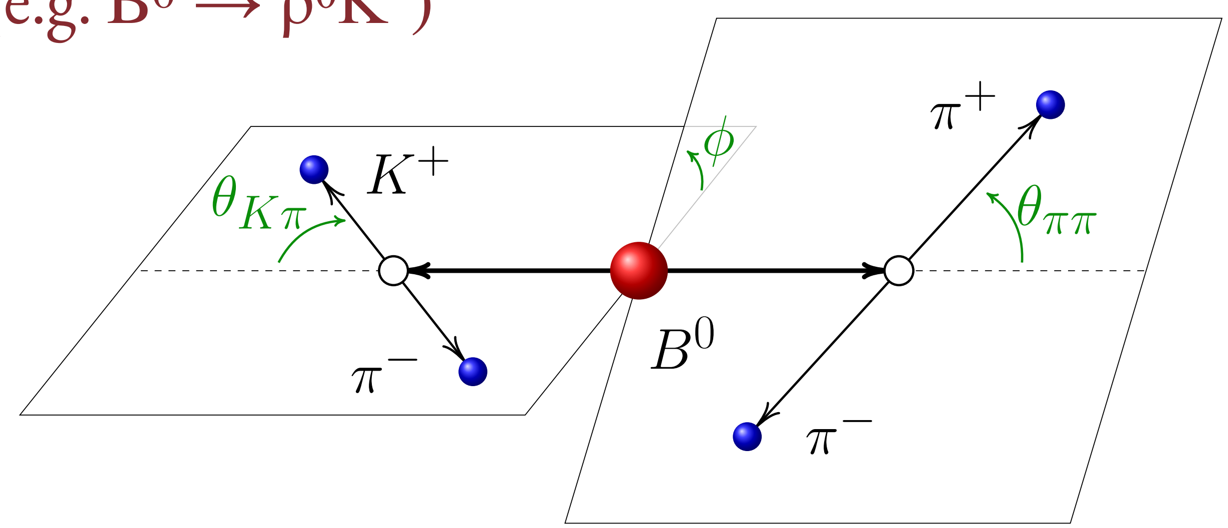


- Three helicity angles: $\theta_1$, $\theta_2$, $\phi$
- Two invariant masses: $m_{(p1p2)}$, $m_{(p3p4)}$

Decay rate given by

$$\frac{d^5\Gamma}{d\Omega dm_{\pi^+\pi^-} m_{\pi^+\pi^-}} \propto K(A_i, m_{\pi^+\pi^-}, m_{\pi^+\pi^-}) F(\Omega)$$

[Illustrative plots - pseudoexperiments]

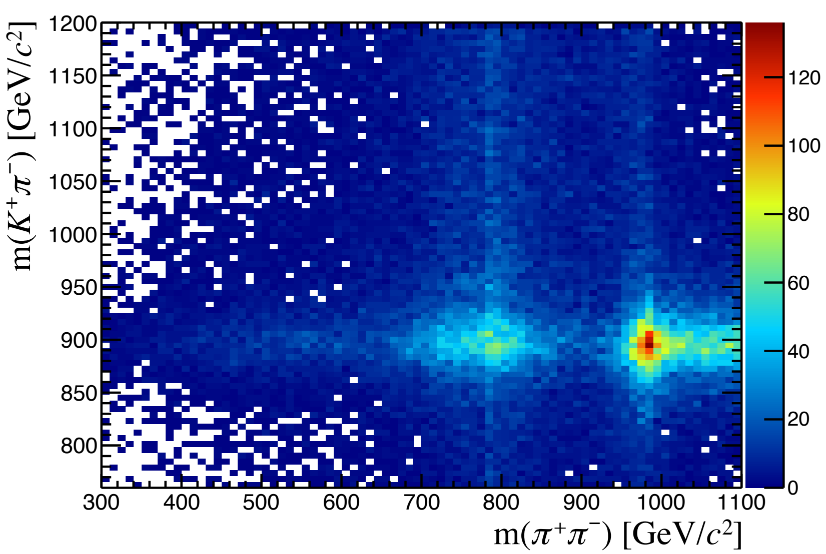


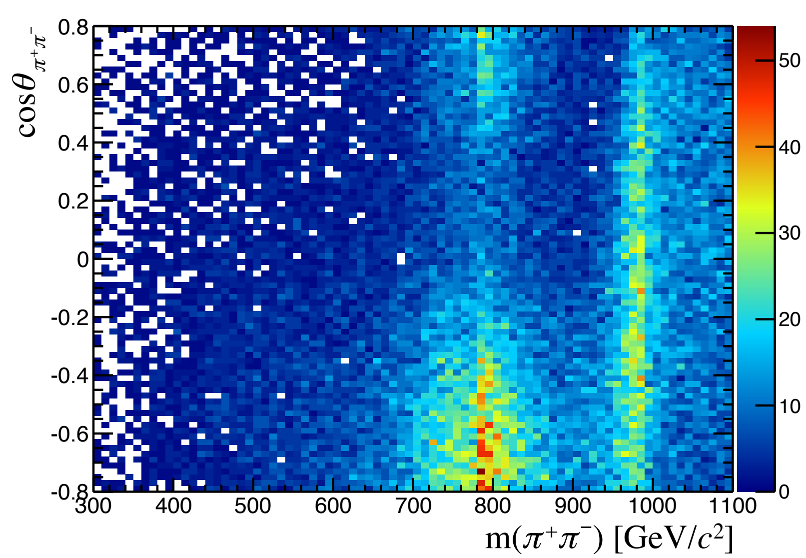


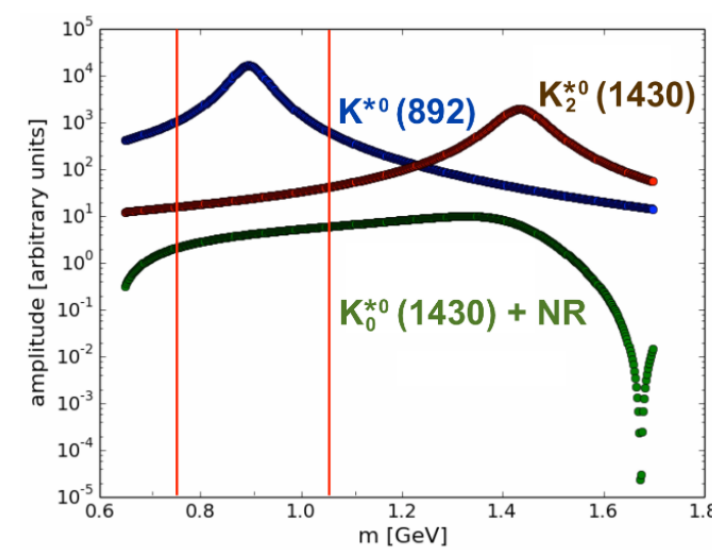

# The $B^0 \rightarrow \rho^0(\pi^+\pi^-)K^*(K^+\pi^-)^0$ decay

Universität Zürich[UZH]

**Charmless b-hadron that proceeds via**

- Double Cabibbo suppressed tree
- A gluonic $b \rightarrow s$ penguin

Comparable amplitudes: more sensitive to CP violation effects

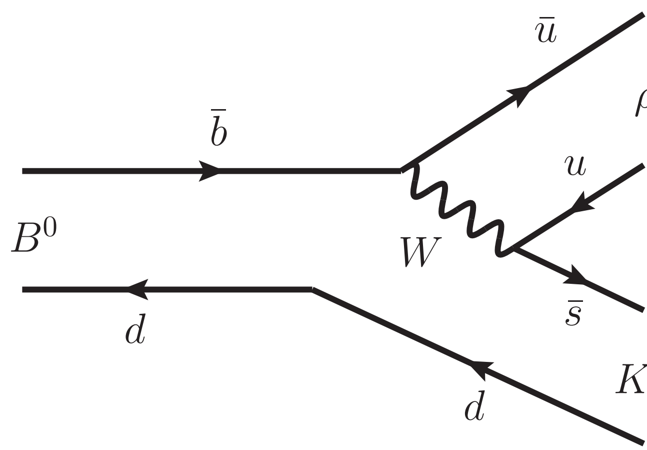


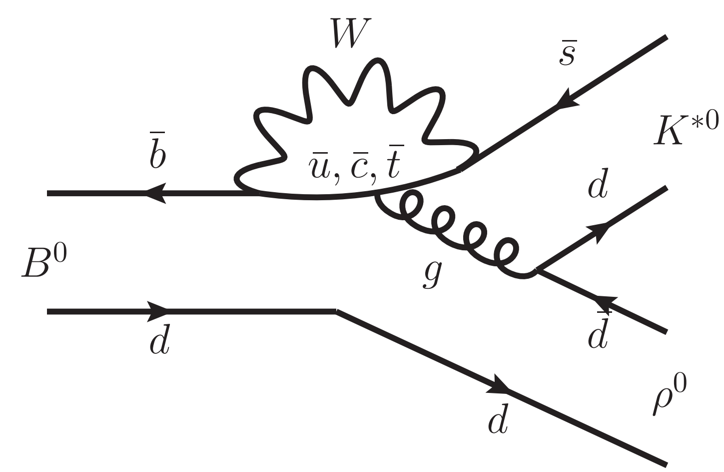


**Self-tagged decay:**
$$\begin{cases} B^0 \rightarrow (\pi^+\pi^-)(K^+\pi^-) \\ \overline{B}^0 \rightarrow (\pi^-\pi^+)(K^-\pi^+) \end{cases}$$

**+ EWP penguin**

Access to CP asymmetries:

$$a_{CP}^{dir} = \frac{|\mathcal{A}|^2 - |\bar{\mathcal{A}}|^2}{|\mathcal{A}|^2 + |\bar{\mathcal{A}}|^2} = \frac{-2rsin\delta sin\phi}{1 + r^2 + 2rcos\delta cos\phi}$$

**In the absence of NP contributions:**

$$\phi = arg[(V_{tb}V_{ts}^*)/(V_{ub}V_{us}^*)] \Rightarrow \sin\phi = \sin\gamma_{CKM}$$

**"$B \rightarrow VV$ puzzle": expected $f_L \gg f_{||}, f_{\perp}$ not seen in purely penguin modes**

[LHCb, JHEP 03 (2018) 140, PRD 90, 052011 (2014)]

# Selecting the signal

[LHCb-PAPER-2018-042]

Strategy designed to improve the signal significance and reduce possible physics contributions under the signal

- Boosted Decision Tree and mass vetoes to reject combinatorial and charm contributions
- Analysis performed with ~11k signal events and purity of 83%

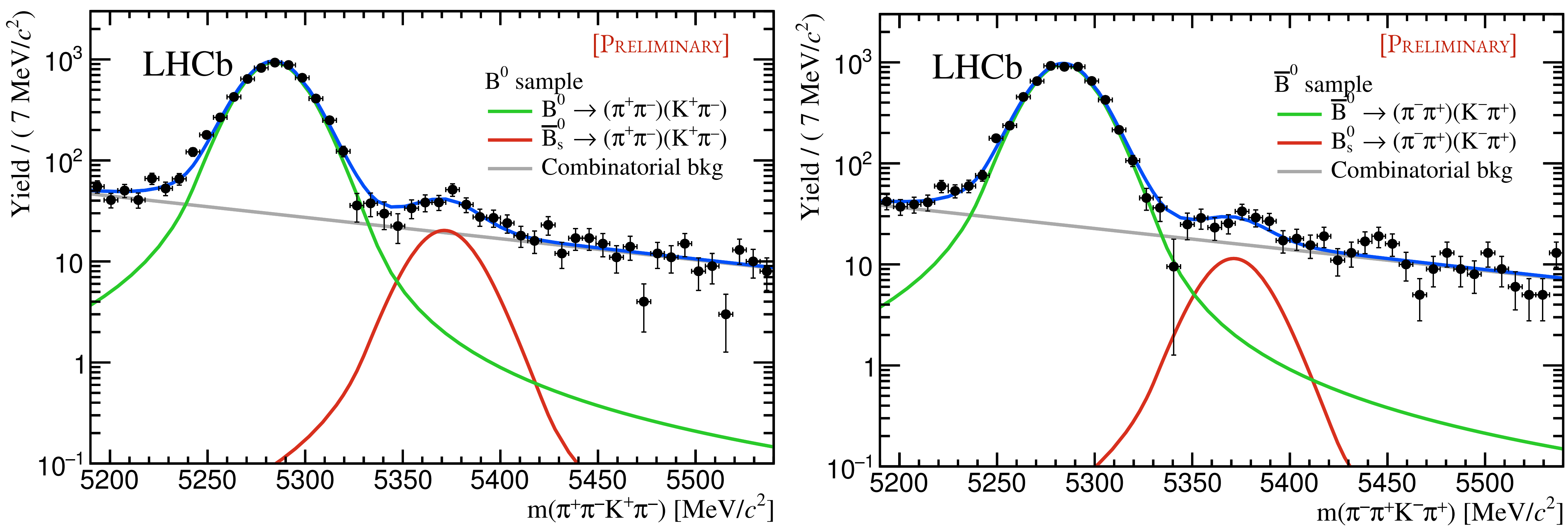

# The $B^0 \to \rho^0(\pi^+\pi^-)K^*(K^+\pi^-)^0$ decay

[LHCb-PAPER-2018-042]

## Nominal model accounts for 10 decay channels

- $\rho^0$: Gounaris-Sakurai
- $\omega$, $K^*(892)^0$: relativistic spin-1 Breit-Wigners
- $f_0(500)$: spin-0 Breit-Wigner
- $f_0(980)$: Flattè
- $f_0(1370)$: spin-0 Breit-Wigner
- $(K\pi)_0$: Lass with a Form Factor

| $A_i$ | $g_i(\theta_{\pi\pi}, \theta_{K\pi}, \phi)$ | $R_i(m_{\pi\pi}, m_{K\pi})$ |
|---|---|---|
| $A^0_{\rho K^*}$ | $\cos\theta_{\pi\pi}\cos\theta_{K\pi}$ | $M_\rho(m_{\pi\pi})M_{K^*}(m_{K\pi})$ |
| $A^{\|\|}_{\rho K^*}$ | $\frac{1}{\sqrt{2}}\sin\theta_{\pi\pi}\sin\theta_{K\pi}\cos\phi$ | $M_\rho(m_{\pi\pi})M_{K^*}(m_{K\pi})$ |
| $A^{\perp}_{\rho K^*}$ | $\frac{i}{\sqrt{2}}\sin\theta_{\pi\pi}\sin\theta_{K\pi}\sin\phi$ | $M_\rho(m_{\pi\pi})M_{K^*}(m_{K\pi})$ |
| $A^0_{\omega K^*}$ | $\cos\theta_{\pi\pi}\cos\theta_{K\pi}$ | $M_\omega(m_{\pi\pi})M_{K^*}(m_{K\pi})$ |
| $A^{\|\|}_{\omega K^*}$ | $\frac{1}{\sqrt{2}}\sin\theta_{\pi\pi}\sin\theta_{K\pi}\cos\phi$ | $M_\omega(m_{\pi\pi})M_{K^*}(m_{K\pi})$ |
| $A^{\perp}_{\omega K^*}$ | $\frac{i}{\sqrt{2}}\sin\theta_{\pi\pi}\sin\theta_{K\pi}\sin\phi$ | $M_\omega(m_{\pi\pi})M_{K^*}(m_{K\pi})$ |
| $A_{\rho(K\pi)}$ | $\frac{1}{\sqrt{3}}\cos\theta_{\pi\pi}$ | $M_\rho(m_{\pi\pi})M_{(K\pi)}(m_{K\pi})$ |
| $A_{\omega(K\pi)}$ | $\frac{1}{\sqrt{3}}\cos\theta_{\pi\pi}$ | $M_\omega(m_{\pi\pi})M_{(K\pi)}(m_{K\pi})$ |
| $A_{f_0(500)K^*}$ | $\frac{1}{\sqrt{3}}\cos\theta_{K\pi}$ | $M_{f_0(500)}(m_{\pi\pi})M_{K^*}(m_{K\pi})$ |
| $A_{f_0(980)K^*}$ | $\frac{1}{\sqrt{3}}\cos\theta_{K\pi}$ | $M_{f_0(980)}(m_{\pi\pi})M_{K^*}(m_{K\pi})$ |
| $A_{f_0(1370)K^*}$ | $\frac{1}{\sqrt{3}}\cos\theta_{K\pi}$ | $M_{f_0(1370)}(m_{\pi\pi})M_{K^*}(m_{K\pi})$ |
| $A_{f_0(500)(K\pi)}$ | $\frac{1}{3}$ | $M_{f_0(500)}(m_{\pi\pi})M_{(K\pi)}(m_{K\pi})$ |
| $A_{f_0(980)(K\pi)}$ | $\frac{1}{3}$ | $M_{f_0(980)}(m_{\pi\pi})M_{(K\pi)}(m_{K\pi})$ |
| $A_{f_0(1370)(K\pi)}$ | $\frac{1}{3}$ | $M_{f_0(1370)}(m_{\pi\pi})M_{(K\pi)}(m_{K\pi})$ |

Dominant uncertainties come from the pollution of $a_1(1260)$ resonance

# Fit results - projections



[LHCb-PAPER-2018-042]

Fitter implemented using Ipanema framework and similar strategy for kinematic effects

[arXiv:1706.01420]

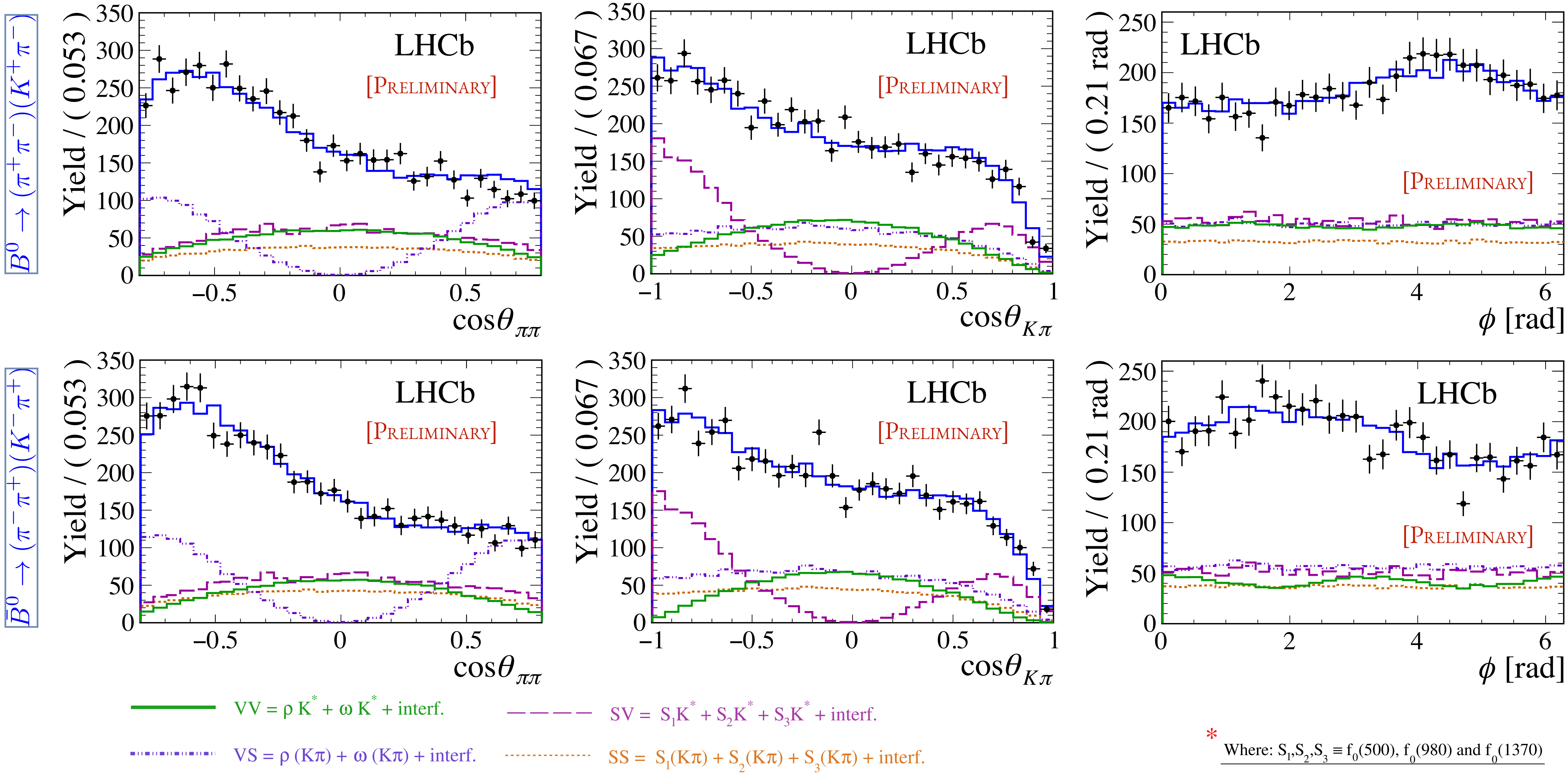


* Where: $S_1, S_2, S_3 \equiv f_0(500)$, $f_0(980)$ and $f_0(1370)$

# Fit results - projections

[LHCb-PAPER-2018-042]

Fitter implemented using Ipanema framework and similar strategy for kinematic effects

[arXiv:1706.01420]

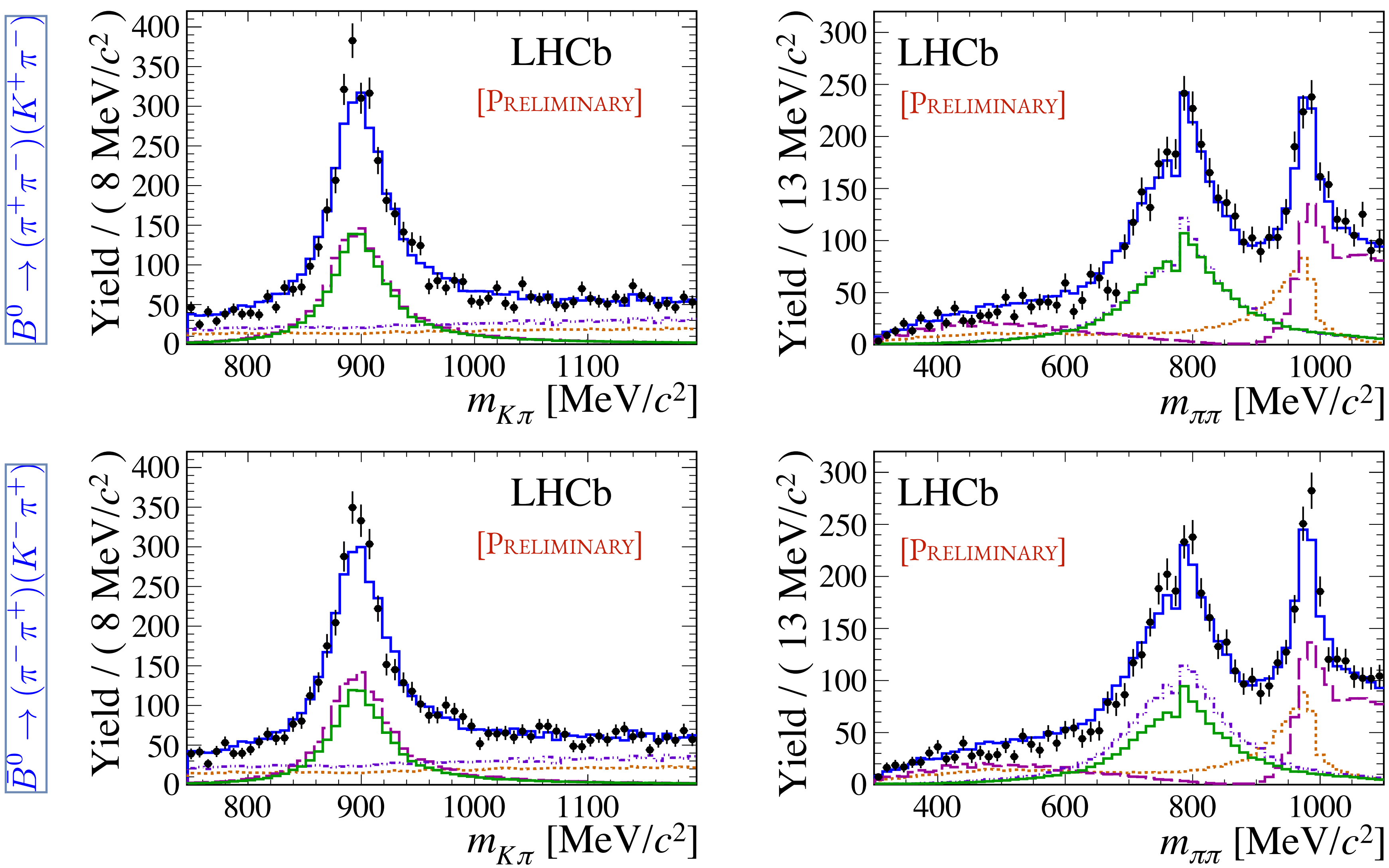


VV = ρ K* + ω K* + interf.

SV = $S_1K^* + S_2K^* + S_3K^*$ + interf.

VS = ρ (Kπ) + ω (Kπ) + interf.

SS = $S_1$(Kπ) + $S_2$(Kπ) + $S_3$(Kπ) + interf.

* Where: $S_1,S_2,S_3 \equiv f_0(500)$, $f_0(980)$ and $f_0(1370)$

# Fit results

[LHCb-PAPER-2018-042]

## First measurements of several individual magnitude and phase

[PRELIMINARY]

| Parameter | $CP$ average | $CP$ asymmetry |
|---|---|---|
| $\lvert A^{0}_{\rho K^*}\rvert^2$ | $0.316 \pm 0.039 \pm 0.074$ | $-0.75 \pm 0.07 \pm 0.17$ |
| $\lvert A^{\parallel}_{\rho K^*}\rvert^2$ | $0.701 \pm 0.038 \pm 0.084$ | $-0.049 \pm 0.053 \pm 0.019$ |
| $\lvert A^{\perp}_{\rho K^*}\rvert^2$ | $0.668 \pm 0.036 \pm 0.068$ | $-0.187 \pm 0.051 \pm 0.026$ |
| $\lvert A^{0}_{\omega K^*}\rvert^2$ | $0.019 \pm 0.010 \pm 0.012$ | $-0.61 \pm 0.37 \pm 0.39$ |
| $\lvert A^{\parallel}_{\omega K^*}\rvert^2$ | $0.0050 \pm 0.0029 \pm 0.0031$ | $-0.30 \pm 0.54 \pm 0.28$ |
| $\lvert A^{\perp}_{\omega K^*}\rvert^2$ | $0.0020 \pm 0.0019 \pm 0.0015$ | $-0.21 \pm 0.86 \pm 0.41$ |
| $\lvert A_{\omega(K\pi)}\rvert^2$ | $0.026 \pm 0.011 \pm 0.025$ | $-0.47 \pm 0.33 \pm 0.45$ |
| $\lvert A_{f_0(500)K^*}\rvert^2$ | $0.532 \pm 0.048 \pm 0.098$ | $-0.056 \pm 0.091 \pm 0.042$ |
| $\lvert A_{f_0(980)K^*}\rvert^2$ | $2.42 \pm 0.13 \pm 0.25$ | $-0.022 \pm 0.052 \pm 0.023$ |
| $\lvert A_{f_0(1370)K^*}\rvert^2$ | $1.29 \pm 0.09 \pm 0.20$ | $-0.094 \pm 0.071 \pm 0.037$ |
| $\lvert A_{f_0(500)(K\pi)}\rvert^2$ | $0.174 \pm 0.021 \pm 0.039$ | $0.30 \pm 0.12 \pm 0.09$ |
| $\lvert A_{f_0(980)(K\pi)}\rvert^2$ | $1.184 \pm 0.079 \pm 0.073$ | $-0.083 \pm 0.066 \pm 0.023$ |
| $\lvert A_{f_0(1370)(K\pi)}\rvert^2$ | $0.139 \pm 0.028 \pm 0.039$ | $-0.48 \pm 0.17 \pm 0.15$ |
| $f^{0}_{\rho K^*}$ | $0.164 \pm 0.015 \pm 0.022$ | $-0.622 \pm 0.085 \pm 0.086$ |
| $f^{\parallel}_{\rho K^*}$ | $0.435 \pm 0.016 \pm 0.042$ | $0.188 \pm 0.037 \pm 0.022$ |
| $f^{\perp}_{\rho K^*}$ | $0.401 \pm 0.016 \pm 0.037$ | $0.050 \pm 0.039 \pm 0.015$ |
| $f^{0}_{\omega K^*}$ | $0.68 \pm 0.17 \pm 0.16$ | $-0.13 \pm 0.27 \pm 0.13$ |
| $f^{\parallel}_{\omega K^*}$ | $0.22 \pm 0.14 \pm 0.15$ | $0.26 \pm 0.55 \pm 0.22$ |
| $f^{\perp}_{\omega K^*}$ | $0.096 \pm 0.094 \pm 0.091$ | $0.34 \pm 0.81 \pm 0.37$ |

[PRELIMINARY]

| Parameter | Strong phases, $\frac{1}{2}(\delta_{\overline{B}} + \delta_B)$ [rad] | Weak phases, $\frac{1}{2}(\delta_{\overline{B}} - \delta_B)$ [rad] |
|---|---|---|
| $\delta^{0}_{\rho K^*}$ | $1.57 \pm 0.08 \pm 0.18$ | $0.123 \pm 0.084 \pm 0.036$ |
| $\delta^{\parallel}_{\rho K^*}$ | $0.795 \pm 0.030 \pm 0.068$ | $0.014 \pm 0.030 \pm 0.026$ |
| $\delta^{\perp}_{\rho K^*}$ | $-2.365 \pm 0.032 \pm 0.054$ | $0.000 \pm 0.032 \pm 0.013$ |
| $\delta^{0}_{\omega K^*}$ | $-0.86 \pm 0.29 \pm 0.71$ | $0.03 \pm 0.29 \pm 0.16$ |
| $\delta^{\parallel}_{\omega K^*}$ | $-1.83 \pm 0.29 \pm 0.32$ | $0.59 \pm 0.29 \pm 0.07$ |
| $\delta^{\perp}_{\omega K^*}$ | $1.58 \pm 0.43 \pm 0.63$ | $-0.25 \pm 0.43 \pm 0.16$ |
| $\delta_{\omega(K\pi)}$ | $-2.32 \pm 0.22 \pm 0.24$ | $-0.20 \pm 0.22 \pm 0.14$ |
| $\delta_{f_0(500)K^*}$ | $-2.28 \pm 0.06 \pm 0.22$ | $-0.002 \pm 0.064 \pm 0.045$ |
| $\delta_{f_0(980)K^*}$ | $0.385 \pm 0.038 \pm 0.066$ | $0.018 \pm 0.038 \pm 0.022$ |
| $\delta_{f_0(1370)K^*}$ | $-2.757 \pm 0.051 \pm 0.089$ | $0.076 \pm 0.051 \pm 0.025$ |
| $\delta_{f_0(500)(K\pi)}$ | $-2.80 \pm 0.09 \pm 0.21$ | $-0.206 \pm 0.088 \pm 0.034$ |
| $\delta_{f_0(980)(K\pi)}$ | $-2.982 \pm 0.032 \pm 0.057$ | $-0.027 \pm 0.032 \pm 0.013$ |
| $\delta_{f_0(1370)(K\pi)}$ | $1.76 \pm 0.10 \pm 0.11$ | $-0.16 \pm 0.10 \pm 0.04$ |
| $\delta^{\parallel-\perp}_{\rho K^*}$ | $3.160 \pm 0.035 \pm 0.044$ | $0.014 \pm 0.035 \pm 0.026$ |
| $\delta^{\parallel-0}_{\rho K^*}$ | $-0.772 \pm 0.085 \pm 0.061$ | $-0.109 \pm 0.085 \pm 0.034$ |
| $\delta^{\perp-0}_{\rho K^*}$ | $-3.931 \pm 0.085 \pm 0.065$ | $-0.123 \pm 0.085 \pm 0.035$ |
| $\delta^{\parallel-\perp}_{\omega K^*}$ | $-3.41 \pm 0.52 \pm 0.73$ | $0.84 \pm 0.52 \pm 0.16$ |
| $\delta^{\parallel-0}_{\omega K^*}$ | $-0.97 \pm 0.41 \pm 0.57$ | $0.57 \pm 0.41 \pm 0.17$ |
| $\delta^{\perp-0}_{\omega K^*}$ | $2.44 \pm 0.51 \pm 0.82$ | $-0.28 \pm 0.51 \pm 0.24$ |

# Selected results

[LHCb-PAPER-2018-042]

[PRELIMINARY]

| | Observable | QCDF from Ref. [4] | pQCD from Ref. [11] | This work |
|---|---|---|---|---|
| $f^0_{\rho K^*}$ | *CP* average | $0.22^{+0.03+0.53}_{-0.03-0.14}$ | $0.65^{+0.03+0.03}_{-0.03-0.04}$ | $0.164 \pm 0.015 \pm 0.022$ |
| | *CP* asymmetry | $-0.30^{+0.11+0.61}_{-0.11-0.49}$ | $0.0364^{+0.0120}_{-0.0107}$ | $-0.622 \pm 0.085 \pm 0.086$ |
| $f^\perp_{\rho K^*}$ | *CP* average | $0.39^{+0.02+0.27}_{-0.02-0.07}$ | $0.169\ ^{+0.027}_{-0.018}$ | $0.401 \pm 0.016 \pm 0.037$ |
| | *CP* asymmetry | $--$ | $-0.0771^{+0.0197}_{-0.0186}$ | $0.050 \pm 0.039 \pm 0.015$ |
| $\delta^{\parallel-0}_{\rho K^*}$ | Strong phase [rad] | $-0.7\ ^{+0.1+1.1}_{-0.1-0.8}$ | $-1.61\ ^{+0.02}_{-3.06}$ | $-0.772 \pm 0.085 \pm 0.061$ |
| | Weak phase [rad] | $0.30^{+0.09+0.38}_{-0.09-0.33}$ | $-0.001^{+0.017}_{-0.018}$ | $-0.109 \pm 0.085 \pm 0.034$ |
| $\delta^{\parallel-\perp}_{\rho K^*}$ | Strong phase [rad] | $\equiv 0$ | $0.01\ ^{+0.02}_{-4.30}$ | $3.160 \pm 0.035 \pm 0.044$ |
| | Weak phase [rad] | $\equiv 0$ | $-0.003^{+0.025}_{-0.024}$ | $0.014 \pm 0.035 \pm 0.026$ |

**[Summary]**

- **First observation of CP violation in $B^0 \to VV$ angular distributions**
- **Low values for longitudinal polarisation might suggest the importance of EWP diagrams**

Universität Zürich[UZH]

# Amplitude analyses of Charm decays

## LHCb results : $\mathcal{L} = 3\,\mathrm{fb}^{-1}$ – 2011 + 2012 dataset

**Dalitz plot analysis of $D^+ \to K^- K^+ K^+$ decays**

[LHCb-PAPER-2018-039]

**Search for CP violation through an amplitude analysis of $D^0 \to K^+ K^- \pi^+ \pi^-$ decays**

[arXiv:1811.08304]

Paul Signac
[The Papal Palace in Avignon]

# $D^+ \rightarrow K^+K^-K^+$ Dalitz-plot analysis

**Further understanding on the resonant structure of the decays**

- **Information about the $K^-K^+$ scattering amplitudes**

**Analysis performed with ~110k signal events and purity of 90% with 2 $fb^{-1}$**

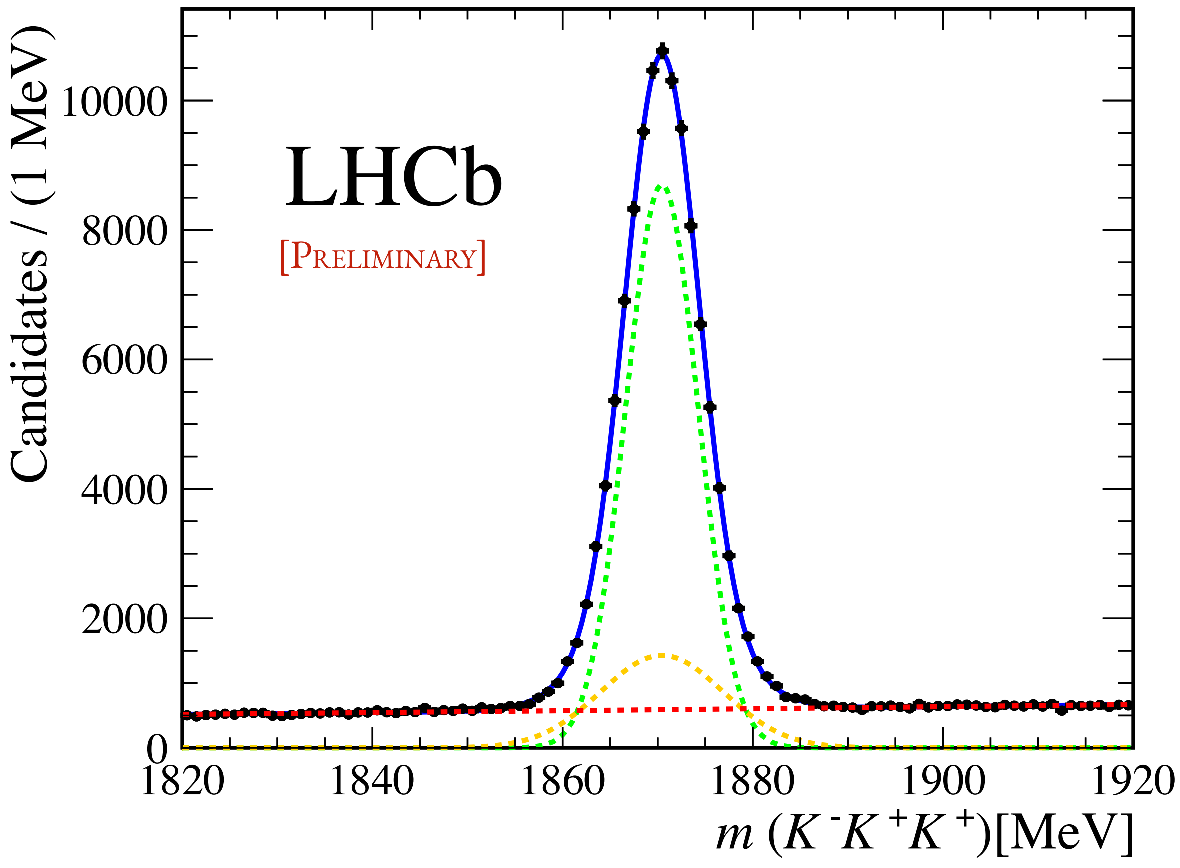


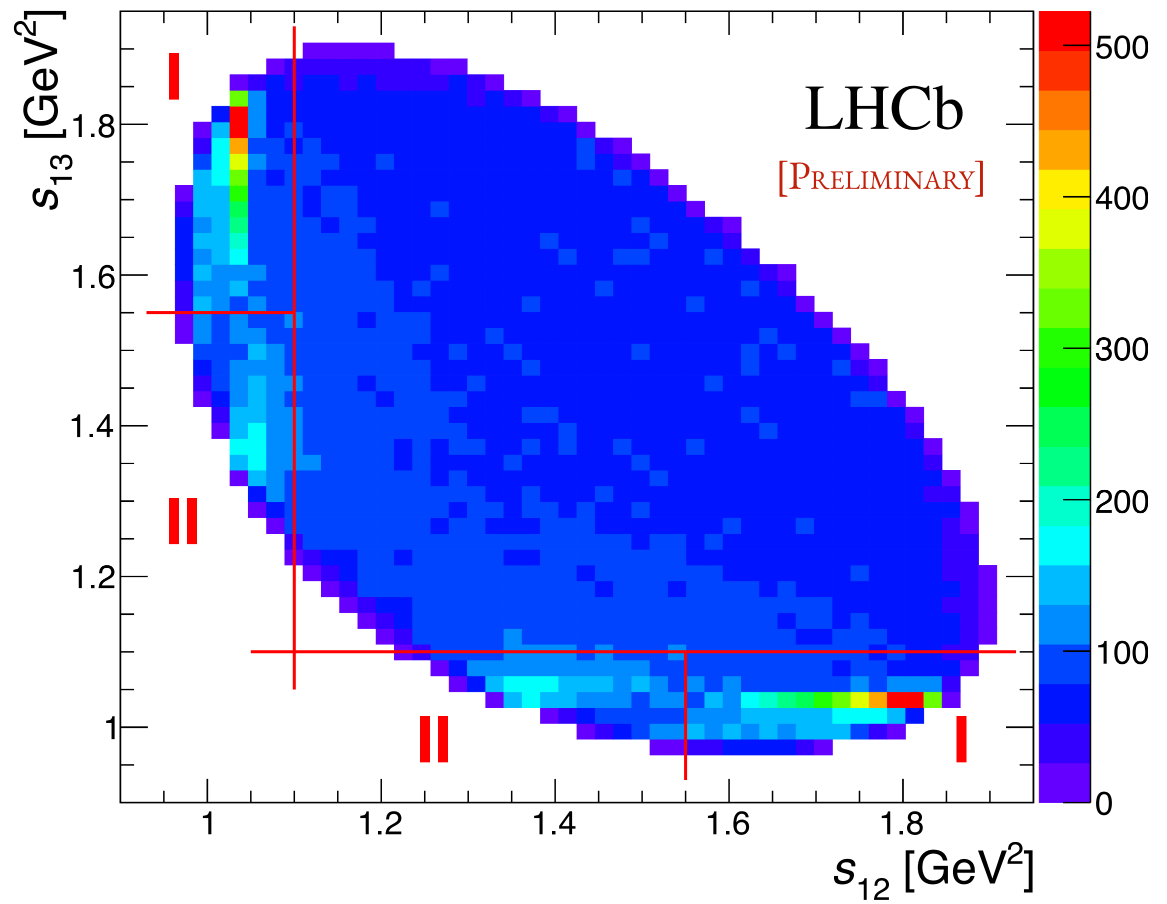

# $D^+ \to K^+K^-K^+$ Isobar model

Universität Zürich[UZH]

[LHCb-PAPER-2018-039]

## Canonical approach for the DP

- **Several resonances considered, e.g. $f_0(980)$, $f_2(1270)$, $a_0(1540)$, $\varphi(1020)$, and others**

| Resonance | Magnitude | Phase[°] | Fraction (%) |
|---|---|---|---|
| $f_0(980)$ | 3.12±0.15 | -59.0±5.0 | 23.7±3.0 |
| $f_0(X)$ | 3.46±0.46 | 13.1±7.7 | 25.4±5.0 |
| $\phi$ | 1[fix] | 0[fix] | 6.17±0.48 |
| sum | | | 55.4±5.9 |

**Large interference in the S-wave and limited understanding of underlying dynamics**

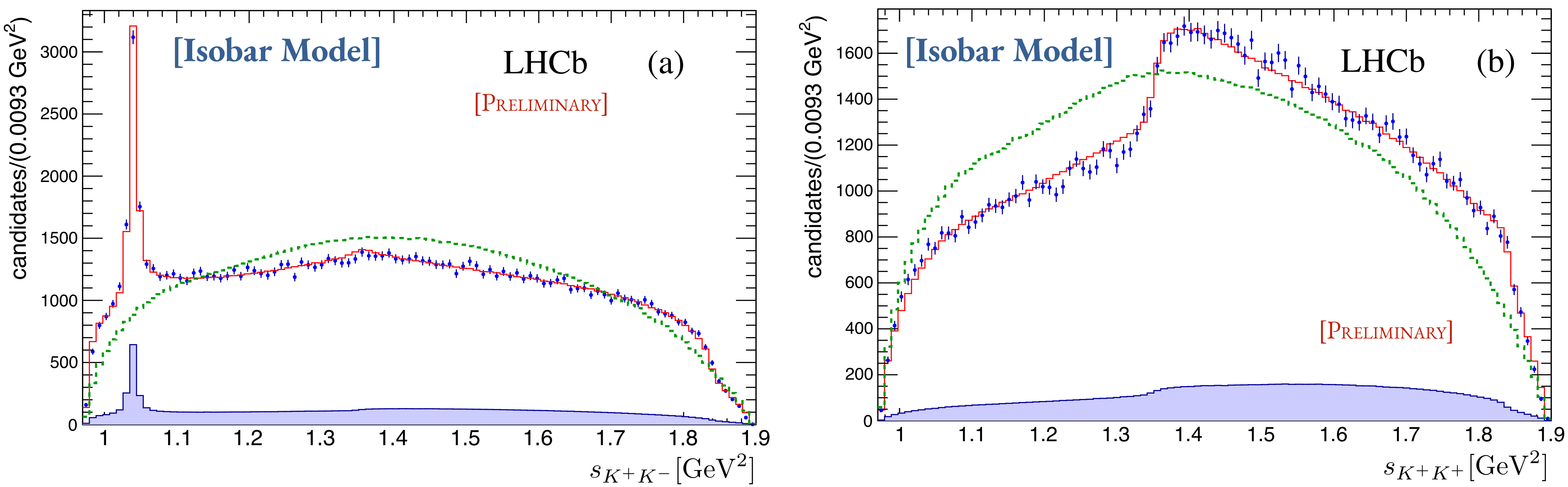

# $D^+ \to K^+K^-K^+$ phenomenological model

[LHCb-PAPER-2018-039]

**Assuming the annihilation dominance**

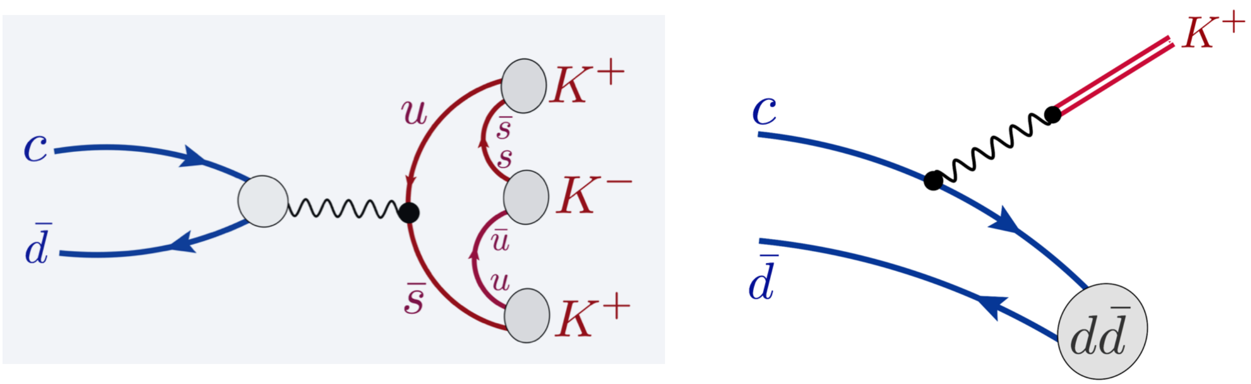

**The decay amplitude can be expressed as**

[Phys. Rev. D 98, 056021 (2018)]

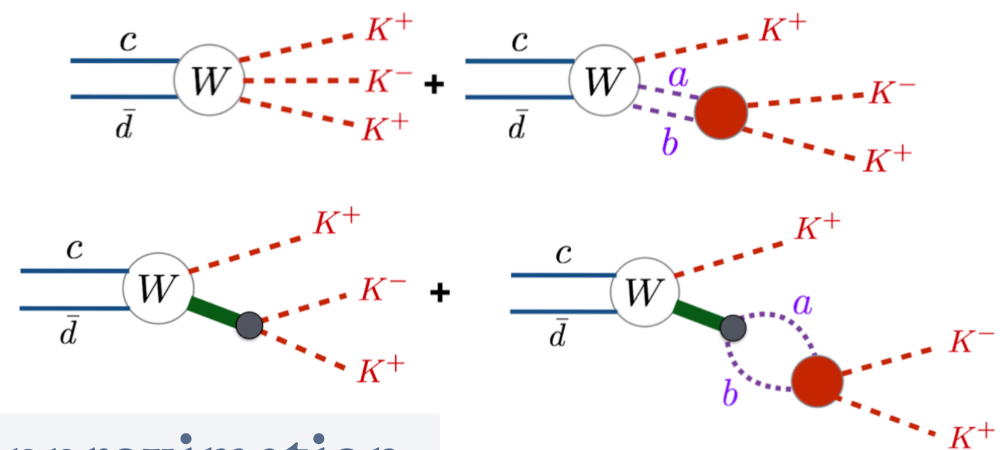

**→ goes beyond the (2+1) approximation**

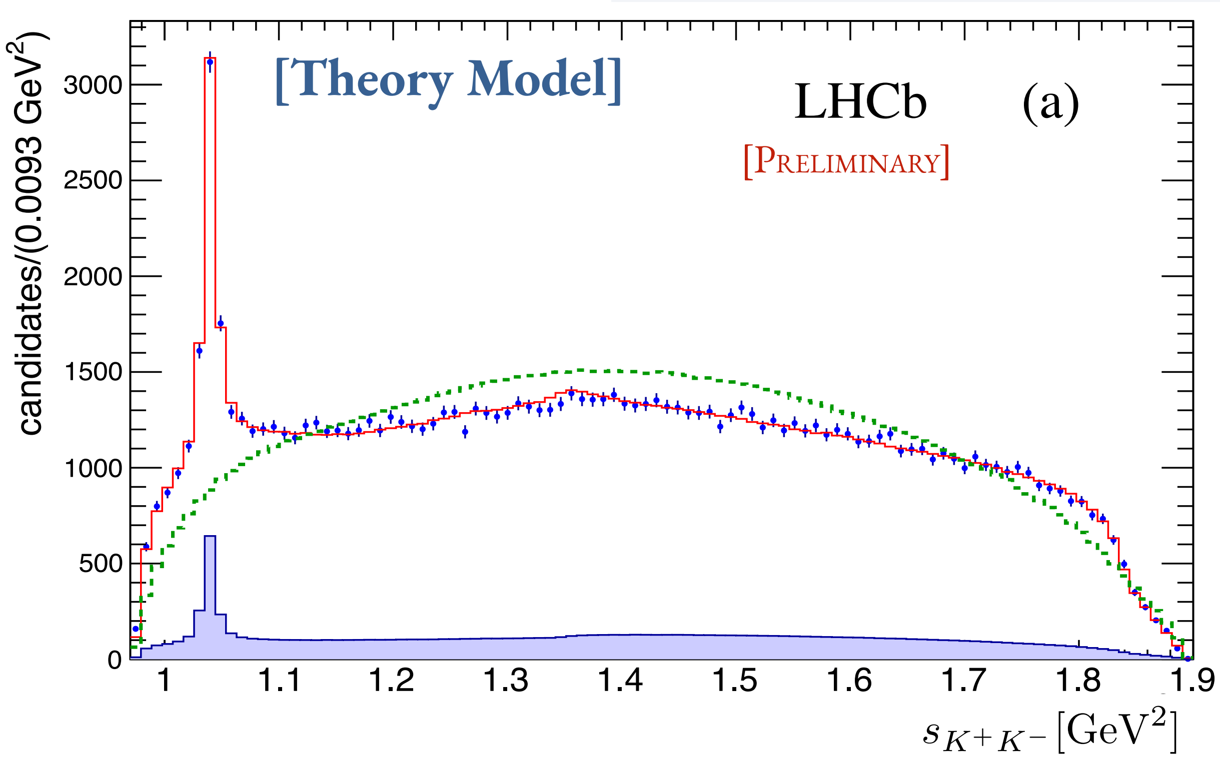


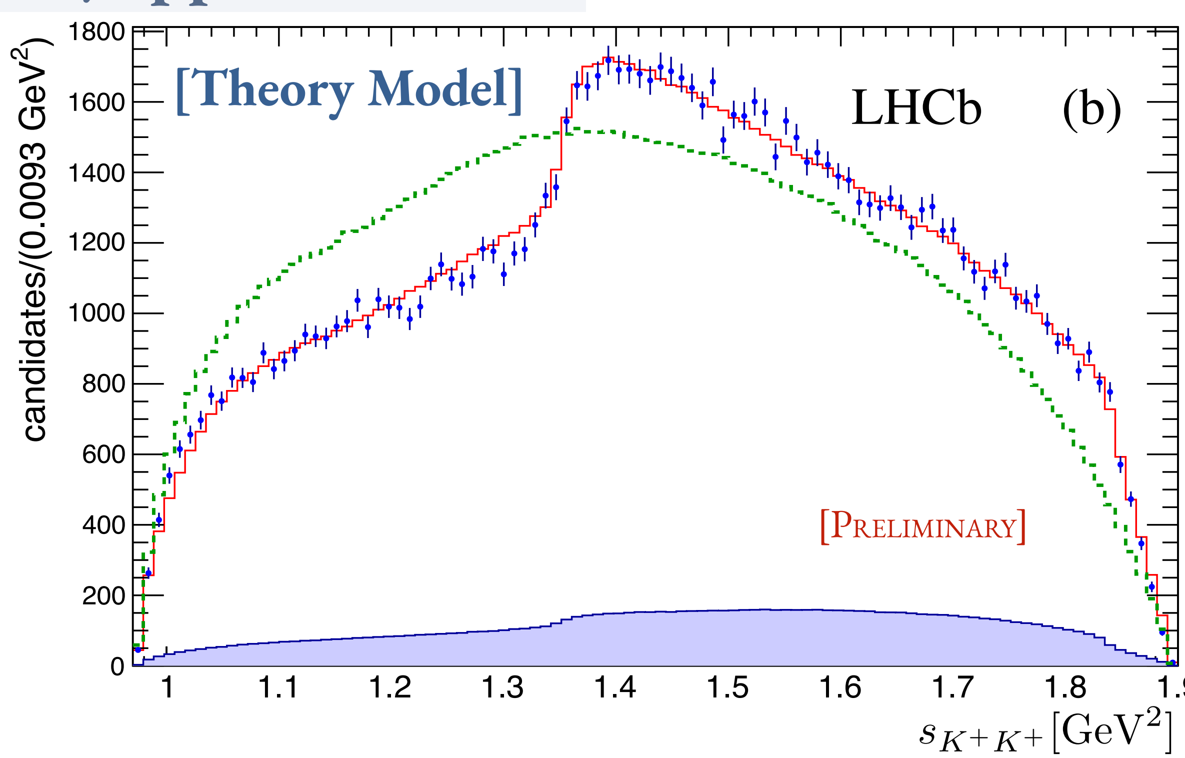

# $D^+ \rightarrow K^+K^-K^+$ phenomenological model

[LHCb-PAPER-2018-039]

**Assuming the annihilation dominance**

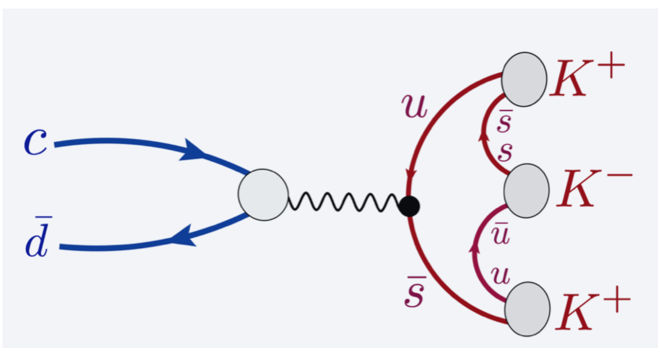


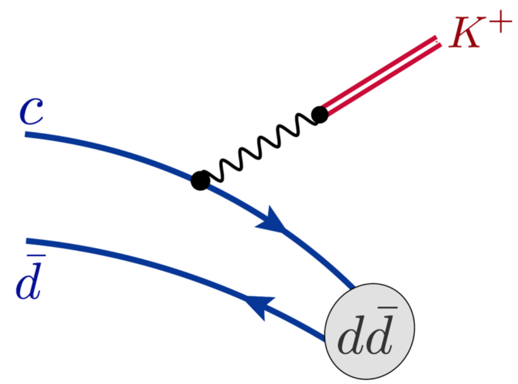


**The decay amplitude can be expressed as**

[Phys. Rev. D 98, 056021 (2018)]

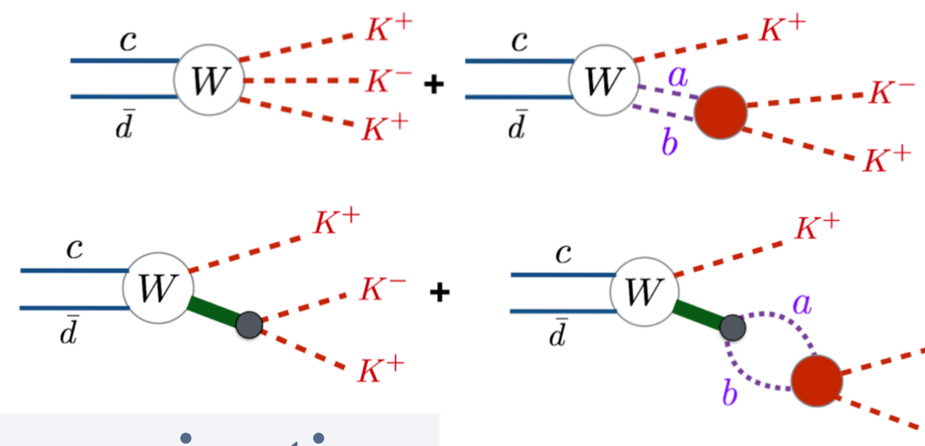


**→ goes beyond the (2+1) approximation**

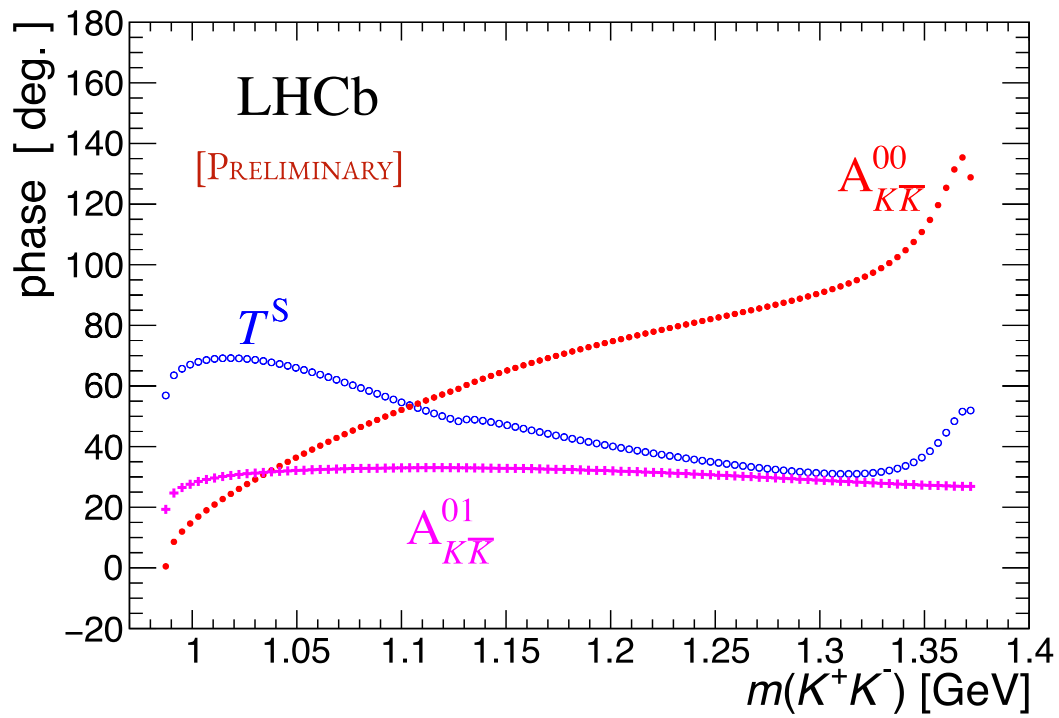


**Better description of the data with a much more clear physics content:**

- *e.g.* resonant structure (nonresonant, $\varphi(1020)$, $a_0(980)$ and mixture of $f_0(980)$ and $f_0(1370)$)
- phase shifts/inelasticities in $K^-K^+$ scattering

Universität Zürich[UZH]

LHCb

# Amplitude analyses of Charm decays

---

## LHCb results : $\mathcal{L} = 3\,\mathrm{fb}^{-1} - 2011 + 2012$ dataset

**Dalitz plot analysis of $D^+ \rightarrow K^-K^+K^+$ decays**

[LHCb-PAPER-2018-039]

**Search for CP violation through an amplitude analysis of $D^0 \rightarrow K^+K^-\pi^+\pi^-$ decays**

[arXiv:1811.08304]

Paul Signac
[The Papal Palace in Avignon]

# $D^0 \rightarrow K^+K^-\pi^+\pi^-$ decays

[arXiv:1811.08304]

## Search for CP violation in an unprecedented statistics

- **Beyond quasi-two body approach - also considering resonances to 3-body**

## Analysis performed with ~160k signal events and purity of 83%

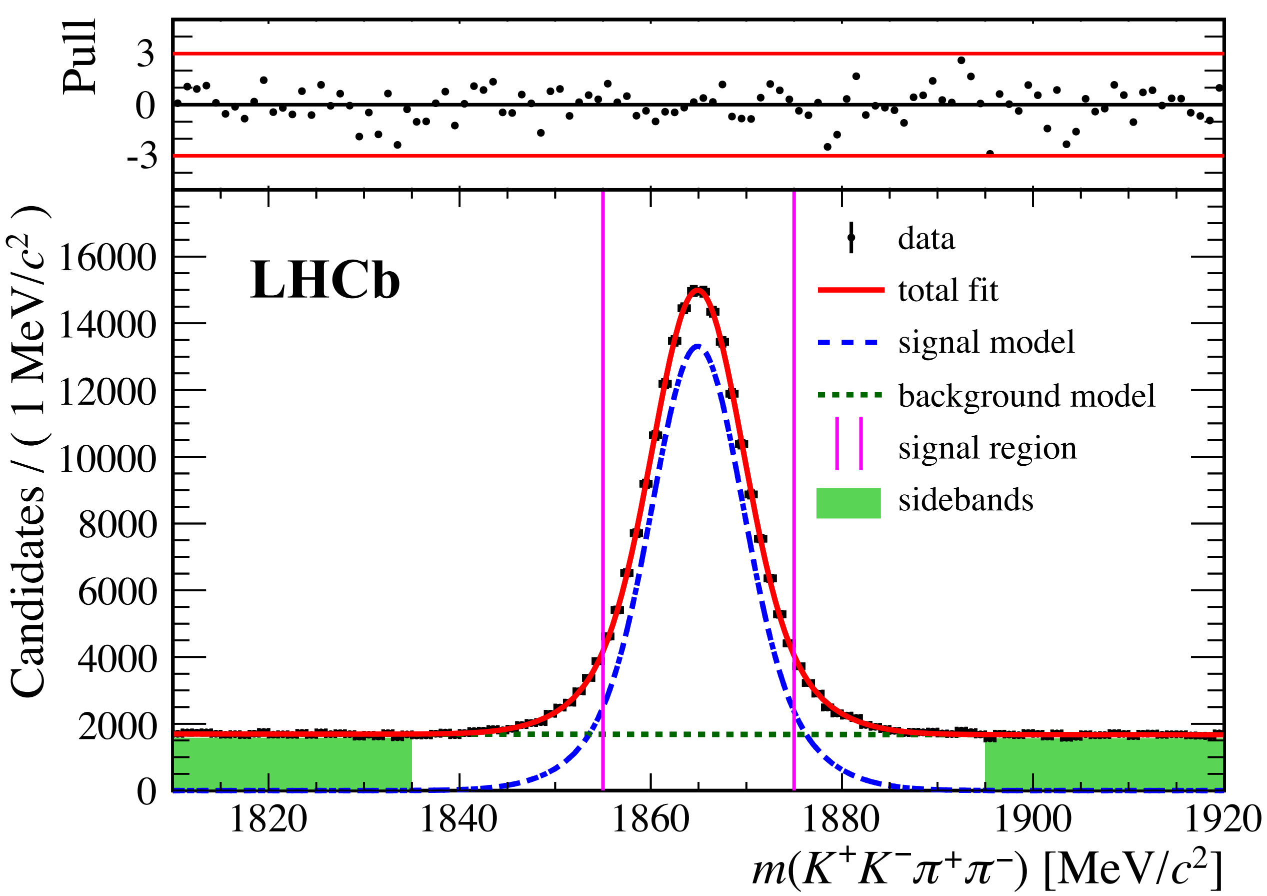


| | $KK$ | $\pi\pi$ | $K\pi$ | $KK\pi$ | $K\pi\pi$ |
|---|---|---|---|---|---|
| $J^P = 0^+$ | $a_0(980)$ $f_0(980)$ $f_0(1370)$ | $f_0(980)$ $f_0(1370)$ | $K_0^*(1430)$ | | |
| $J^P = 1^+$ | | | | $a_1(1260)$ | $K_1(1270)$ $K_1(1400)$ |
| $J^P = 1^-$ | $\phi(1020)$ | $\rho(770)$ $\omega(782)$ $\rho(1450)$ | $K^*(892)$ $K^*(1680)$ | | $K^*(1410)$ $K^*(1680)$ |
| $J^P = 2^+$ | $f_2(1270)$ $a_2(1320)$ | $f_2(1270)$ | $K_2^*(1430)$ | | $K_2^*(1430)$ |

S-waves are treated with the K-matrix formalism for the $\pi\pi$ and KK systems

# Fit results - projections

[arXiv:1811.08304]

## Similar projections as quasi-two-body method (+26)

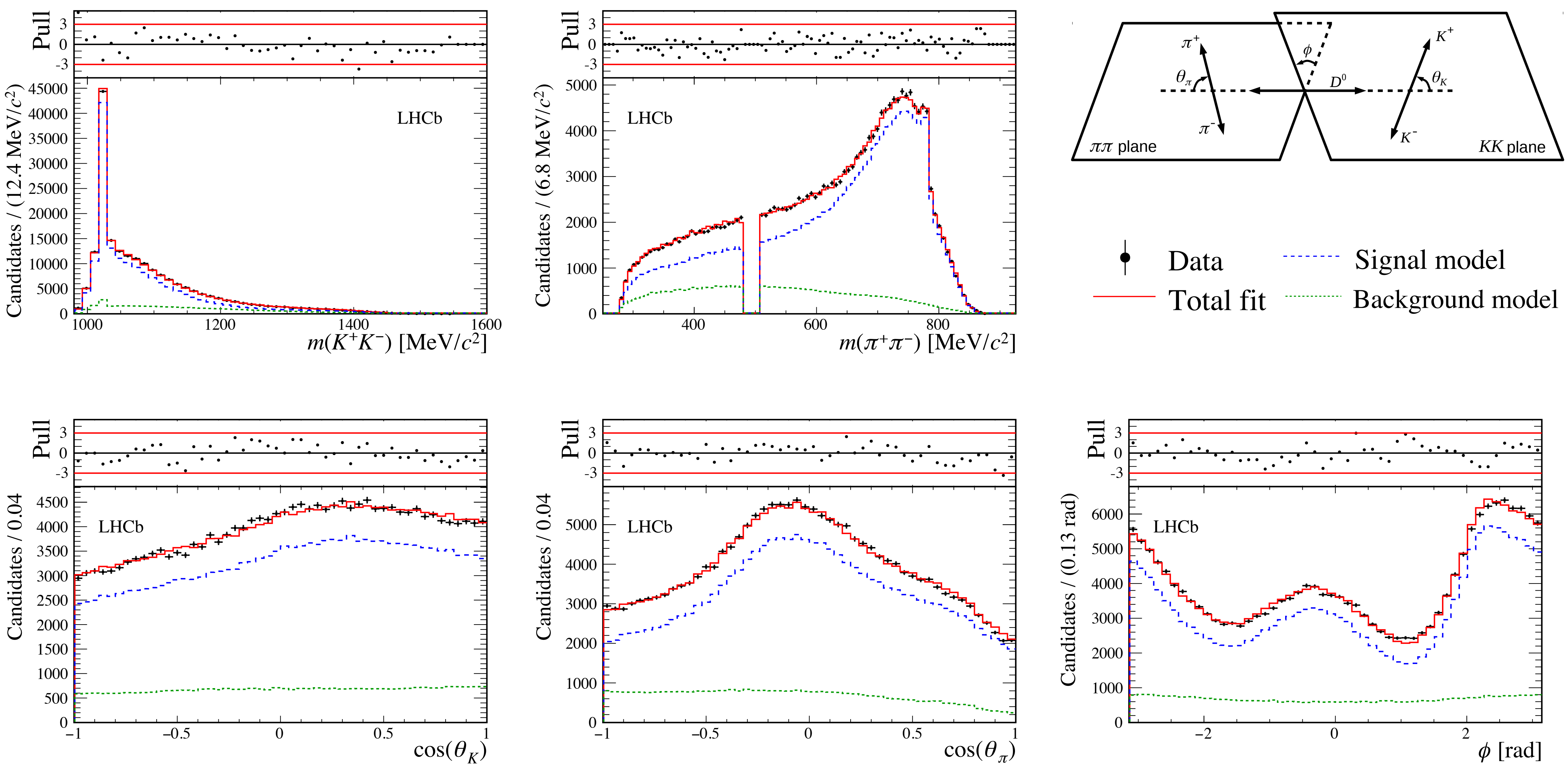

Universität Zürich[UZH]

# Fit results

[arXiv:1811.08304]

| Amplitude | Fit fraction [%] | $\mathcal{A}^{CP}$ [%] |
|---|---|---|
| $D^0 \to [\phi(1020)(\rho-\omega)^0]_{L=0}$ | $23.82 \pm 0.38 \pm 0.50$ | $-1.8 \pm 1.5 \pm 0.2$ |
| $D^0 \to K_1(1400)^+ K^-$ | $19.08 \pm 0.60 \pm 1.46$ | $-4.5 \pm 2.1 \pm 0.3$ |
| $D^0 \to [K^-\pi^+]_{L=0}[K^+\pi^-]_{L=0}$ | $18.46 \pm 0.35 \pm 0.94$ | $2.0 \pm 1.8 \pm 0.7$ |
| $D^0 \to K_1(1270)^+ K^-$ | $18.05 \pm 0.52 \pm 0.98$ | $-2.6 \pm 1.7 \pm 0.2$ |
| $D^0 \to [K^*(892)^0 \overline{K}^*(892)^0]_{L=0}$ | $9.18 \pm 0.21 \pm 0.28$ | $-4.3 \pm 2.2 \pm 0.5$ |
| $D^0 \to K^*(1680)^0 [K^-\pi^+]_{L=0}$ | $6.61 \pm 0.15 \pm 0.37$ | $2.6 \pm 2.2 \pm 0.4$ |
| $D^0 \to [K^*(892)^0 \overline{K}^*(892)^0]_{L=1}$ | $4.90 \pm 0.16 \pm 0.18$ | $-2.6 \pm 3.2 \pm 0.3$ |
| $D^0 \to K_1(1270)^- K^+$ | $4.29 \pm 0.18 \pm 0.41$ | $3.3 \pm 3.5 \pm 0.5$ |
| $D^0 \to [K^+K^-]_{L=0}[\pi^+\pi^-]_{L=0}$ | $3.14 \pm 0.17 \pm 0.72$ | $5.1 \pm 5.1 \pm 3.1$ |
| $D^0 \to K_1(1400)^- K^+$ | $2.82 \pm 0.19 \pm 0.39$ | $-1.3 \pm 6.0 \pm 1.0$ |
| $D^0 \to [K^*(1680)^0 \overline{K}^*(892)^0]_{L=0}$ | $2.75 \pm 0.15 \pm 0.19$ | $6.2 \pm 5.2 \pm 1.5$ |
| $D^0 \to [\overline{K}^*(1680)^0 K^*(892)^0]_{L=1}$ | $2.70 \pm 0.11 \pm 0.09$ | $-2.5 \pm 3.9 \pm 0.4$ |
| $D^0 \to \overline{K}^*(1680)^0 [K^+\pi^-]_{L=0}$ | $2.41 \pm 0.09 \pm 0.27$ | $2.4 \pm 3.7 \pm 1.1$ |
| $D^0 \to [\phi(1020)(\rho-\omega)^0]_{L=2}$ | $2.29 \pm 0.08 \pm 0.08$ | $-0.1 \pm 3.3 \pm 0.5$ |
| $D^0 \to [K^*(892)^0 \overline{K}^*(892)^0]_{L=2}$ | $1.85 \pm 0.09 \pm 0.10$ | $-3.0 \pm 5.0 \pm 0.7$ |
| $D^0 \to \phi(1020)[\pi^+\pi^-]_{L=0}$ | $1.49 \pm 0.09 \pm 0.33$ | $5.8 \pm 6.1 \pm 0.8$ |
| $D^0 \to [K^*(1680)^0 \overline{K}^*(892)^0]_{L=1}$ | $1.48 \pm 0.08 \pm 0.10$ | $1.3 \pm 5.3 \pm 0.6$ |
| $D^0 \to [\phi(1020)\rho(1450)^0]_{L=1}$ | $0.98 \pm 0.09 \pm 0.05$ | $7.5 \pm 8.5 \pm 1.1$ |
| $D^0 \to a_0(980)^0 f_2(1270)^0$ | $0.70 \pm 0.05 \pm 0.08$ | $1.5 \pm 7.2 \pm 1.3$ |
| $D^0 \to a_1(1260)^+ \pi^-$ | $0.46 \pm 0.05 \pm 0.22$ | $-10.6 \pm 11.7 \pm 7.0$ |
| $D^0 \to a_1(1260)^- \pi^+$ | $0.45 \pm 0.06 \pm 0.16$ | $-8.7 \pm 13.7 \pm 2.9$ |
| $D^0 \to [\phi(1020)(\rho-\omega)^0]_{L=1}$ | $0.43 \pm 0.05 \pm 0.03$ | $2.4 \pm 11.0 \pm 1.4$ |
| $D^0 \to [K^*(1680)^0 \overline{K}^*(892)^0]_{L=2}$ | $0.33 \pm 0.05 \pm 0.06$ | $8.5 \pm 14.3 \pm 3.5$ |
| $D^0 \to [K^+K^-]_{L=0}(\rho-\omega)^0$ | $0.27 \pm 0.04 \pm 0.05$ | $21.3 \pm 12.5 \pm 2.8$ |
| $D^0 \to [\phi(1020) f_2(1270)^0]_{L=1}$ | $0.18 \pm 0.02 \pm 0.07$ | $3.6 \pm 13.3 \pm 3.0$ |
| $D^0 \to [K^*(892)^0 \overline{K}_2^*(1430)^0]_{L=1}$ | $0.18 \pm 0.02 \pm 0.02$ | $6.1 \pm 10.8 \pm 1.8$ |
| | $129.32 \pm 1.09 \pm 2.38$ | |
| | $9242/8121 = 1.14$ | |

Large contributions from states as φ(1020) (ρ -w)$^0$, $K_1$ and S-wave

**No sign of $\not{C}P$ is observed (sensitivity ranging from 1-15%) - at the SM at the order of $10^{-3}$**

20 x larger statistics is expected for Run-II dataset

## Summary

- Multibody decays provide promising probes for the Standard Model

  - First measurement of a large S-wave contribution in $B^0_s \to \overset{(-)}{K^0} K^{\pm}\pi^{\mp}$
  - First observation of $\not{CP}$ in $B^0 \to VV$ angular distributions
  - New avenues in the search for $\not{CP}$ and in the understanding of the underlying physics in charm decays

- Synergy between theory-experiment is paramount

- Larger datasets from the LHCb Run-II+ upgrade will provide in the future the possibility to fully explore the potential of the field

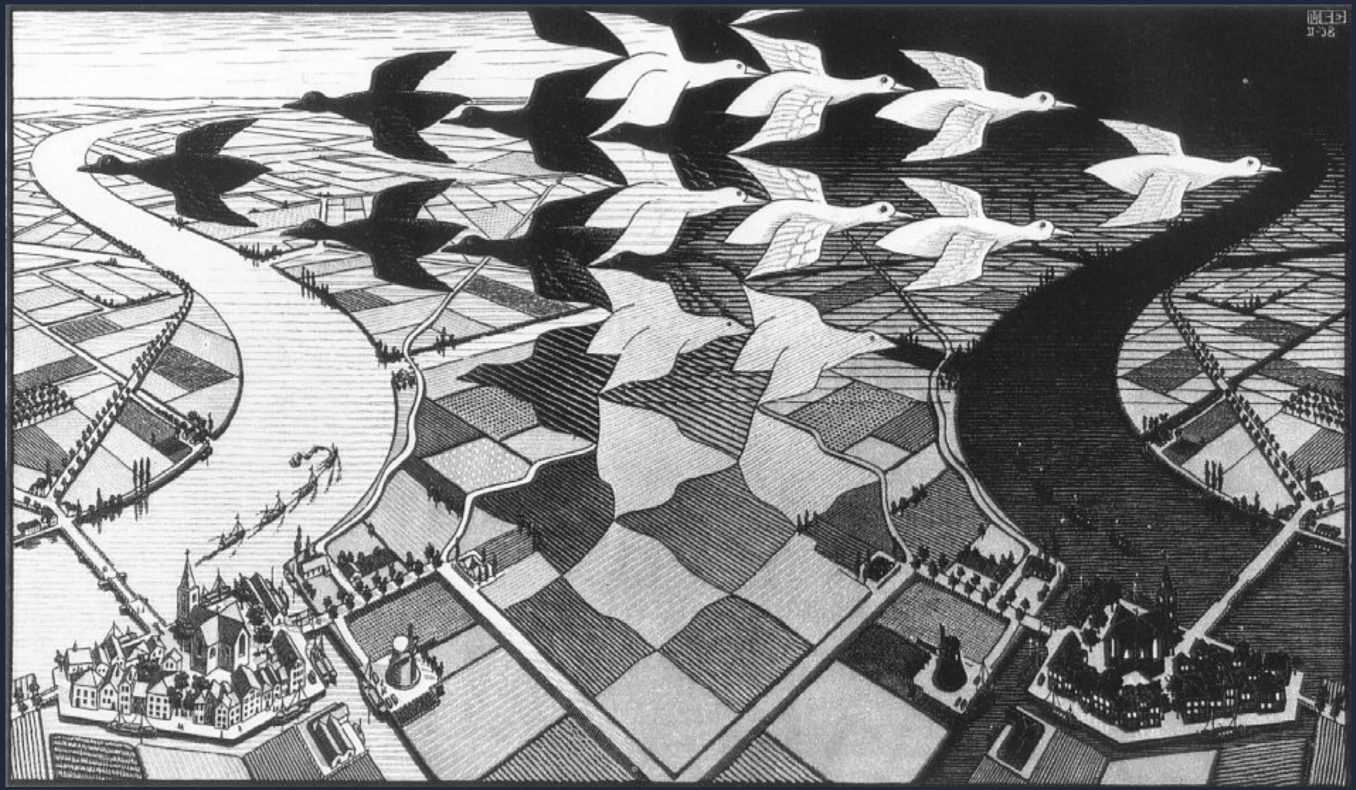

M.C. Escher
[Day and Night]

Les Nabis (“the Prophets”), *i.e.* artists who set the pace for painting in France in the 1980s

(re-incarnation) synergy between theorists and experimentalists in the pursue to understand the dynamics of multibody decays

P. Serusier
[The Talism]